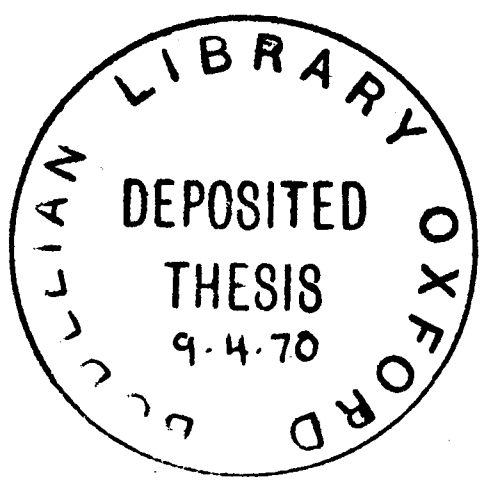
VORTEX FORMATION IN A TWO-DIMENSIONAL PERIODIC WAKE

by

K. Th. Wiese Nielsen

Brasenose College

Thesis submitted for the Degree of Doctor of Philosophy
at the University of Oxford



Department of Engineering Science
Parks Road
Oxford

Hilary Term, 1970

ABSTRACT

Flow visualization techniques have been used for quantitative determination of the distribution of vorticity in a two-dimensional incompressible periodic wake formed behind a bluff body at a Reynolds number of 1.5×10^4.

Following the suggestion of Gerrard (1966) the vorticity distribution in the wake was considered as an ordered subdivision of the shed circulation into no more than three identifiable and measurable parts. This permitted a single algebraic summation of the circulation quantities involved.

To trace the history of the transport of circulation in the formation region of the wake, a technique was developed which used small countable particles ejected from the point of separation into one of the shear layers. The number rate of ejection of particles was known and controlled accurately so that the particle density could be related to the vorticity in the shear layer. Having established that the particles remain implicitly with the rotational fluid, it is shown that the quantity of circulation transferred to any location is proportional to the number of particles carried into the same region.

By application of flow visualization techniques developed for this specific purpose, the number of particles carried to any region of interest in the wake could be determined. By means of these measurements, all the terms in the proposed circulation distribution equation was evaluated independently and the equation shown to be satisfied.

Not only do these results verify the Gerrard flow model; but also they provide the first known quantitative information concerning the actual distribution and history of the circulation

within the formation region. In the case of the final vortex strength comparison is possible with the work of other investigators and here good agreement was found.

As the particles are a vital tool in the investigation considerable efforts were devoted towards establishing the validity of their use as a flow marker in accelerating and shearing flows. This phase included also the solution of the mechanical problems of handling and measurement associated with the controlled ejection of particles into the shear layer. This work is described separately in Part II of the thesis.

The third part of the thesis is devoted to a general wake inquiry in which the particle technique is employed to explore certain subsidiary aspects of the wake flow not covered in Part I. These topics included the determination of the size of the dead fluid region, measurements of the injection mode of circulation into the dead fluid region and also effects of the ambient turbulence upon the formation of region and residual vortex strength in the fully formed vortices.

ACKNOWLEDGEMENTS

I am in particular indebted to my supervisor Dr. C.J. Wood for counteracting despondency with encouragement and inspiration while at times tempering my exuberance with caution.

I wish also to thank both Mr. M. Byford for his unfailing and very competent technical assistance during the research program, and Mrs. M. Matheson for her care while typing the thesis.

The work was performed under Science Research Council Contract B/SR/3271 whose support is gratefully acknowledged. For personal support since June 1968 on Research Contract AT/2057/034 I would like to thank the Ministry of Technology.

For their permission to take leave of absence and loan of instrumentation I am also in great debt to Dr. P. Squires and Professor J. Warburton of Desert Research Institute, University of Nevada. Their assistance made this work possible.

Finally, I would like to thank my wife for her encouragement, patience and the understanding with which she accepted this endeavour also.

LIST OF CONTENTS

		Page
TITLE		
FRONTISPIECE		i
ABSTRACT		ii
ACKNOWLEDGEMENT		iv
LIST OF CONTENTS		v
LIST OF ILLUSTRATIONS		vii
LIST OF TABLES		ix
NOTATION		x
PART I	QUANTITATIVE DETERMINATION OF THE VORTICITY DISTRIBUTION IN THE WAKE	
Chapter I	Introduction	
	The Two-Dimensional Periodic Wake	1
	Vorticity Distribution in the Periodic Wake	1
	The Gerrard Hypothesis concerning Vorticity Distribution	4
Chapter II	Assessment of Methods for the Experimental Inquiry	
	Applicable Flow Visualization Techniques	7
	Flow Visualization at Oxford	9
	The Concept of using Particles to Trace the Vorticity Distribution	11
Chapter III	Equations for Interpretation of the Experimental Data	
Section I	The Gerrard Hypothesis Expressed in Algebraic Terms	14
	The Marking of Rotational Fluid with Particles	17
	The Relationship between the Distribution of Particles and the Circulation Balance	19
	The Circulation Balance Expressed in Terms of Particle Counts	21
Section 2	Independent Determination of the Circulation Distributed in the Dead Fluid Region	24
	The Dead Fluid Region	24
	Formulation of the Particle Accumulation Balance in the Dead Fluid Region	26

Chapter IV	The Experimental Equipment	
	The Towing Tank and Trolley	31
	The Bluff-Based Model	32
	The Particle Emitting System and Procedures	33
	The Illumination System	37
	The Equipment for Still Photography	38
	" " " Cine Film "	39
	The Fibre Optics Timing System	40
	Correlation of Time and the Cine Film Record	41
Chapter V	Experimental Procedures and Results	
Section 1	Solution of the Circulation Balance	44
	The Total Loss of Circulation in the Formation Region	47
Section 2	Verification of the Value of Γ_c by the Particle Accumulation Balance	57
Chapter VI	Summary and Conclusions	65
PART II	THE PROPERTIES OF THE PARTICLES	
Chapter VII	The Static Properties of the Particles	69
	Determination of Particle Size	69
	Numerical Count of Particles in Bulk Volumes	78
	Effects on the Solution Viscosity due to the Presence of Solid Particles	78
Chapter VIII		
Section 1	Particle Response to Non-Shearing Unsteady Flow	
	Particle Response to Acceleration in the Flow Field	80
Section 2	Particle Response when Immersed in a Shearing Flow	84
	Quantitative Determination of the Particle Response to Shearing Flows	86
PART III	A GENERAL WAKE INQUIRY	
Chapter IX		
Section 1	Particle Motion History in the Wake	92
	Determination of the Downstream Counting Zone	96
	Particle Motion History in the Dead Fluid Region	97
	Determination of the Boundaries of the Dead Fluid Region	100
	Timing of the Particle Entry into the Dead Fluid Region	103
Section 2	Effects of Ambient Residual Turbulence	106
Section 3	Effects of Turbulence upon the Residual Vortex Strength	109
REFERENCES		111

LIST OF ILLUSTRATIONS

Fig. No.		Page
Frontispiece	A Starry Night (by Vincent Van Gogh)	i
PART I		
1:1	The Gerrard Filament Model	4
2:1	A Series of One-Second Long Smoke Puffs interspaced with a Two-Second Pause at 3.1 km ASL.	8
2:2	A Periodic Wake at Re $\tilde{=}$ 1.5×10^4	10
3.1	The Gerrard Filament Model (repeat of Fig. 1:1)	14
3:2	Visualization of Circulation Distribution Paths	15
3:3	Visualization of Simplified Circulation Distribution	17
3:4	Visualization of Particle Distribution Concept	18
3:5	Distribution of Vorticity within the Shear Layer	19
3:6	General Appearance of the Dead Fluid Region	25
3:7	Accumulation of Particles in the Dead Fluid Region (qualitative)	27
3:8	Sketch showing the Family of Solutions of Eq. 3:15 for Several Values of α	28
3:9	Sketch showing $\bar{N}_c$ Plotted versus Elapsed Ejection Time	29
4:1	The Experimental Equipment	30
4:2	The Bluff-Based Model	33
4:3	The Particle Ejection Mechanism	34
4:4	Timing Signal Appearance on Cine Film	41
5:1	The Concept of Outer Shear Layer Velocity = U_1	44
5:2	Wake Photograph as used for the Determination of U_1	45
5:3	The x, y and θ Coordinates as Measured on Flow Photographs by use of the Travelling Microscope	47
5:4	Strength of the Fully Formed Vortices (in Non-dimensional Terms) as a Function of Distance downstream of the Bluff Base	48
5:5	Discrimination Criteria for Particle Streaks as they are seen in the Microscope Eyepiece	49
5:6	Particles recorded in the Wake at an Exposure of 0.003 second	51

5:7	The Location and Boundaries of the Region in which all N_l and N_u Counts were Taken	51
5:8	Normalized Frequency Distribution of the Span of Ratios of N_l/N_u	54
5:9	$\frac{\Gamma_c}{\Gamma_o}$ as a Function of the Ratio $\frac{N_l}{N_u}$	56
5:10	Particle Counts $\bar{N}_c$ as a Function of Elapsed Ejection Time	60
5:11	The Mean Value of the $\bar{N}_c$ Counts (Fig. 5:10) Superimposed upon the Solution Set of Eq. 3:15	62
PART II		
7:1	The Characteristic Stacking Geometry of the Cubic and Rhombohedral Lattices	71
7:2	The Significant Volumes of Cubic and Rhombohedral Stacking Lattices	72
7:3	The Probability Distribution for the Co-ordination Number which is obtainable with a given Stacking Mode	74
7:4	The Experimentally obtained Stacking Modes of Polystyrene Particles in a vibrated, lubricated Bed	76
7:5	Occupancy by Solid Matter in Percent of Unit Volume as a Function of the Co-ordination Number C_o, for Monosized Spheres in Systematic Assemblies	77
8:1	The General Arrangement of the Equipment used in the Determination of the Particle Behaviour in Strong Velocity Gradients in the Shear Layer	87
8:2	Particle Paths in the Shear Layers	89
PART III		
9:1a-k	A Complete Vortex Shedding Cycle shown at 0.04 sec. per Frame Number	93
9:2	The Exact Dimensions of the Downstream Counting Zone in the Wake	96
9:3	Ejection of Dye into the Periodic Wake	97
9:4	The Translation and Rotation Exhibited by the Pairs of Particles visualized by following and marking their Position at 0.02 sec intervals during 1½ cycle	99
9:5a-h	The Periodic Injection of Particles into the Dead Fluid Region shown at 0.04 sec per Frame Number	101

9:6	The Timing of Ejection Mode into the Dead Fluid Region within the Cycle	103
9:7	The Dimensions and Boundaries of the Dead Fluid Region	104
9:8	A Lateral View of the Particle Ejection and the Wake formed under Conditions of High Residual Turbulence	105
9:9a-c	The Effects of Residual Turbulence upon orderly Wake Formation	108

LIST OF TABLES

Table I	Particle Ejection Sequence Data	36
Table II	Comparison of Outer Shear Layer Velocities for Three Types of Blunt-Based Sections	46

NOTATION

Symbol		
C	Volume Concentration of Solids in Liquids	(page 78)
C_o	Coordination Number	(" 70)
D	Particle Diameter	
H	$(\text{Velocity})^{-1}$ × (Height of Field in Focus)	(page 26)
K	A Proportionality Constant	(" 21)
N_o	The Number of Particles Ejected into the Shear Layer per Cycle	
N_1	The Number of Particles Present in the Fully Formed Vortices	
N_u	The Number of Particles Transported during each Cycle to the Fully Formed Vortices in the Opposite Row	
N_c	The Number of Particles Transported during each Cycle to the Dead Fluid Region	
$\bar{N}_c$	The Number of Particles Present at any time in the Dead Fluid Region	
U or u	Velocity	
U_s	Inner Wake Velocity	(page 44)
U_∞	Free Stream Velocity	(" 91)
U_1	Outer Stream Velocity	(" 44)
V	Volume	
V_P	Volume of Particle-(s)	
V_F	Volume of Fluid	
d	Height of the Illuminated Zone	
h	Model Base Width	
t	Time	
x-y	Cartesian Coordinates	
Γ_o	The Total Circulation Shed per Second at the point of Separation	
Γ_c	Circulation Transported to the Dead Fluid Region	
Γ_{ab}	Circulation Transported to the Opposite Row in the Wake	
Γ	Strength of the Fully Formed Vortices Downstream in the Wake	
α	The Ratio Expressed by $N_c/N_o = \alpha$	

β	A Void Coefficient	(page 71)
γ	An Occupation Coefficient	(" 74)
ξ	Vorticity	
θ_{1-2-3}	Angular Coordinates	
λ	The Einstein Constant	(" 78)
μ	Significant Dimensions in Microns	
ν	Kinematic Viscosity	
ρ	Density	
τ	Period of the Vortex Shedding Cycle	

PART I

QUANTITATIVE DETERMINATION OF THE VORTICITY DISTRIBUTION IN THE WAKE

CHAPTER ONE

INTRODUCTION

The Two-Dimensional Periodic Wake

This thesis is concerned with an experimental investigation of the two-dimensional wake in an incompressible flow downstream of a bluff body. The specific topics which are studied are limited to the range in which the wake displays a regular periodic vortex pattern.

The periodic wake has stimulated much interest by virtue of its fascinating features. The extent of this interest is indicated by the abundance of literature which has been presented on every aspect of the subject.

A number of survey papers provide a comprehensive review of the features and the state of the understanding of these wake flows. The first of these was by Goldstein (1938) who provided a lucid introduction to the early work on these subjects. This paper was followed with reviews by Krzywoblocki (1953), Rosenhead (1953), Batchelor (1956),Wille (1960), Nash (1962), Marris (1964), Morkovin (1964), Wille (1966), Roshko (1967), and Nash (1967)*.

Every phase of research on periodic wake in the subsonic flow regime is surveyed in detail in these reviews. Although they are of great general interest, much of the material which they treat is not relevant to the present problem and discussion of these papers is therefore omitted except where points of interest to the problem at hand have been considered.

Vorticity Distribution in the Periodic Wake

The reviews reveal that in the domain of the classical vortex street alone, studies have been performed upon many

---

* A brief review on recent work on periodic wakes including approximately 300 references is under preparation for publication as a University of Oxford Engineering Report by the author.

different aspects. These include among others: the Von Karman stability problem, the changes in flow pattern of the wake and its transition to turbulence, the relationships between the dimensions of the vortex trail and the body which causes the trail to form and the problems associated with the spatial distribution of vorticity in the wake.

The present investigation is concerned only with the last of these. By comparison with the other aspects it has been subjected to treatment by very few authors. The paucity of investigations has not been caused by lack of interest as much as by the absence of a way of making such an investigation.

In order that questions can be posed and ultimately answered about distribution of vorticity in the periodic wake, the rate at which vorticity is being generated and shed from the points of separation on a bluff body must be established first.

Fage and Johansen (1927) investigated this, in what appears to be the first detailed experimental investigation of the structure of the periodic wake. Using hot wire anemometers they examined the wake formed by a variety of shapes ranging from flat plates mounted transverse to the flow to slender ogival bodies with blunt bases. By this method they succeeded in obtaining data for the vorticity shedding rate and also the magnitude of the remaining circulation in the first fully formed vortices downstream in the wake. It appears that they were the first to deduce the rate of vorticity shedding from measurements of the increased velocity in the outer boundary of the shear layer springing from the points of separation.

When the circulation remaining in the downstream vortices was compared with that which was created in one shedding cycle,

a loss of approximately 50% was found, although no attempt was made to explain the mechanism causing the loss.

Roshko (1955) supported the findings by Fage and Johansen concerning the rate of vorticity shedding. By introducing an "early wake pressure" concept, he justified the use of a "free streamline velocity" which was larger than the mainstream velocity far removed from the bluff body. When the vorticity discharge was deduced from this "free streamline velocity", the apparent loss was similar to that found by Fage and Johansen. Nevertheless, the discrepancy still remained unexplained in detail.

It is however accepted that vortices of opposite rotation may annihilate each other when meeting. Even when no claims are made about eventual modes of meeting, this hypothesis is most plausible when applied to a wake where vortices of both signs are formed. It explains immediately how only a fraction of the original vorticity may survive the transfer through the vortex formation region of the wake to become part of a regular vortex.

Indications of the occurrence of vorticity annihilation by just such a mechanism can be had from the experimental data contributed by Schaeffer and Eskinazi (1959). When an oversight in their assumptions concerning the vortex centre's location was corrected by a method contributed by Hooker (1936), it was shown that the lateral spacing between two rows of viscous vortices increased downstream and while this widening process of the street was going on, vorticity was simultaneously being cancelled by interaction between the rows. This merely suggests, however, that such a mechanism can be active, while the initial problem concerning the nature of the vorticity loss and distribution stand virtually unsolved, and only sparse

knowledge exists concerning the magnitude of the loss of vorticity.

This loss was estimated to be as high as 50% by Fage and Johansen (1927), while Eskinazi (1967) suggests that the value is in the neighbourhood of 33%.

The Gerrard Hypothesis Concerning Vorticity Distribution

Although several investigators, among them Roshko (1955) and Wood (1964), have concurred in their opinions concerning the approximate magnitude, few have commented in detail upon the exact causes for, and the nature of the mechanism responsible for the distribution and subsequent loss of vorticity in the formation region. It was not until 1966 that a detailed mechanism was suggested.

The suggestion was made by Gerrard (1966), who discussed the loss in terms of an actual transfer of vorticity bearing fluid from one side of the wake to the other as shown in Fig. 1:1.

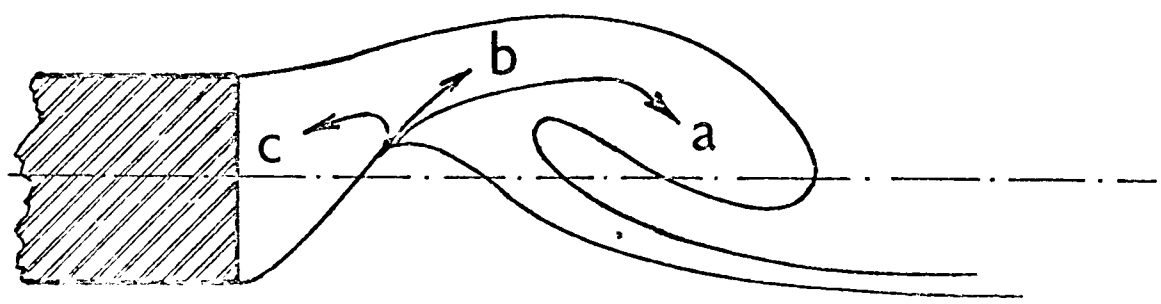


Fig. 1:1 The Gerrard Filament Model

As each new vortex begins to form behind the blunt trailing edge, its growth is sustained by the introduction of circulation from the shear layer. Such a vortex is shown forming in the upper row in Fig. 1:1. Eventually the growing vortex is strong enough to induce a transverse motion which

draws the opposite (in Fig. 1:1, the lower row) shear layer across the wake. The amount of fluid involved in the transverse movement is substantial and must therefore include fluid from the external stream. This external fluid cannot cross the filament lines indicated in Fig. 1:1 by solid lines and therefore the rotational fluid must have crossed also and become entrained by the growing vortex and the shear layer just upstream of the nascent vortex. A quantity of this transferred fluid also penetrates into the relatively quiet region immediately behind the bluff base. These three suggested entrainment paths are shown by arrows "a", "b" and "c", while the formation region itself is outlined by the continuous filament lines in Fig. 1:1.

It is of importance to recognize that the fluid which is carried across the wake possesses vorticity that is opposite in the rotational sense to that vorticity which it encounters when being entrained by the opposite shear layer (path "b"), the nascent vortex (path "a") and in the internal region (path "c").

It follows that when such elements of opposed vorticity are entrained the effect must be a cancellation, with an ensuing decrease in the vorticity available for subsequent vortex formation. Furthermore, because the rotational fluid has been transferred, its vorticity is no longer available to feed the next vortex on the lower side.

From the preceding paragraphs, it is clear that the Gerrard model provides a plausible explanation of several important aspects of the wake development. Not only is it the only model to be proposed so far; but also, by defining the flow mechanism in terms of vorticity transport, it gives a clear

suggestion that it might be rewarding to investigate further the flow in these terms.

It was this suggestion that led the present author to consider the use of flow visualization methods to trace the history of the vorticity as it passes from the boundary layers into the vortex trail.

A recent paper by Zdravkovich (1969) gave support for this decision. Using a moveable smoke filament, he marked the rotational fluid in the shear layer on one side only of the wake formed by a cylinder.

Subsequent photographic records revealed that a quantity of smoke from the marked shear layer appeared eventually in the vortex cores in the opposite row in the wake.

Of course, these results were qualitative only. Zdravkovich had no way of estimating either the proportion of the smoke that was transferred or the amount of circulation it represented. However, the idea is very much of interest in that it represents a development of thought which was parallel to the work of this author. By using a similar selective injection technique with countable particles instead of smoke, the present flow visualization method was designed not only to demonstrate that rotational fluid crosses the wake; but also to determine the proportion which does so.

CHAPTER TWO

ASSESSMENT OF METHODS FOR THE EXPERIMENTAL ENQUIRY

Applicable Flow Visualization Techniques

Flow visualization techniques have been utilized in investigations of fluid flow phenomena from the dawn of interest in this branch of science.

Among the nearly innumerable variations in approach and choice of media, two particular methods have emerged and become widely used.

First, the use of a continuous fluid flow marker such as a smoke or a dye. The indicator is allowed to distribute itself according to the motion in the flow field undergoing investigation. The use of this method was demonstrated in classical simplicity by Reynolds in his classical demonstration of transition.

The second approach involves the use of small gas or solid particles in temporary or permanent suspension in the fluid. Media and applications are here also too numerous to recall in total, but among the more successful have been applications of plastic spheres, Schmiescheck (1936), kerosene droplets, Zdravkovich (1969), and hydrogen bubbles, Clutter et al (1959), suspended in the fluid, aluminium dust or lycopodium spores, Goldstein (1938), distributed on fluid surfaces, and a rather distinctive choice by Hooker (1936), who developed a taste for elixirs composed of alcohol and condensed milk.

The term "very small particles" should be qualified in the sense that the size of the tracing particles should be small with respect to the scale of the phenomenon of interest.

This tracing particle concept has been used in a very large scale range. For example, Fage and Townend (1932) used an ultra microscope to follow the movement of particles smaller

than 1μ in diameter in air flow. At the other extreme, coherent smoke puffs of about 50 metres in diameter were used by Nielsen and Berry (1968) to trace the flow motion in alto-cumulus lenticularis clouds at altitudes ranging from 3 to 10 kilometres above sea level as shown in Fig. 2:1.



Fig. 2:1 A series of one-second long smoke puffs inter-spaced with a two-second pause at 3.1 km. A.S.L.

With due compensation for the scale, the principles were entirely the same as used in any flow visualization scheme.

With proper care and preparation the methods using particles in suspension allow the acquisition of accurate, qualitative information about flow motion with respect to velocity and direction.

These methods have therefore been utilized by a large number of investigators in even more numerous applications. Prandtl and Tietjens (1934) and subsequently Goldstein (1938) provided comprehensive reviews of earlier work with solid particle methods, while Clutter et al (1959) gave a detailed account of the use of the hydrogen bubble technique in water

towing tanks. Both they and Wood (1967) have demonstrated how rather accurate results can be obtained by combining the principles of either gas or solid tracer particles with analytical techniques and a convenient data retrieval system. Yet more recent and elaborate systems still under further development have been used by Kline (1967) and Kline et al (1967) in large scale tracking of hydrogen bubble paths with subsequent computerized data treatment.

Flow Visualization at Oxford

The techniques employed by Wood in Oxford are based upon still photography of small, neutrally bouyant,spherical polystyrene particles suspended in water. The fluid motion is created either by letting the water flow over some bluff body fastened in the transparent test-section of a recirculating flow tunnel, or by towing a body through still water in a tank.

The paths of the fluid in the water are made visible by illuminating a cross section of the cloud of suspended particles with mercury vapour lamps and photographing the particle movement in the wake. Due to their sphericity each particle acts as a small lens when illuminated and scintillates brightly on the dark background. The strong contrast between the illuminated particles and the background makes it easy to record their tracks on suitably timed photographs. Furthermore, the flashing mercury lamplight breaks the particle path streaks into rows of dots. Together these features provide the facility to measure both directions and velocities in the flow field.

Photographs of the wake similar to Fig. 2:2 provide the bulk of the data about the motion of the flows. There are, however, far too many particle streaks on each photograph to

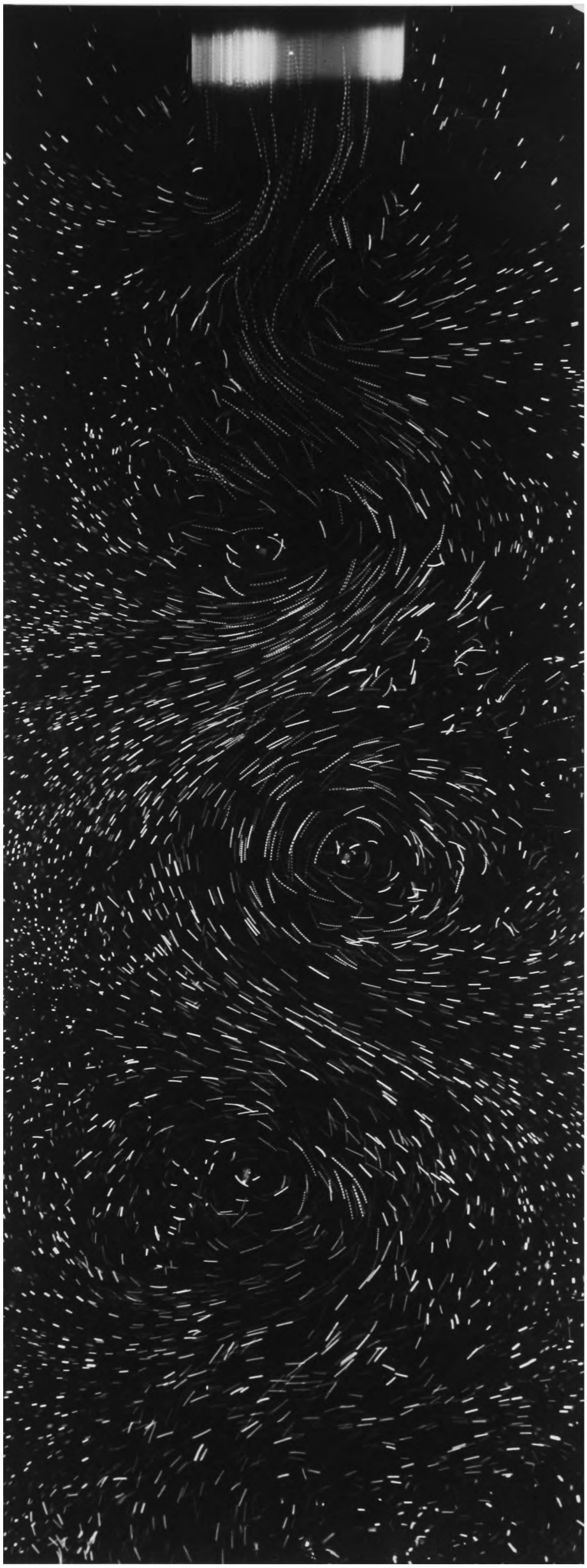


Fig. 2:2 Periodic wake at Re = 1.5×10^4 photographed at 1/10 sec.

measure them manually. Therefore a travelling microscope coupled to a digital recorder was added to the facilities to expedite the analysis. When required the digital output can be treated directly by computer to yield quantitative information about parameters which include: flow field velocities, base pressures and directions, while by integration of tangential velocity components on suitable circles in the fully formed vortices, the magnitude of the remaining circulation can be estimated.

The capabilities of the present techniques and equipment are, however, limited to the extent that they can only provide information about circulation in the fully formed vortices.

The present author improved the system by the addition of a cine camera technique which yielded a large amount of sequential wake photographs. Examination of these yielded much reliable information as will be shown later.

The Concept of Using Particles to Trace the Vorticity Distribution

Nevertheless, at the present state of development, the Oxford flow - visualization method could yield no information concerning the Gerrard Hypothesis of vorticity transfer in the near wake.

The essential need was for a method by which the rotational fluid could be masked specifically and identified in a quantitative manner so that its distribution could be determined at all stages during the vortex formation process.

If it is accepted that a smoke or dye stream or any other suspension of particles will follow the path of a fluid flow, then the concept of a technique using small discrete and countable particles obeying the same laws as the smoke particles becomes very attractive. Such a technique could conceivably

be developed for use as a tracer to mark and follow vorticity in a selective manner and to be capable of yielding quantitative results.

The possibility of using tracer particles in the form of the aforementioned polystyrene spheres was therefore considered at once on the basis of their previous successful use at Oxford in other flow visualization programs.

The main requirements for the use of discrete particles as a tracing media are, in general terms:

The particles must be introduced into the shear layer in such a way that an invariant and measurable proportionality coefficient relate the distribution of particles to the distribution of vorticity elements.

The particles must remain with the fluid - and therefore with the vorticity elements into which they originally were injected and entrained.

The subsequent distribution of particles must be measurable and must be capable of interpretation in the terms of the original proportionality coefficient mentioned in the preceding paragraphs in order that the vorticity distribution can be assessed quantitatively.

The development and initial application of a flow visualization technique satisfying these requirements were discussed by Nielsen (1969).

This development included a thorough investigation of the problem of obtaining a controlled and measurable injection of particles and also the analogy between particle and vorticity distribution,when known quantities of particles are placed solely within vorticity bearing shear layers.

This phase is presented as a separate entity in Part II

of the thesis. It suffices therefore here to state that such a method has been devised, tested exhaustively and found to be reliable.

The subsequent chapters in Part I of the thesis are concerned exclusively with the use of the method and the information which has been gained about the particle and vorticity distribution in the wake.

CHAPTER III

EQUATIONS FOR THE INTERPRETATION OF THE EXPERIMENTAL DATA

The Gerrard Hypothesis Expressed in Algebraic Terms

Inasmuch as the desire and need for a satisfactory flow visualization technique expressed in Chapter 1 has been fulfilled, it is now convenient to return to the treatment of the main thesis topic - the demonstration of the validity of the hypothesis suggested by Gerrard concerning the flow in the formation region of a two-dimensional, incompressible periodic wake.

He postulated the occurrence of a periodic flow reversal and entrainment of vorticity along three distinct paths in the formation region as shown in Fig. 1:1, which is repeated here.

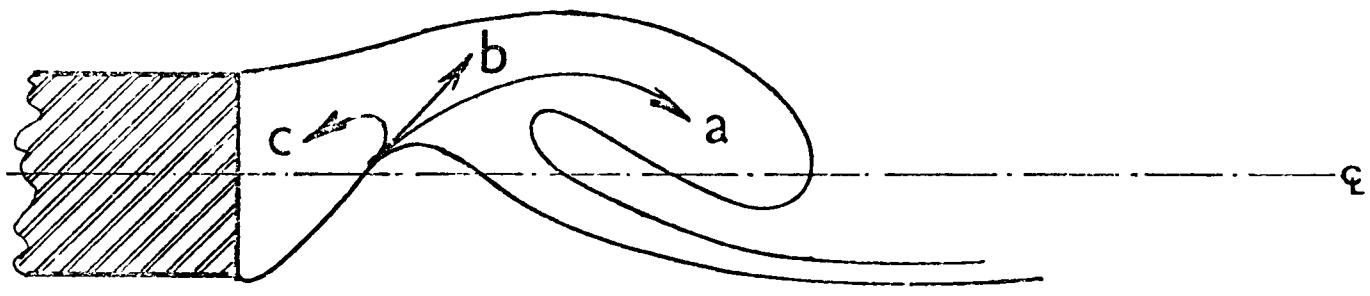


Fig. 3:1 The Gerrard Filament Model

In order to develop and examine the Gerrard model it is necessary to express the circulation distribution by an algebraic statement.

The components of the displaced flow marked respectively as "a", "b" and "c" in Fig. 3:1 include rotational fluid from the shear layer. Thus each component carries vorticity in two-dimensions and has a corresponding circulation which is denoted here by Γ_a, Γ_b and Γ_c.

If the total circulation shed per cycle from each separation point is denoted by Γ_o and if Γ is defined to be

the final strength of the fully formed vortex immediately after its separation from the shear layer, then a circulation balance can be established with reference to Fig. 3:2.

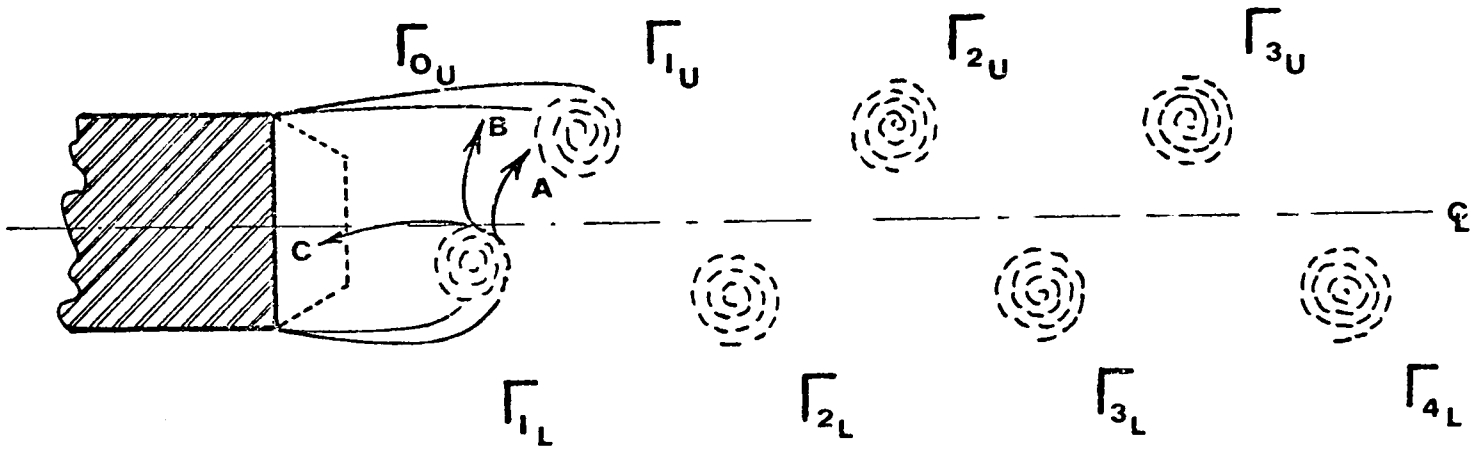


Fig. 3:2 Visualisation of Circulation Distribution Paths

Considering the balance of anti-clockwise circulation on the lower side of the wake, the Gerrard model may be described by stating that three quantities Γ_a, Γ_b, and Γ_c are removed from the lower shear layer during each whole cycle (one vortex shed from each side).

The subsequent history of these components does not influence the fact that their removal constitutes a loss in the lower side of anti-clockwise circulation equal to $(\Gamma_{a_l} + \Gamma_{b_l} + \Gamma_{c_l})$.

During the same cycle a corresponding transfer of clockwise circulation takes place in which quantities Γ_{a_u}, Γ_{b_u} and Γ_{c_u} are removed from the upper shear layer. The Gerrard model states that the Γ_a and the Γ_b components are entrained respectively in the lower shear layer and in the growing vortex. Being of the opposite sign to the circulation present there, this entrainment causes a further reduction of Γ_{a_u} and Γ_{b_u} in the final strength of the lower vortex so that:

$$\Gamma_l = \Gamma_{o_l} - [\Gamma_{a_l} + \Gamma_{b_l} + \Gamma_{c_l}] - [\Gamma_{a_u} + \Gamma_{b_u}] \qquad 3.1$$

The conditions for lateral symmetry demand that:

$$\Gamma_{a_l} = -\Gamma_{a_u} = \Gamma_a$$

$$\Gamma_{b_l} = -\Gamma_{b_u} = \Gamma_b$$

$$\Gamma_{c_l} = -\Gamma_{c_u} = \Gamma_c$$

The same equations apply to the upper shear layer as well, so on either side of the wake the balance of circulation can be expressed by:

$$\Gamma = \Gamma_o - 2\Gamma_a - 2\Gamma_b - \Gamma_c \qquad 3.2$$

In order to measure the magnitude of the various circulation quantities in Eq. 3.2, it is now necessary to consider the regions into which the circulation is distributed.

The Gerrard hypothesis postulates three such regions as shown in Fig. 3:2: the nascent vortex, the region immediately behind the bluff body (path "c") and the opposite row in the wake (paths "a" and "b").

The quantities of circulation which are transferred across the wake respectively into the vortex as Γ_a and into the shear layer just ahead of the vortex cause jointly a net reduction in circulation on that side from which they were removed. A reliable distinction between these quantities Γ_a and Γ_b was impaired by the chosen experimental methods as discussed in detail (see page 97) in Part III of the thesis. This lack of discrimination does not cause any concern however, because the initial interest is concentrated upon the determination of the total loss of circulation. It therefore suffices to consider Γ_a and Γ_b not as individual components but as a lumped quantity:

$$\Gamma_a + \Gamma_b = \Gamma_{ab} \qquad 3.3$$

by substitution into Eq. 3.2

$$\Gamma = \Gamma_o - \Gamma_c - 2\Gamma_{ab} \qquad 3.4$$

The distribution is thus conceptualized as shown in Fig. 3:3

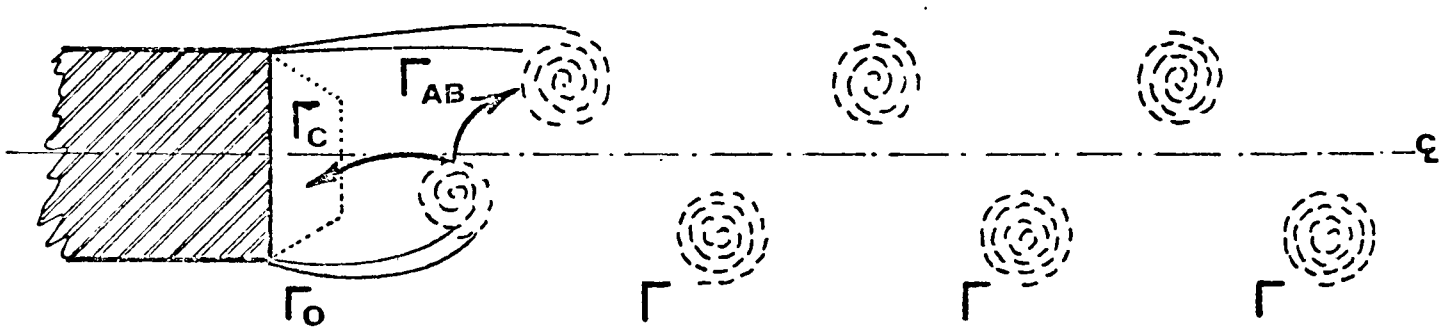


Fig. 3:3 Visualisation of Simplified Circulation Distribution

It remains to establish the relationship between the circulation balance Eq. 3.4 and the method which was developed for tracing the distribution of the shed circulation throughout the wake.

The Marking of Rotational Fluid with Particles

This method (discussed in Part II of the thesis) is evolved around the principle of emitting particles at a constant rate from one of the separation points where also the vorticity is generated and shed, thus marking only the rotational fluid on that side. If the particles are emitted from the lower point of separation, their distribution may be related to the distribution of vorticity originating in that shear layer.

The particle distribution is expressed in terms of four distinct quantities as shown in Fig. 3:4.

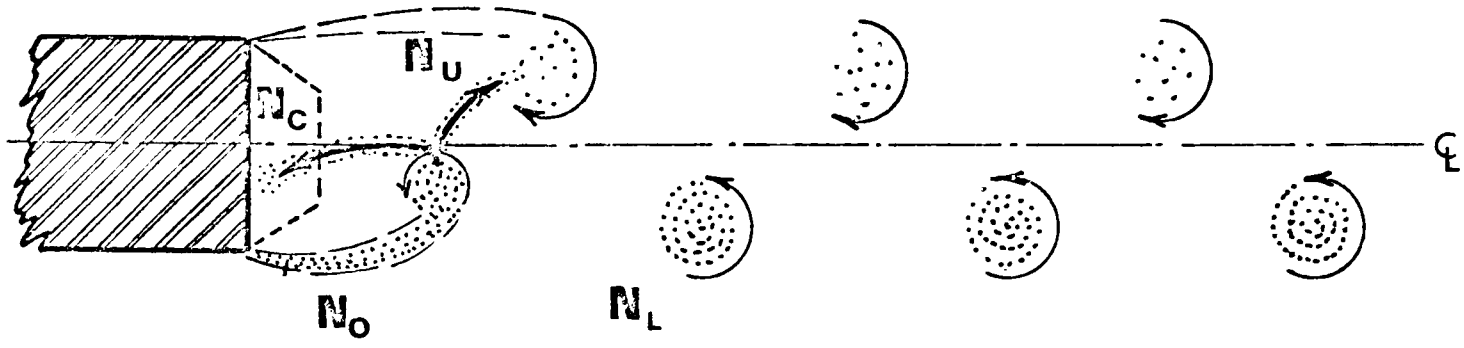


Fig. 3:4 Visualisation of Particle Distribution Concept

These terms are:

N_o: which is the total number of particles which during one cycle are emitted into the vorticity bearing shear layer.

N_1: which is the number of particles which terminate their travel in the wake in the fully formed vortices on the particle ejecting side.

N_u: which is the number of particles which are transferred across the wake with the fluid which also bears the vorticity defined as Γ_{ab}. These particles terminate their travel in the fully formed vortices which form on the opposite side of the particle ejection side.

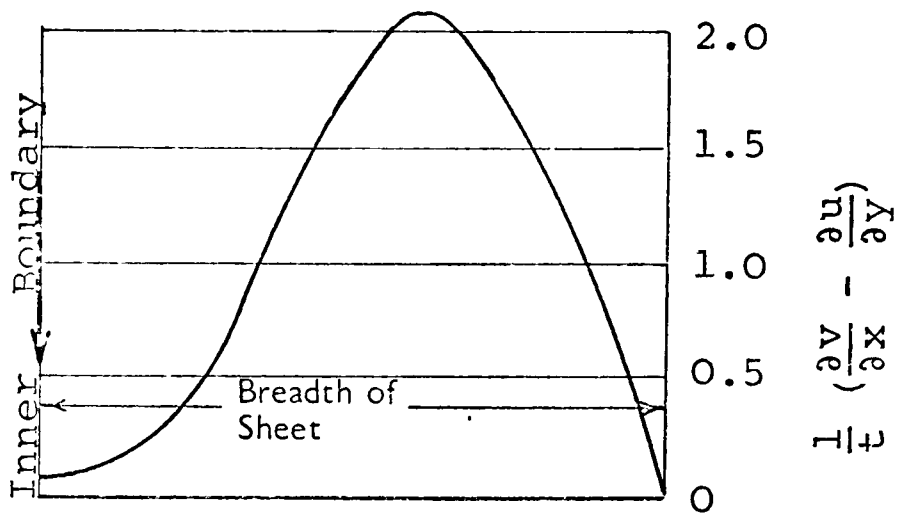
N_c: which is the total number of particles that entrain in the fluid penetrating once during a cycle into the quiescent region behind the bluff base.

The particle distribution balance in the wake within one cycle can therefore be expressed by:

$$N_o = N_u + N_1 + N_c \qquad 3.5$$

The Relationship Between the Distribution of Particles and the Circulation Balance

The relationship between Γ and N is considered first in the shear layer. Although the rate of particle emission can be made constant, the subsequent distribution of particles across the shear layer is not known. Furthermore, although the transverse distribution of vorticity in the shear layer is known to be of the form shown in Fig. 3:5, it is almost certainly a periodic function of time.



After Fage and Johansen (1927)

Fig. 3:5 Distribution of Vorticity Within the Shear Layer

Thus it is not easy to justify an assumption of proportionality between N_o and Γ_o.

The difficulty need not be insurmountable however, provided that care is taken in assessing the implications of the assumptions that are made.

The basis of the analysis is that during one shedding cycle a known number of particles is injected entirely within a Lagrangian area A_s which contains all the rotational fluid leaving the separation point during that cycle. Irrespective of how the particles and the vorticity are distributed this

area A_s may be subdivided into N_o smaller areas A_p each containing a single particle.

It is important that no vorticity bearing fluid should be omitted from consideration, therefore it is necessary that:

$$\sum_{1}^{N_o} A_p = A_s.$$

Because it is associated with an area where there is a vorticity distribution $\xi(x,y)$ each particle may also be associated with a specific circulation Γ given by

$$\Gamma_p = \iint_{A_p} \xi dA.$$

The sum of the circulation about all sub-areas is equal to the total circulation Γ_o about A_s so that:

$$\sum_{1}^{N_o} \Gamma_p = \Gamma_o.$$

The variation in Γ_p is, of course, quite unknown. However, it is sufficient to consider an average value K such that:

$$K = \frac{1}{N_o} \sum_{1}^{N_o} \Gamma_p = \Gamma_o/N_o. \qquad 3.6$$

As the particles move with the flow, they remain associated with individual prescribed areas A_p (these remain constant in an incompressible, two-dimensional flow). The vorticity moves with the fluid also, so that each individual particle remains associated with its own circulation Γ_p. Thus when the original shear layer area A_s is subdivided and a subset N of the original particles is found within one of the wake vortices, it remains true that

$$\Gamma = \sum_{1}^{N} \Gamma_p.$$

In this situation the average circulation $\bar{K}$ per particle is given by:

$$\bar{K} = \frac{1}{N} \sum_{1}^{N} \Gamma_p$$

so that

$$\Gamma = \bar{K}N.$$

Clearly, if the new value of N is to be utilized to estimate the new value of Γ, then $\bar{K}$ must be known. In the present work it is assumed that $\bar{K} = K$, that is:

$$\frac{1}{N} \sum_{1}^{N} \Gamma_p = \frac{1}{N_o} \sum_{1}^{N_o} \Gamma_p \qquad 3.7$$

In other words, it is assumed that when part of the shear layer is transferred across the wake and entrained into the other side, the particles which are transferred are truly representative of the distribution in the original shear layer. This is not an unreasonable assumption since in the proposed flow model a whole section of the shear layer is transferred during each cycle.

Having established the concept of an invariant constant of proportionality K which is the mean circulation per particle in all regions of the flow, it can be stated that

$$N_o = (K^{-1})\Gamma_o \qquad 3.8$$

$$N_u = (K^{-1})\Gamma_{ab} \qquad 3.9$$

$$N_c = (K^{-1})\Gamma_c \qquad 3.10$$

and, by the same arguments which were used to develop Eq. 3.4,

$$N_1 = (K^{-1})(\Gamma + \Gamma_{ab}) \qquad 3.11$$

The Circulation Balance Expressed in Terms of Particle Counts

It is now possible to combine Eqs. 3.9 and 3.11.

$$\frac{N_1}{N_u} = \frac{(K)^{-1}(\Gamma + \Gamma_{ab})}{(K^{-1})(\Gamma_{ab})} = \frac{\Gamma}{\Gamma_{ab}} + 1$$

to get

$$\Gamma_{ab} = \frac{\Gamma}{N_{1/N_u} - 1}$$

using the expression to eliminate Γ_{ab} from Eq. 3.4 we obtain

$$\Gamma_o = \Gamma_c + \Gamma\left|1 + \frac{2}{N_{1/N_u} - 1}\right| \qquad 3.12$$

All terms in Eq. 3.12 can now be evaluated directly since:

Γ_o: is the total amount of vorticity which is shed during each cycle from the separation point. If in the boundary layer at the point of separation the streamlines are parallel to the x-axis the rate at which vorticity leaves the point can be estimated by taking the integral $u(\frac{\partial u}{\partial y})dy$ across the boundary layer.

$$\frac{d\Gamma}{dt} = \int_{y_1}^{y_2} u\left(\frac{\partial u}{\partial y}\right) dy.$$

Integrating with respect to y yields

$$\frac{d\Gamma}{dt} = \frac{u_2^2 - u_1^2}{2}$$

Hence

$$\Gamma_o = \int_o^\tau \frac{d\Gamma}{dt}dt = \int_o^\tau \frac{u_2^2 - u_1^2}{2} = \frac{u_2^2 - u_1^2}{2} x\tau \qquad 3.13$$

where u_2 and u_1 are the boundary velocities in the sheet. Eq. 3-13 was used by Fage and Johansen (1927) who concluded that it yields accurate values of $d\Gamma/dt$ for sheets where the radius of curvature is large compared with the length of the sheet. Therefore it applies to the present investigation.

Evaluation of the magnitude of Γ_o by use of Eq. 3.13 requires therefore only determination of the velocities in the sheet boundaries. For this measurement,

methods are at hand.

Γ: is the vorticity remaining in the fully formed vortices. It can be measured on flow photographs as demonstrated by Wood (1967), see page 11, Chapter 2.

N_l/N_u: is the ratio of the numbers of particles located in the fully formed vortices at their peak strength positions. The particles are counted also on the flow photographs.

The ability to estimate these three terms in Eq. 3.12 leaves only one unknown term. This is the quantity of vorticity Γ_c which is carried to the interior of the formation region of the wake and annihilated there by vorticity of opposite sign arriving one half cycle later.

The validity of this proposed model will be demonstrated if an independent evaluation of the quantity of circulation Γ_c can be performed which agrees well with the magnitude established for Γ_c by evaluation of Eq. 3.12.

CHAPTER III, SECTION 2

The Independent Determination of the Circulation Distributed in the Dead Flow Region

Γ_c is that quantity of circulation which, according to Gerrard, is deposited in the interior of the formation region. To estimate the magnitude of this quantity use is again made of the results of Part II of the thesis, in which it was shown that particles remain with the elements of circulation in which they originally were entrained.

If it can be shown that some fraction of the total number of particles originating in the shear layer are found at the end of each cycle in the "c" region, the Gerrard model becomes yet more plausible.

If, in addition, the rate of arrival of these particles can be determined and compared with the total output rate of particles, an independent quantitative estimate would be had of Γ_c which subsequently could be compared with the value of Γ_c deduced by the methods utilized in the previous section.

The Dead Fluid Region

The region occupied by the circulation Γ_c is normally known as the dead fluid region. Its general appearance is shown on the next page.

The physical boundaries of this region and the details of the transfer of circulation into it were deduced from cine and still photographs of the particle movement, as described in Part III on the inquiry into the general feaures of the wake.

This study included the observation of approximately 2000 shedding cycles and showed that the process by which particles, and hence circulation, are transferred into the dead fluid region, is not continuous, but a brief intense event. It is

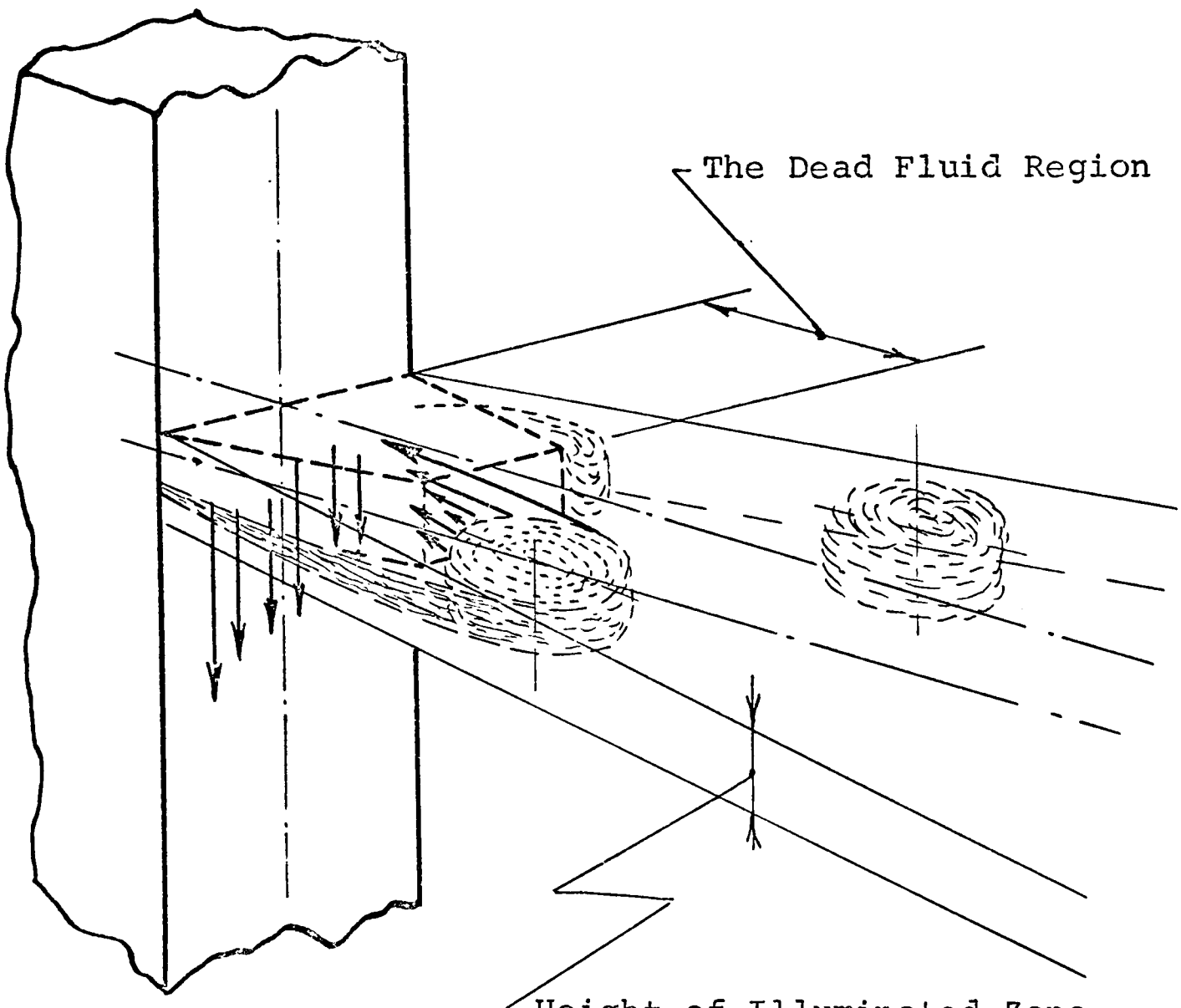


Fig. 3:6 General Appearance of Dead Fluid Region

initiated shortly after the nascent vortex has grown to a small but discernible size and stops just before the fully grown vortex is separated from the shear layers. It was also observed that after the particles have entered the dead fluid region and the circulation they represent has been cancelled by the arrival of particle free, but circulation laden fluid of opposite rotation; although remaining implicitly within the lateral boundaries of the dead fluid region, they do not any more participate in the wake movement, but sink slowly away.

It is imperative to note that at this stage the particles no longer represent circulation.

Because the particles sink slowly in water (specific

gravity = 1.05) they cannot remain in the dead fluid region, but must sink vertically along the span of the model of the illuminated zone. Particles do not sink into the dead fluid region from above as the initial injection of particles takes place in one plane only and there are no particles in the tank above the illuminated region.

Formulation of the Particle Accumulation Balance in the Dead Fluid Region

In the dead fluid region a balance therefore exists between the periodic injection of N_c particles per cycle and the loss by sinking. If this loss is proportional to the total number $\bar{N}_c$ of particles actually present in the dead fluid region at any instant the balance may be expressed in the following equation

$$\frac{d\bar{N}_c}{dt} = N_c f(t) - H\bar{N}_c \qquad 3.14$$

in which:

f(t): is the function which specifies how the particle injection rate varies during the cycle.

H: is a constant such that $H\bar{N}_c$ is equal to the rate of loss of particles due to sinking. The magnitude of H = 0.22 particles sec^{-1} was established in Parts II and III from measurements of the particle sinking velocity and the height of the illuminated zone.

The input function f(t) is cyclic with a period τ. Therefore the solution of Eq. 3.14 will also be periodic in the steady state. In addition, there will also be a transient past representing the initial increase in the mean value $\bar{\bar{N}}_c$ of $\bar{N}_c$ over the first several cycles, as shown in Fig. 3:7.

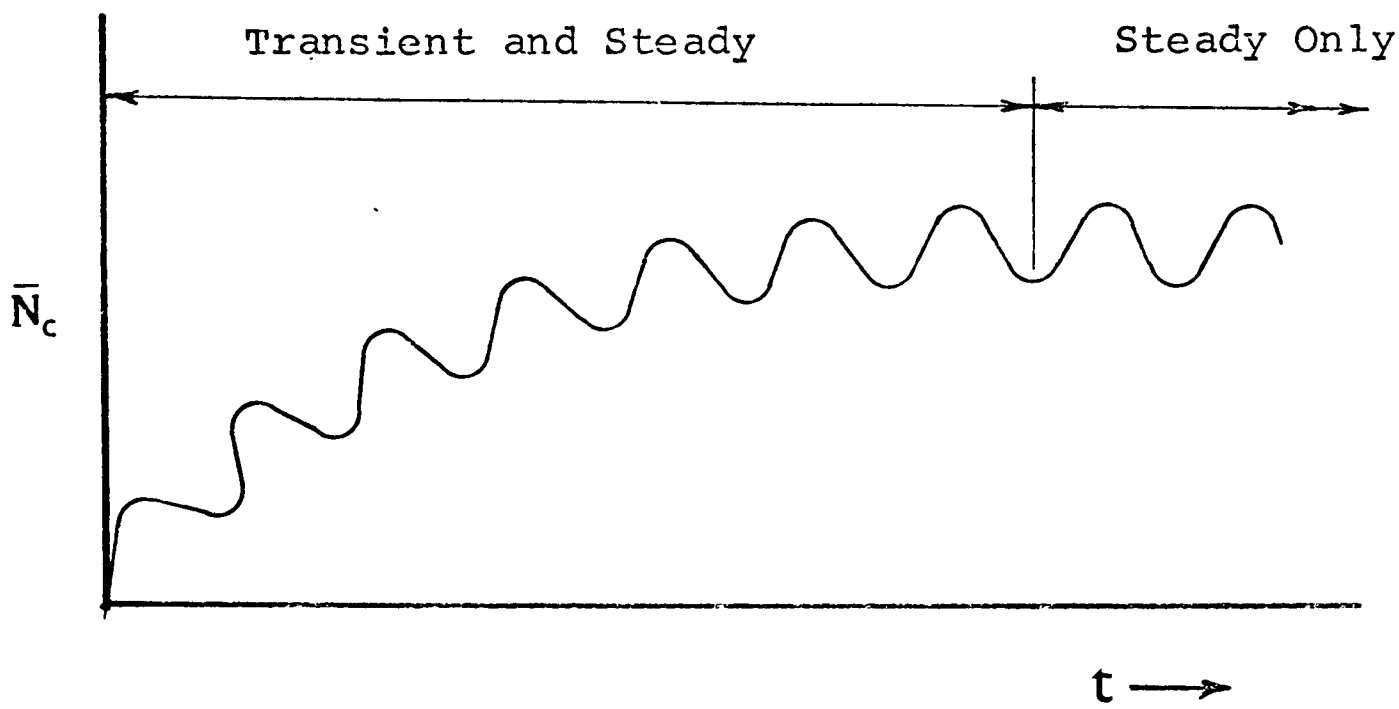


Fig. 3:7 Accumulation of Particles in the Dead Fluid Region (qualitative)

Because the duration of the experimental runs in the towing tank was relatively short, the accumulation time between the start of particle injection and taking the photographs was always within this initial rise. Therefore, the transient part of the solution of Eq. 3.14 is of interest rather than the steady state periodic part.

Furthermore, although the aforementioned accumulation time could be measured with good accuracy (page103, Part III), it was difficult to relate the time of the photograph to the phase within the shedding cycle.

For this reason it was decided to neglect the periodic aspects of the solution of Eq. 2.14 and make no attempts to specify the exact form of the function f(t), but rather to consider the transient growth of the mean value of $\bar{N}$ which was denoted earlier by $\bar{\bar{N}}_c$.

These considerations allow simplification of Eq. 3.14

since instead of the instantaneous particle injection rates $N_c f(t)$ we use the mean rate $\frac{N_c}{\tau}$ to obtain:

$$\frac{d\bar{\bar{N}}_c}{dt} = \frac{N_c}{\tau} - H\bar{\bar{N}}_c \qquad 3.15$$

The solution for this equation yields for $t > o$

$$\bar{\bar{N}}_c = \frac{N_c}{H\tau}(1 - e^{-Ht}) \qquad \text{for } \bar{\bar{N}}_c = o \text{ at } t = o$$

Subsequent division by N_o which was defined as the total number of particles ejected per cycle gives the form

$$\frac{\bar{\bar{N}}_c}{N_o} = \frac{\alpha}{H\tau}(1 - e^{-Ht}) \qquad 3.16$$

The ratio $\frac{N_c}{N_o} = \alpha$ is that proportion of the ejected particles which are carried into the dead fluid region and its exact value can now be deduced in two steps.

Firstly, Eq. 3.16 is solved for $\bar{\bar{N}}_c$ in terms of t with:

$H = 0.22$ particles sec^{-1}, $\tau = 1.47$ sec, and

$N_o = 540$ particles per cycle

(which were the values used in all experimental work) while holding α constant at several values between 1 and O.

When these solutions were plotted they yielded a family of curves as shown in Fig. 3:8, where each curve represents one particular value of α.

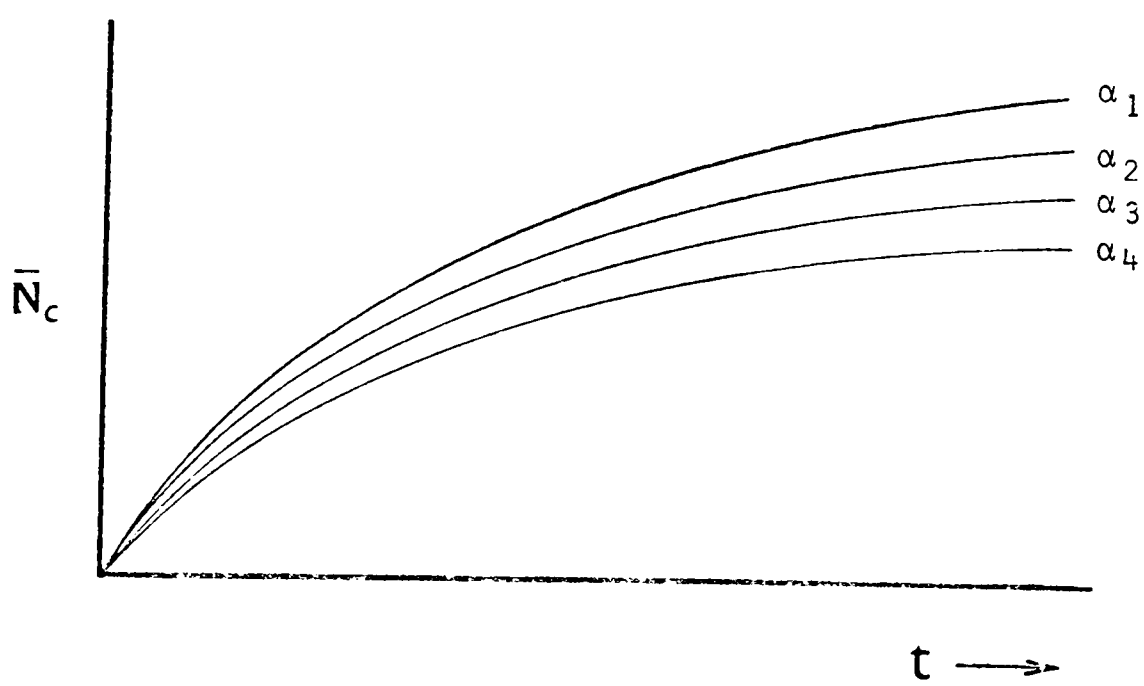


Fig. 3:8 Sketch Showing the Family of Solutions of Eq. 3.16 for several values of α.

Since α is represented by several curves, it is necessary for completion of the solution to ascertain by experimental means which of these curves represent the true value of α.

This completion can be accomplished by taking instantaneous particle counts $\bar{N}_c$ of the accumulation in the dead fluid region. The subsequent plotting of each value of $\bar{N}_c$ will yield a set of data points, through which the mean curve can be drawn. These counts will occur at somewhat random times within the cycle, nevertheless when a large number of values of $\bar{N}_c$ are plotted, the mean curve through these points will represent the desired average count $\bar{\bar{N}}_c$, as shown in Fig. 3:9.

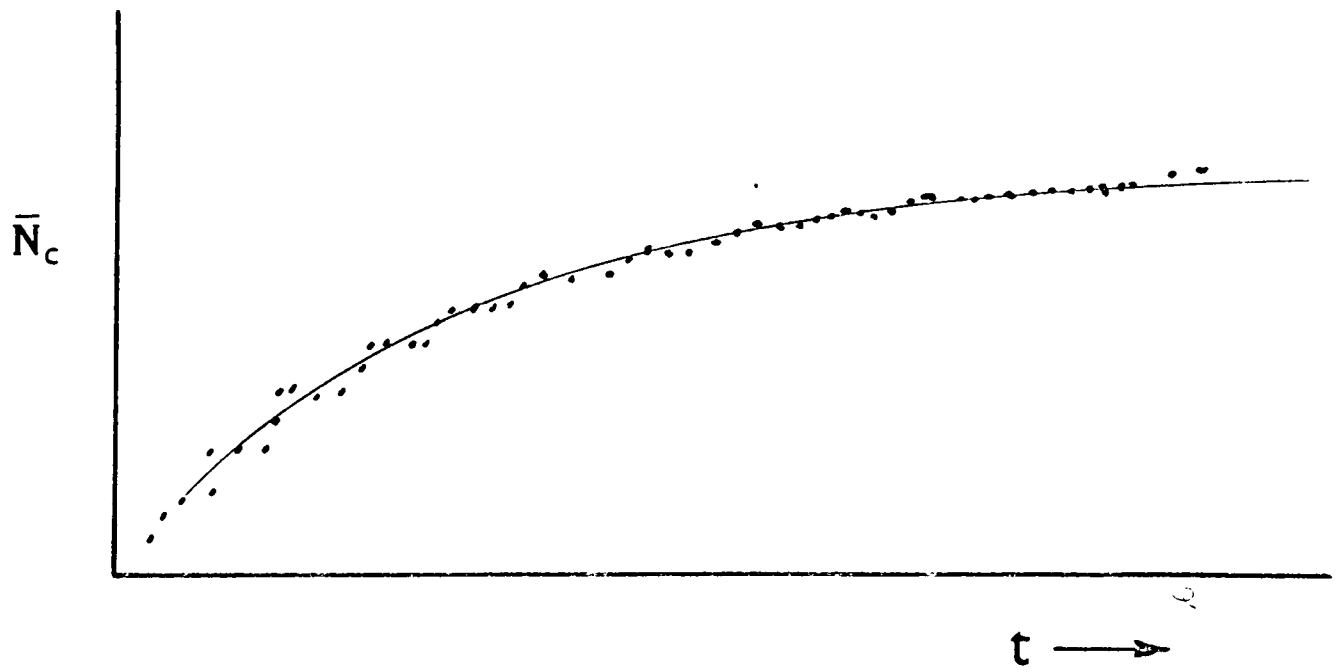


Fig. 3:9 Sketch Showing $\bar{N}_c$ plotted versus Elapsed Ejection Time

Superimposing the experimental mean curve (Fig. 3:9) upon the family of theoretical curves (Fig. 3:8) will then enable the current value of α to be identified.

CHAPTER IV

THE EXPERIMENTAL EQUIPMENT

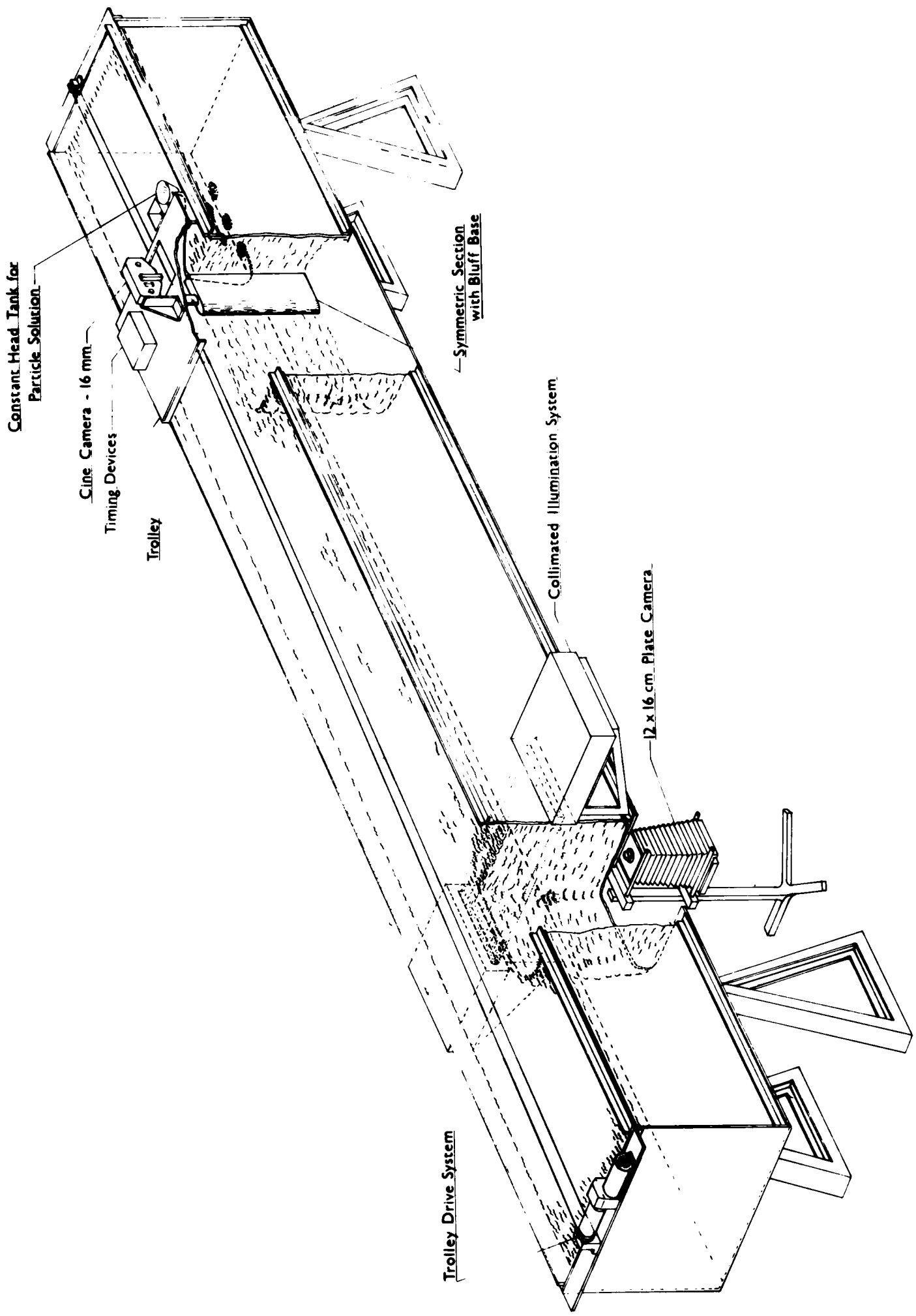


Fig. 4:1 General Arrangement of Experimental Equipment.

The topic for the thesis work - the periodic wake in an incompressible two-dimensional flow - was formed by towing a bluff-based model through still water in a towing tank. In Fig. 4:1 (preceding page) a general assembly is shown of the major components, which together constitute the experimental equipment.

The Towing Tank and Trolley

The tank supports and the load-carrying structure of the towing tank were fabricated from steel profiles; while the sides and the bottom of the tank were equipped with 10 mm thick hardened glass panels of good optical quality. The tank width and length are respectively 0.75 metre x 5.00 metre while the depth is such that the water height can be varied from 0 to 0.5 metre. On top of both sides finely finished rails constitute the track for the trolley rollers.

The trolley is supported in three positions by rollers and is constrained vertically by its weight (20 kg empty), while constraint is supplied in the lateral plane by guide rollers contacting the sides of the two trolley tracks.

The trolley is powered by a 25 watt single phase capacitor induction motor, which through appropriate sets of gears can propel the trolley at several fixed velocities between 9.30 cm/sec and 37.10 cm/sec. The motor and gear box are located on the tank end as shown in Fig. 4:1, and the towing face is applied by a steel cable wound around a spirally-grooved pulley and returns around a pulley at the opposite end of the tank.

The trolley velocities were calibrated by Wood (1967) who determined that within one metre of travel, the velocity fluctuations are less than one percent of the travelling

velocity. A later check by the author revealed no change from the findings of the initial calibration.

The trolley was towed at the lowest available velocity:

$$U_\infty = 9.30 \text{ cm/sec}$$

in all the experimental work, which with the model shown in Fig. 4:1 provided a Reynolds Number of approximately 1.5×10^4. At this Reynolds Number the shear layers can be expected to be laminar at the start, if not until the roll-up into vortices is initiated.

The Bluff-based Model

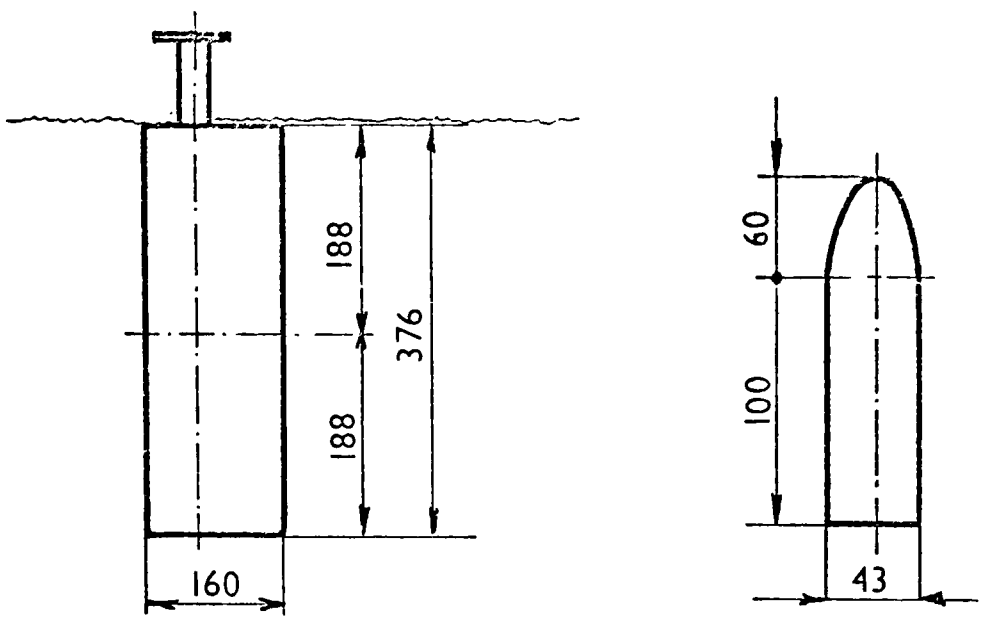
The model has, as indicated in Fig. 4:1, a bluff-based symmetrical cross section. This configuration was chosen because a fixed point of separation as exhibited by this type of section was desired. In addition a series of well-documented experiments performed by Wood (1967) with a very similar model is available for reference in the literature. Furthermore, Fage and Johansen (1927) established the vorticity shedding rates for models similar in cross section to the profile chosen for this investigation.

The model was built on a tubular main stem from 3 mm sheet brass for the sides, while the top and bottom faces and the blunt base were made of 6 mm brass plate. All edges were milled, such that the separation corners were held sharp and true.

The dimensions of the model as well as the general shape are shown in Fig. 4:2.

To minimize stray light reflections, the model was painted flat black after all small cavities such as screw slots and countersunk holes had been sealed.

The accuracy between the tracks for the trolley and the



Dimensions in mm.

Fig. 4:2 The Bluff-based Model.

bottom of the tank is adequate to ensure that the gap between the model bottom and surface of the tank never exceeds 1-1.5 mm, thus preserving the two-dimensionality of the flow. It will be shown later (see page 40) how a similar effect was obtained at the model top.

The Particle Emitting System and Procedures

When the model is towed through the water in the tank, a solution of water and particles are emitted from the point of separation as also shown in Fig. 4:1.

The mechanism for emitting these particles consisted of a conical adjustable head feed tank incorporating a stirring device to insure that the particles are maintained in a uniform suspension in the solution. A feeding tube made of semi-stiff 2 mm inner diameter surgical plastic tubing supplied the solution of particles to the ejection point. This tube terminated at the corner midway between top and bottom of the model. The details of the shape of the outlet are shown in Fig. 4:3 as well as the general system.

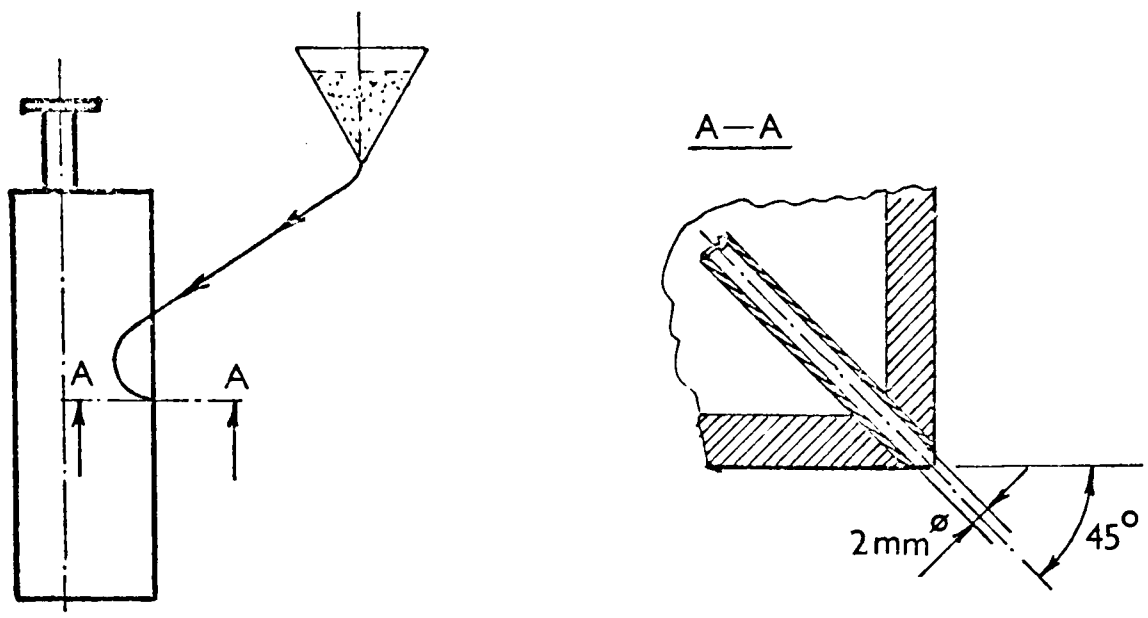


Fig. 4:3 The Particle Ejection Mechanism

A small valve linked to a stopwatch allowed the flow of particle solution to be started and stopped with an accuracy of ± 0.05 sec and all particles not ejected could be recovered to determine the number emitted into the wake. The head which drives the solution through the feed tube and outlet into the shear layer could initially be varied from 0 to 15 cm of water to provide a facility for maintaining a constant head during long experimental runs. It was however determined that the discharge caused less than a 0.30 cm decrease in head during a full run and measurements on cine film photographs of the ejection sequence revealed that changes in the discharge rate were not discernible until the difference in head exceeded 1.5 cm. Therefore a fixed tank position was chosen to eliminate the complications associated with devising a mechanism providing a constant head.

The actual head employed was determined by the need to eject particles at a velocity which would inject them into but not across and out of the shear layer. Such a suitable head

was established by adjusting the height of the head tank until the particles were injected entirely within the shear layer. This could be observed conveniently on the flow photographs and was confirmed by subsequent measurements on cine film photographs.

These tests led to the conclusion that any head between 6.7 cm and 10.7 cm could be used. At the lower limit particles were observed to trickle down the span of the bluff base inside of the shear layer, while at the upper limit the ejection jet began to penetrate the shear layer and place the particles outside in the irrotational flow. To avoid either of the extremes, a head of 8.7 cm was chosen and used throughout the work.

The number rate of particles entering the shear layer is controlled both by the head and also by the concentration of particles in the solution. Since the head had been shown to be restricted to 8.7 cm, a series of tests was performed to ascertain the best compromise between having so many particles in the solution that counting became impossible due to image overlap on the flow photographs and having so few that a representative distribution was not obtained.

During these tests it was revealed that when stirred a solution would flow completely unimpaired until the concentration exceeded 35% when occasional clogging of the feed pipe obstructed the flow.

It was determined also from the cine films that at the other extreme, concentrations as low as 1.0-1.5% provided uniform distribution with ease. The solution strength to be used for all experiments was therefore arbitrarily chosen to be 3% by volume particles to water.

In the subsequent experimental runs this ratio was proven to yield very constant result. The consumption of particles during each run was determined by measuring the height in a calibrated cylinder of a column of the particles which constituted the 3% measure. The height was measured of the columns formed by the particles initially in the solution, and also by those in the remaining solution after completion of a run. The output of particles into the wake was determined by taking the difference of the particle volume before and after the run. All particles not ejected into the wake could be recovered for measurement.

A set of ejection data are presented in Table 1.

TABLE 1

Run No.	Duration to Time Mark in Seconds	Duration of Run in Seconds	Total output of particles cm^3	Output of Particles in cm^3/sec
1	19.5	27.7	0.400	0.0145
2	13.2	21.8	0.320	0.0147
3	5.2	13.5	0.200	0.0148
4	10.9	19.8	0.286	0.0146
5	5.3	13.5	0.193	0.0146
6	FRAMING RATE CHECK			
7	-"-	-"-		
8	11.6	19.8	0.291	0.0147

The particle size was determined earlier as well as the number of particles contained in unit volume, see Chapter VII, Part II, page 69, and gave a count per cm^3 of

$$N/cm^3 = 2.55 \times 10^4 \text{ particles}/cm^3.$$

Therefore, for the average output in Table 1

$$N/sec = N/cm^3 \times \text{vol. output/sec}$$

$$= 2.55 \times 10^4 \frac{P}{cm^3} \times 0.0147 \frac{cm^3}{sec}$$

and

$$N/sec = 375 \text{ particles/sec.}$$

The demonstrated capability for obtaining constant and repeatable ejection data and the appearance of the wakes composed of particle clouds allow good faith in the established ejection rates.

The Illumination System

After their introduction into the wake, the particle motion was recorded by cine and still photography for which the illumination was provided by four 1000 watt mercury vapour arc lamps.

The lamps are mounted in pairs in two housings, which also each contain a light collimating optical system. This system concentrates the light from the point sources into flat parallel sheets of light variable in thickness from about 5 mm to 20 mm. The housings are shown in Fig. 4:1 located on each side of the test section to provide an even, shadowless illumination of the flow.

In addition to the illumination, the Hg lamps provide a convenient timing system. The paths of the particles in the flow are photographed during a finite interval which is chosen to be larger than the intervals between the discharges in the Hg lamps. These discharges occur at 100 cycles/sec, or twice the network frequency, and do therefore break the particle streaks on the flow photographs into rows of dots, where the interval between each dot represents the distance travelled by the particle in 0.01 sec.

The Equipment for Still Photography

All still photographs of the particle motion in the wake were obtained with a 12 cm by 16 cm plate camera equipped with a 20.3 cm f7:7 Kodak Ektar lens while using Kodak Royal X Pan sheet film rated (and used) at 1200 ASA.

The images of the particles are registered upon the emulsion during the brief peak light output of the Hg lamps. The duration of the flash is much shorter than 0.01 sec, therefore the camera shutter only controls the number of dots which are registered on the film emulsion. Hence it was possible to use shutter speeds from 0.003 during which the positions of the particles were registered as single dots, or any longer intervals producing the chain-like rows of dots.

When necessary, compensation against over-exposure was made with neutral density filters.

In general, the scale relationship was maintained at 1:2.5 on the photographs. Increases of this ratio caused unacceptable loss of detail, while decreasing the ratio limited the extent of the wake under surveillance too much.

The exact value of the scale ratio could be determined when measuring the particle streaks since a fixed reference dimension was always present in the form of the base width of the model.

The still photographs provided the source of data from which wake velocities and the strength of the fully developed vortices were computed.

The measurements were made with a two-axis travelling microscope on which the lead screws had been equipped with accurate linear potentiometers which convert the lead screws sled position into D.C. voltage signals. A rotating turntable,

underneath the optical system on the sled controlled by the lead screws, is also fitted with a rotary potentiometer measuring the angular position θ of the turntable. The accuracy of the x-y components is ± 0.005 mm over the measuring range of 10 x 20 cm while the angular position can be measured over 720^{o} with an accuracy of ± 0.1^{o}.

The voltage signals from the θ, x and y potentiometers can be either displayed directly on a digital voltmeter or reproduced on punched paper tape to be treated as data directly on the Oxford University KDF-9 computing facility. For this purpose a program was written to accompany the punched tapes in order that the necessary data could be obtained about the vortex strength and spacing in the wake.

The Equipment for Cine Film Photography

The remainder of the photographic information was obtained by cine filming the wake events. A Bell and Howell Model 240 cine camera was used in conjunction with the still camera for this purpose.

This camera was equipped with a 13 mm, f:1.7 Elgeet lens and used Kodak 4-X Negative film type 7224 at framing speeds of nominally 25, 32 and 48 frames per second. The lens opening was held at f:5.6 in all sequences to ensure correct depth of field. Changes in light intensity were compensated for, by the use of neutral density filters as before. The type 7224 film is nominally rated at ASA 500; but by forced development, it was feasible to obtain usable results in conditions requiring ratings as high as ASA 1200.

The cine camera was mounted on the trolley on the centre line of the model above and behind the model base. From this position three complete cycles of the wake could be included in

the image frame. Optical interference from waves on the top of the water surface was eliminated by photographing the wake through a Perspex plate mounted on the upper end of the model. The lower surface of this perspex plate was just submerged such that a ripple-free upper surface was provided.

In addition to the elimination of optical interference, this plate provided an end-plate effect which, by preventing surface waves, helped to maintain the two-dimensionality of the flow towards the upper end of the model.

The cine film technique was designed to provide a continuous record of the particle motion in the wake, such that counts could be made on the individual frames to determine the number of particles in any location at any desired instant. This timing facility was particularly important in the process of estimating α which required accurate measurements of the time history of $\bar{N}_c$, i.e. the number of particles in the dead fluid region (as discussed in Chapter 3).

The value of $\bar{N}_c$ depends upon the elapsed time from the start of the particle ejection. The opening of the particle ejection valve can take place at any time before the moving model enters the illuminated zone. Thus, the start of ejection is not recorded on the cine film and it is therefore imperative to establish a time reference which determines the elapsed time to one particular cine film frame.

This reference was obtained by starting a stopwatch as the ejection valve was opened and stopping it simultaneously with the imprint of a time mark on the film.

The Fibre Optics Timing System

To provide this imprint a 0.3 mm diameter multistrand fibre optics lead was installed in the camera such that its face

was located in front of the film plate just above the edge of the rotary shutter. The light from the face was directed towards one corner of the film frame by deflecting the light beam with a 1 mm^2 mirror mounted between the shutter and the film surface.

The light signal was provided by firing AGB-1 flash bulbs, the light from which was focused upon the other end of the filter optics lead. The flash bulb and the stopwatch, which recorded the time from the start of the flow of particle solution to the firing of the flash, were both triggered by a cam on the moving trolley.

Fig. 4:4 shows the appearance of the timing signal peak and subsequent decay when recorded at 48 frames per second.

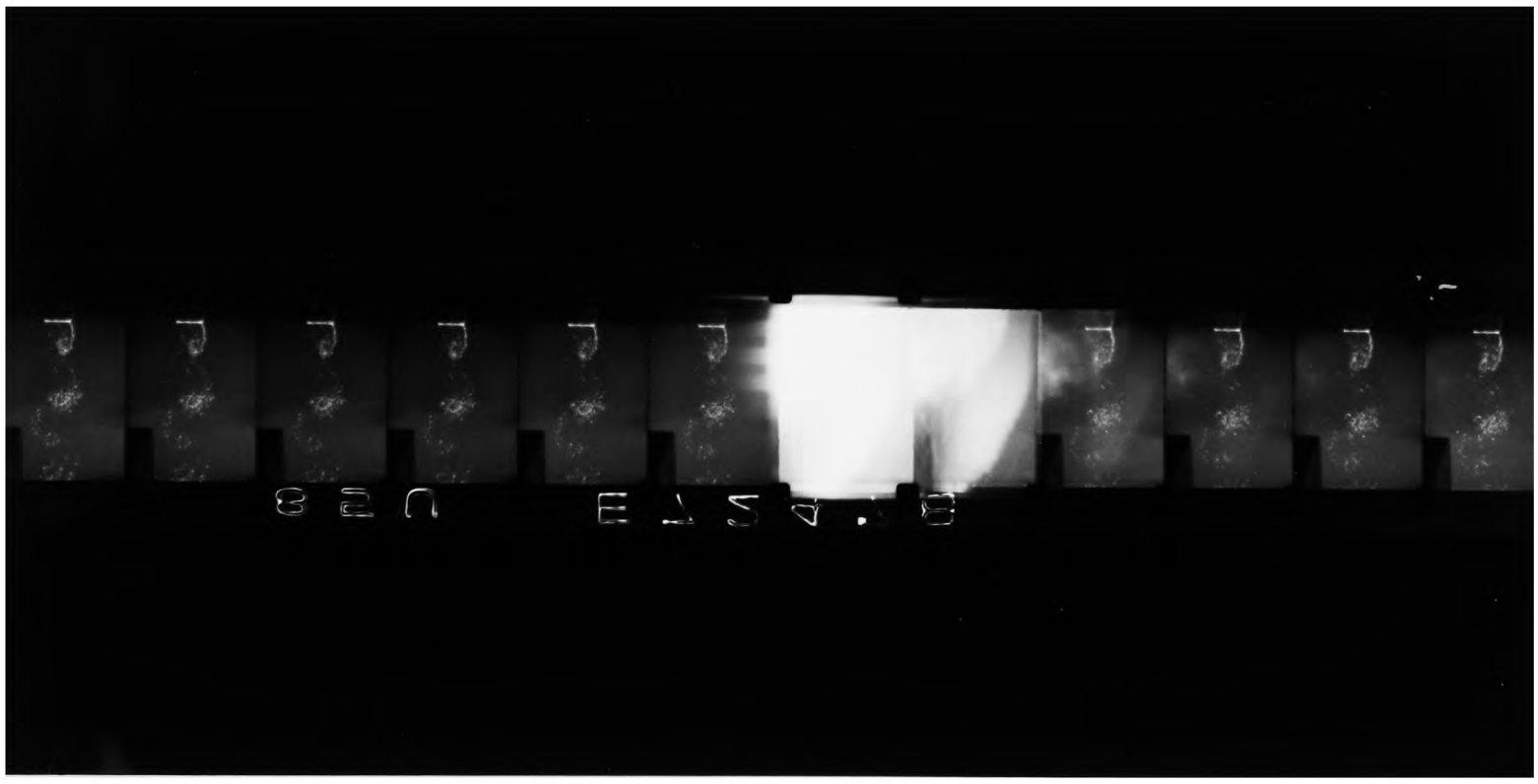


Fig. 4:4 Imprint of the Timing Signal on the Cine Film.

Correlation of Time and the Cine Film Records

The correlation between particle counts and the time of the events was established by regarding the time interval between the frames as constant, although necessarily different

for different framing rates. This required a calibration of the framing rates.

A crude assurance of repeatability was obtained by using the camera only with a fully wound spring motor. The duration of the filming sequences varied, however, in length, with the consequent possibility of errors being introduced in the latter part of the film due to spring motor rundown.

The true framing rate was established and calibrated by cine filming a 100 cm engraved ruler while moving the trolley at the velocity used in all experimental work. The camera settings and exposures were fixed at the settings used throughout the work. Since the trolley speed already was established, the true framing rates could conveniently be deduced from the photographic record.

The framing rates were found constant when using the spring motor from fully to 75% wound. This was adequate throughout the experimental runs, since the demands never exceeded 10-15% of the motor capacity.

The calibration of the framing rate and all subsequent cine film analysis was carried out with the aid of a "SPECTO" Motion Analyzer.

This device is in principle a simple cine film projector in which the film can be stopped, started and reversed at will at several projection speeds. What is even more useful, any single frame can be projected almost indefinitely without damaging the film or emulsion by overheating. This feature of long exposure and a positively engaged frame counter allowed precise correlation between time and any event occurring in the wake while under observation.

CHAPTER V

EXPERIMENTAL PROCEDURES AND RESULTS

The Equations for the Interpretation of the Data

Using the equipment and the flow visualization techniques described in the previous chapter, it is now possible to estimate the magnitude of each term in the relationships for the circulation balance Eq. 3.12 and verify the solution of the expression for the particle balance in the dead fluid region Eq. 3.15, by experimental means.

These relationships were presented in Chapter 3 in the form

$$\Gamma_o = \Gamma_c + \Gamma \left| 1 + \frac{2}{\frac{N_1}{N_u} - 1} \right| \qquad 3.12$$

and

$$\frac{d\bar{\bar{N}}_c}{dt} = \frac{N_c}{\tau} - H\bar{\bar{N}}_c. \qquad 3.15$$

CHAPTER V, SECTION 1

Solution of the Circulation Balance

The terms required for obtaining a solution for Eq. 3.12 will be considered first:

Γ_o was defined to be the total circulation which is shed from the point of separation per cycle. It was also shown that the rate at which circulation is shed can be estimated by use of the expression in Eq. 3.13.

Hence

$$\Gamma_o = \frac{(U_1^2 - U_2^2)}{2} \times (\tau) \qquad 5.1$$

where τ is the period of the cycle and

U_1 is the velocity of the flow in the mainstream just outside of the boundary layer, but level with the point of separation as shown in Fig. 5:1.

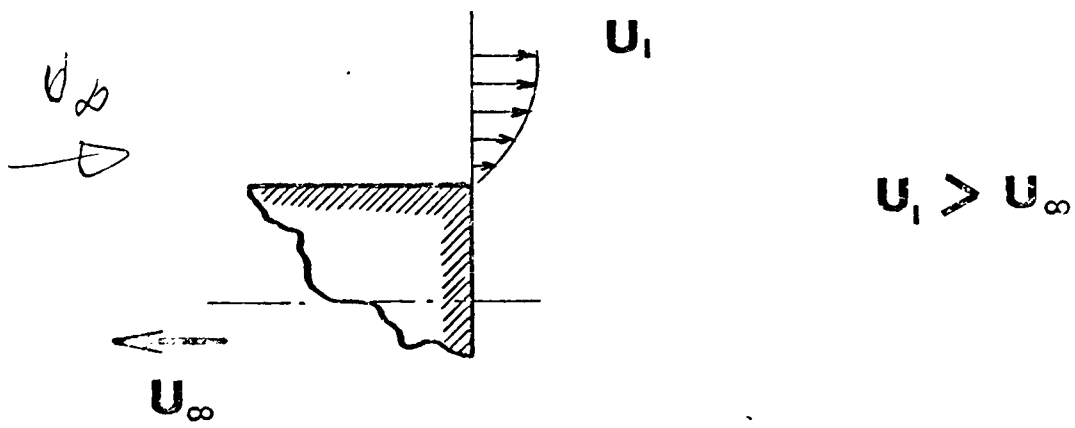


Fig. 5:1 Concept of Outer Shear Layer Velocity

At this point U_1 is nil and therefore

$$\Gamma_o = \frac{\overline{U_1^2}}{2} \times \tau \qquad 5.2$$

Photographs of the wake as shown below in Fig. 5:2 formed in a suspended cloud of particles were used to determine the magnitude of U_1.

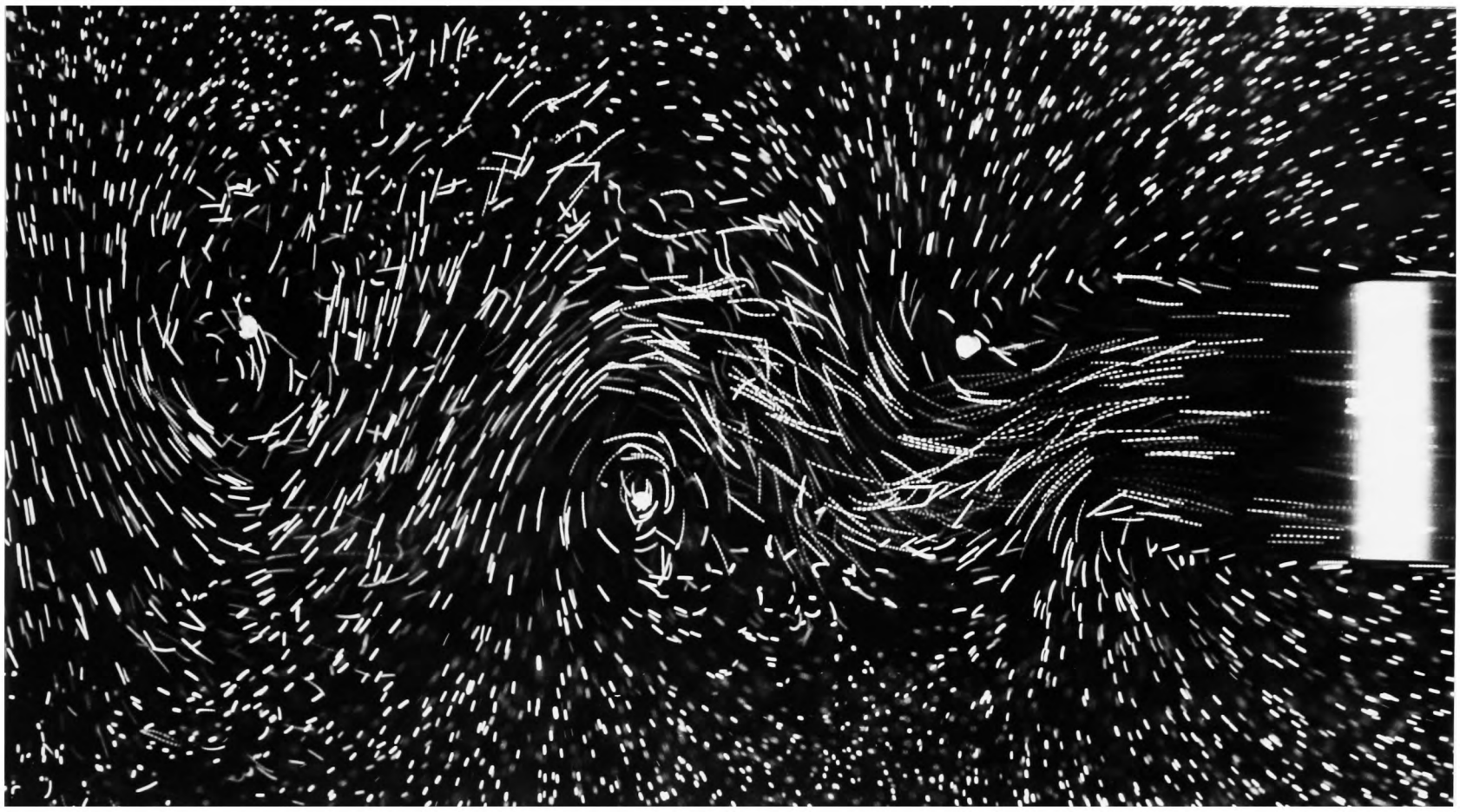


Fig. 5:2 Wake Photograph as used for the Determination of $\bar{U}_1$

Particle streaks on approximately forty wake photographs were measured on the travelling microscope and yielded a ratio between the mean outer wake velocity $\bar{U}_1$ and the free stream velocity U_∞ of:

$$\frac{\bar{U}_1}{U_\infty} = 1.139 \bar{\sim} 1.14,$$

When comparing this value with data established by other investigators for models of similar configurations under similar conditions the following relationships exist.

Investigator and model type	Chord Width / Base Width	U_1/U_∞	Remarks Concerning the Model Shape
Fage & Johansen 1927 Model A	3.18	1.15	Pointed Nose Ogival Front
Fage & Johansen 1927 Model B	9.15	1.16	Pointed Nose Ogival Front
Nielsen 1969	4.50	1.14	Round Nose Elliptical Front

Due to the good agreement the established value of $\bar{U}_1$ can be used with confidence. By substitution of U_1 into Eq. 5.2, Γ_o can be deduced by calculation of

$$\tau_o = \frac{(1.14 \cdot U_\infty)^2 \times \tau}{2} \qquad 5.3$$

The second term in Eq. 3.12 to be evaluated is the magnitude of the vortex strength Γ remaining in the fully formed vortices after they have just separated from the feeding sheet and started to move downstream in the wake.

The magnitude of Γ was determined by measurements of the particle streaks in the vortices outlined on the flow photographs of the same type as shown in Fig. 5:2. The streaks were measured on the travelling microscope described (page 11) in Chapter 2. This instrument incorporates observing, measuring and recording devices by which x, y and θ coordinate measurements can be taken on the flow photographs.

The photograph of the vortex to be measured is placed upon the turntable with the vortex centre coinciding with the turntable axis. The radius of the measuring circle is held constant (y) which establishes one of the three necessary coordinate measurements shown in Fig. 5:3. The tangential

streak length is measured along the second coordinate axis (x), while the angular displacement (θ) is measured by the changes in position of the turntable.

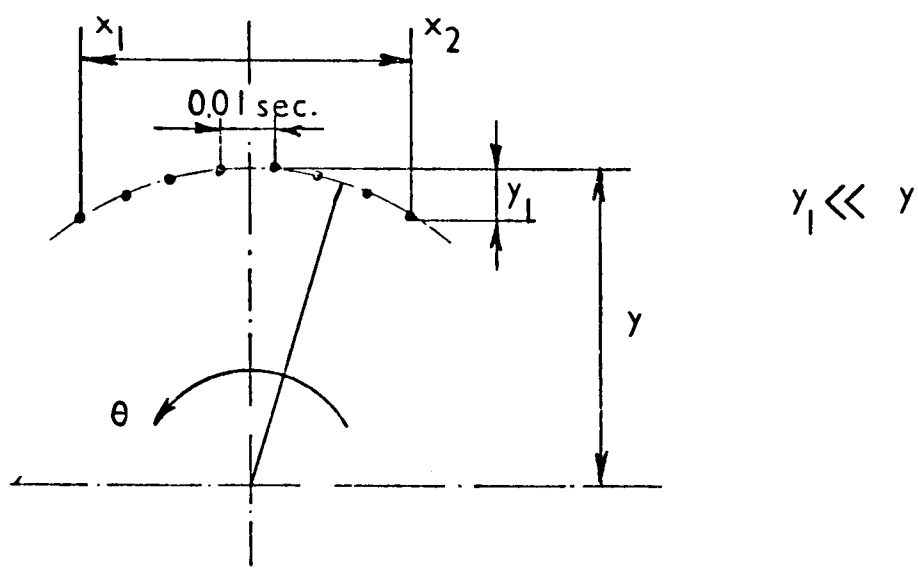


Fig. 5:3 Coordinates Measured on Flow Photographs by Use of the Travelling Microscope

The results from measurements of Γ on approximately forty photographs of wakes produced under identical circumstances are shown in Fig. 5:4. For convenience in all subsequent computations the data in Fig. 5:4 are presented in non-dimensional terms in the form $\Gamma/U_\infty.h$.

The Total Loss of Circulation in the Formation Region

On the basis of the information contained in Fig. 5:4, the vorticity loss in the formation region can now be estimated, because in Eq. 5.3 it was shown that:

$$\Gamma_o = \frac{\bar{U}_1^2 \times \tau}{2} \qquad 5.3$$

When this expression is non-dimensionalized using the same terms U_∞ and h as used earlier for the evaluation of Γ, then

$$\frac{\Gamma_o}{U_\infty x h} = 2.047.$$

By inspection of Fig. 5:4, the maximum value of

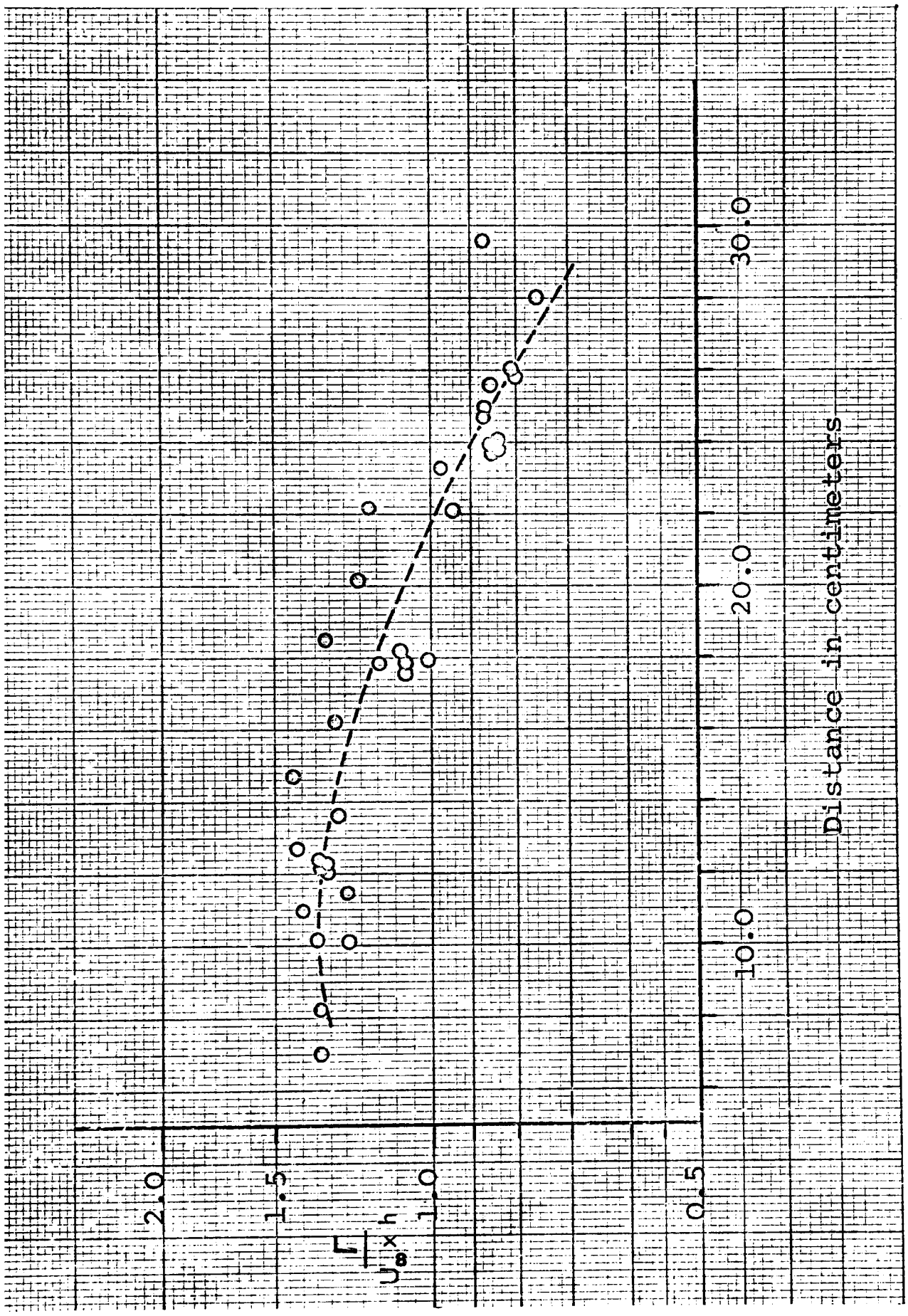


Fig. 5:4 Strength of the Fully Formed Vortices (in Non-dimensional Terms) as a Function of Distance Downstream of the Bluff Base.

$$\frac{\Gamma}{U_\infty xh} \cong 1.35$$

The loss of circulation in the formation region is therefore equal to:

$$1 - \frac{1.35}{2.097} = 0.34 \qquad 5.4$$

When the just established value of the loss of circulation is compared with the value established by Wood (1967) for an identical experimental situation, it is found to be approximately 5% smaller.

Several reasons can be given for this discrepancy. One of these may be the improvement in the accuracy of the measurements which was achieved by discriminating severely between acceptable and non-acceptable particle streaks when seen in the travelling microscope. When these particle streaks were measured, only those streaks were chosen on which it could be clearly observed that the centres of the cross hairs passed over and not by the particle images as shown in Fig. 5:5, thus holding the dimensional error in the y-coordinate measurement below 2% when based upon a mean particle diameter of 0.4 mm and a radius of 10 mm.

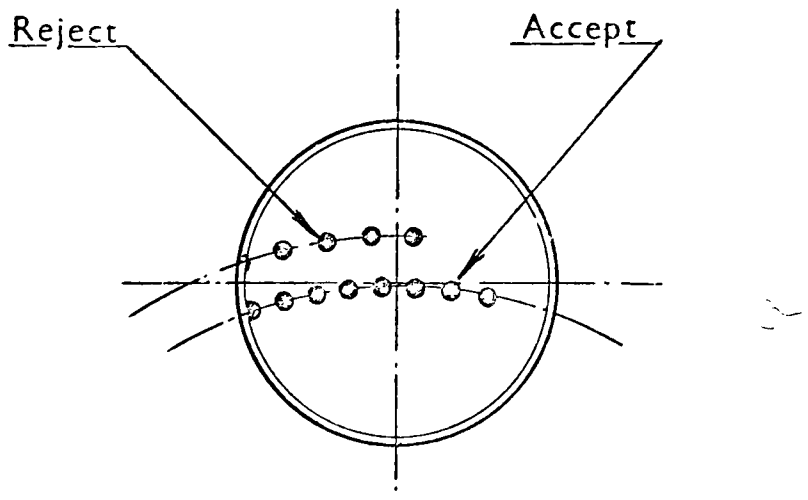


Fig. 5:5 Discrimination Criteria for Particle Streaks as they are seen in the Microscope Eyepiece

For the reasons stated (see page 109) in Part III it was

found beneficial to allow the turbulence to subside in the towing tank for as long as 24 hours between each experimental run. The appearance of the vortices was improved by the longer settling period as well as tighter grouping of the data points was had when the measured vortex strengths were plotted.

In addition to the good agreement with Wood's data, the magnitude of the loss established here compares well with the data obtained by other authors. Fage and Johansen (1927) suggested on the basis of their early work a loss approaching 50%, while Eskinazi (1969) suggests a loss in the vicinity of 33% which is closely approximated by the author's result.

The magnitude of the loss was established by comparison of Γ and Γ_o which also are terms in Eq. 3.12. Knowing their magnitude, it only remains to deduce the value of N_1/N_u in order to complete the solution of 3.12.

This term was defined to be the ratio between the numbers of particles located in the fully formed vortices at their peak strength positions in the wake.

The numerical value of N_1/N_u was established by a simple marking and counting process using the cine film records of the particle distribution in the wake. This method caused very few difficulties since the contrast was very marked between the particle images and the background in the photographs of the wake as illustrated in Fig. 5:6.

The cine film photographs of the vortices containing the particles were projected onto a counting screen in the same scale relationship throughout the data retrieval work, thus assuring that the particles were all counted in the same region of the wake in all cases. This counting region was located



Fig. 5:6 Particles Recorded in the Wake at an Exposure Time of 0.003 Second.

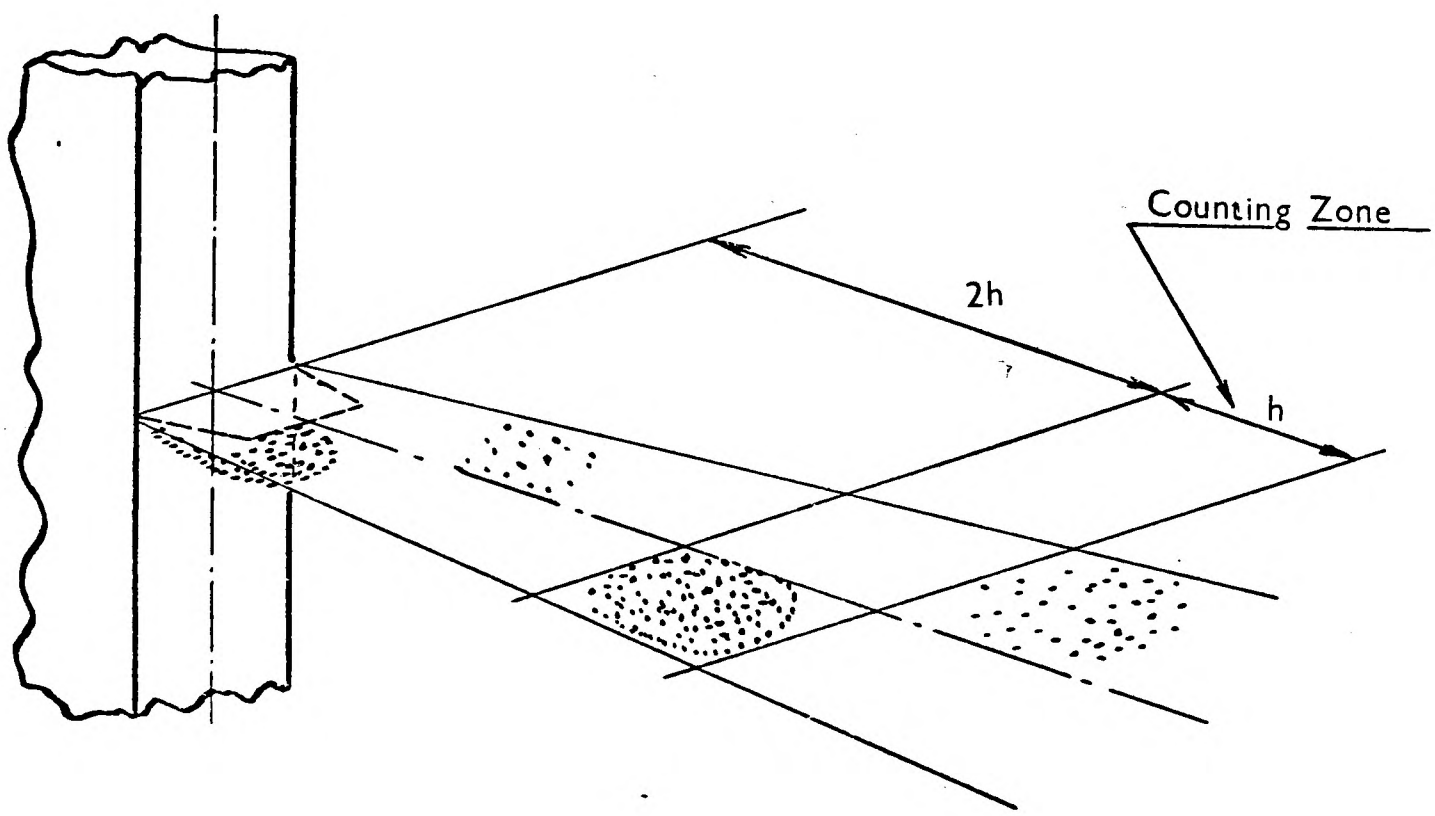


Fig. 5:7 The Location and Boundaries of the Region in which all N_l and N_u Counts were taken.

slightly more than 2 base heights behind the bluff base in the exact position shown in Fig. 5:7.

The exact dimensions of this region were determined in the general inquiry of the wake presented (see page 96) in Part III. For the reasons given there, it suffices here to say that the region shown in Fig. 5:7 is located slightly forward of the region in which the vortex strength was shown to be at its peak, and furthermore the upstream boundary of the counting region coincides with the point at which the sheet feeding the vortex invariably showed the first sign of breaking up thus stopping the growth process.

The exact cine film frame from which the individual particle counts were to be taken was determined by stopping the advancing film when the downstream boundary of the vortex clouds arrived at the downstream boundary of the counting region.

This arrival could be determined within one frame or 0.02 sec accuracy, because the demarcation between the particle cloud and the irrotational fluid on the downstream side was without exception very clear and sharp. The upstream boundary of the cloud was frequently not quite as well defined, but distinguishable in every case. The particles remained generally in close, tight confinement within the vortex clouds after the rolling-up process had ceased and the cloud was proceeding downstream in the wake. This was the case for both the upper row of the vortex clouds from which N_u was deduced and the lower row where the N_l counts were taken.

The actual counting process was accomplished by marking the position of each particle image inside the counting region on an overlay over the counting screen, and using a separate overlay for each new particle cloud count, noting the frame

number and other pertinent data for later counting of the dots.

The possibility of biased judging was eliminated by marking and counting the vortices in the upper and lower row separately and matching the pairs later to calculate the N_l/N_u ratios. To minimize a possible source of error due to particle images overlapping and thus not being included in the counts, random but frequent additional counts were made of the adjacent frames on either side of the initial counting frame. Slight variations never exceeding 2% were at times encountered; but the bulk of the counts either before or after did not differ from the reference frame count, indicating that the ejection and distribution processes are relatively steady and uniform in behaviour.

Approximately 200 particle cloud pairs were evaluated by these methods and yielded the data which are presented in Fig. 5:8.

This histogram shows the full range covered by the counts and that the most predominant value is:

$$N_l/N_u = 5.3 \qquad 5.5$$

Completion of Solution of the Circulation Balance for Γ_c

Since N_l/N_u is now known, adequate information is available to complete the solution which will give a quantitative value of Γ_c, because when the values of Γ and Γ_o (both in the non-dimensional terms) are substituted into Eq. 3.12 they yield

$$\frac{\Gamma_c}{U_\infty h} = 2.047 - 1.35\left[1 - \frac{2}{N_l/N_u - 1}\right]$$

To show the significance in the solution of N_l/N_u it is

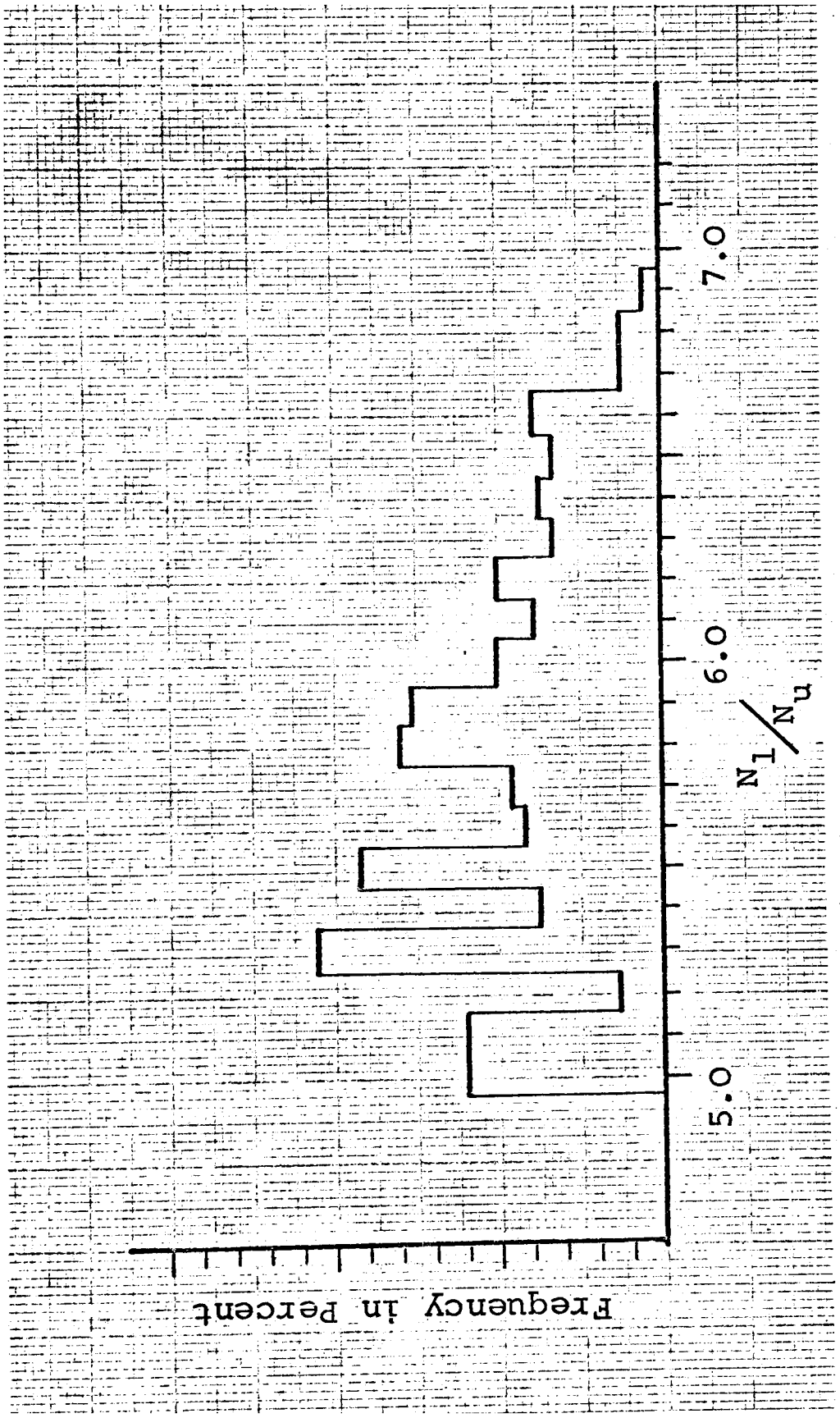


Fig. 5:8 Normalized Frequency Distribution of the Span of Ratios of N_1/N_u.

convenient to plot:

$$\frac{\Gamma_c}{\Gamma_o} \text{ versus } {}^{N_1}/_{N_u}$$

in the form shown in Fig. 5:9.

It is evident by inspection that the aforementioned most predominant value of ${}^{N_1}/_{N_u} = 5.3$ corresponds to

$$\frac{\Gamma_c}{\Gamma_o} \doteq 0.04$$

or in other words approximately 4% of the total shed circulation Γ_o enters the dead fluid region as Γ_c.

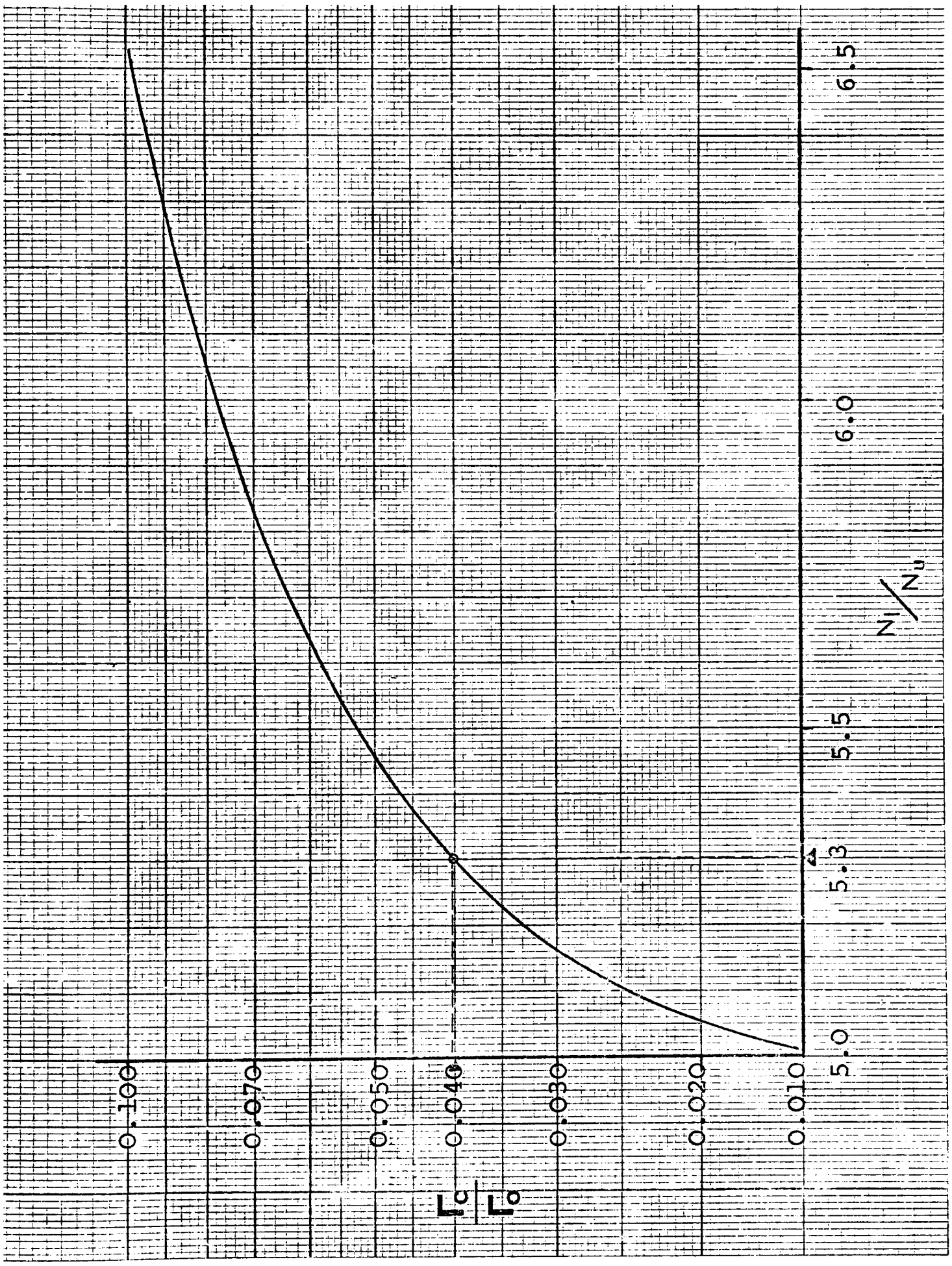


Fig. 5:9 r_c/r_o as a Function of the Ratio N_l/N_u Over the Span Exhibited by N_l/N_u in the Solution of Eq. 3.12.

CHAPTER V, SECTION 2

Verification of the Value of Γ_c by the Particle Accumulation Balance

It now remains to verify the just deduced value of the circulation lost in the dead fluid region Γ_c and the theoretical solution for Eq. 3.15, by taking instantaneous particle counts in the dead fluid region as explained in the last section of Chapter 3 (page 24).

The parameter about which knowledge is required is N_c which was defined as the total number of particles entering the dead fluid region during one cycle. The magnitude of N_c cannot however be measured directly, but will be deduced from the rate of increase of $\bar{N}_c$ which was defined as the total number of particles present in the dead fluid region at any time.

$\bar{N}_c$ is time dependant in the sense that its value depends on the length of the ejection sequence from start until N_c is counted. The ejection could not however be filmed in its entire length since the tank could only be illuminated in a 0.5 metre wide bay. This limitation was overcome by the use of the fibre optics timing system. This system provided a positive signal on one cine film frame at the same instant when a stop-watch recording the duration of the ejection sequence was stopped.

Knowing the framing rate of the cine camera, it became a simple matter to determine the exact "age" of any arbitrary cine film frame. This facility allowed that counts could be taken at any pre-selected intervals or at arbitrary times of the accumulation of particles $\bar{N}_c$ in the dead fluid region. These counts were made on the same cine film records of the wake and projected in the same manner with the same equipment as used

to determine the N_{1/N_u} data.

The dimensions and boundaries of the region in which the particles were to be counted had been established during the general wake investigation presented (see page 104, Fig. 9:2) in Part III of the thesis. For convenience Fig. 9:2 is repeated below.

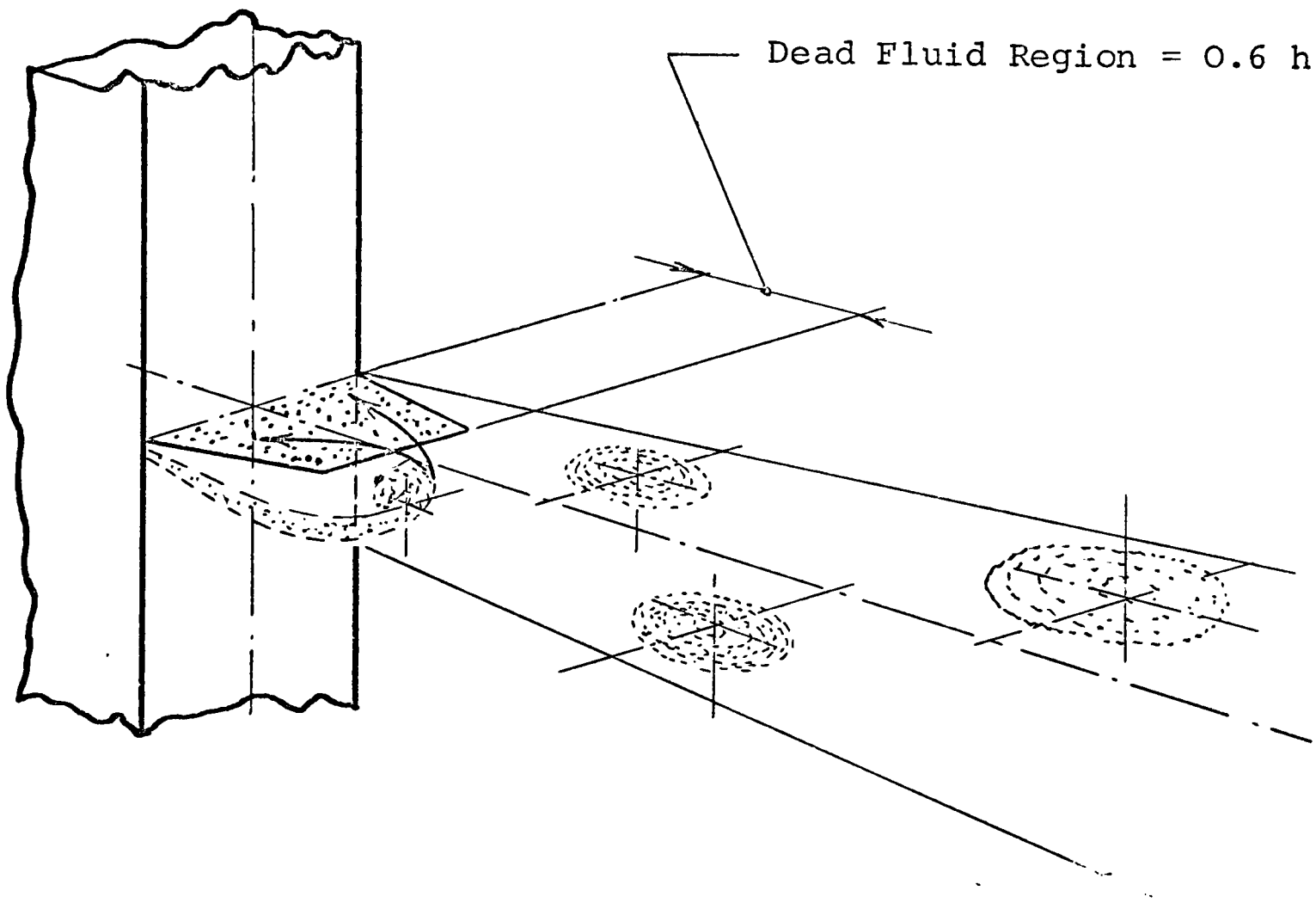


Fig. 9:2 The Dead Fluid Region.

The streamwise length of this region was determined from observations of particle behaviour during the shedding cycle.

The particle movement processes into this region are discussed in detail in Part III. It suffices here to emphasize that none of the particles, which pass across and become counted within the boundaries shown in Fig. 9:2, ever appear again in any other part of the wake. They only sink slowly out of sight along the span of the model while at all times remaining within the boundaries of the dead fluid region.

The possibility must be considered that the restraint on

the streamwise length of the dead fluid region is too severe at 0.6 h. The effect would be indicated as too weak a gradient in the accumulation process during each cycle due to a lower early count. This is preferable however to the alternative choice since if the length was chosen to be excessive, errors may be introduced by counting particles twice - once as $\bar{N}_c$ and later as N_l or N_u, as the particles initially in the formation region may end up in either of the two downstream vortex rows.

On the basis of these considerations, those presented in Chapter 3 and the general wake investigation presented in Part III, the region in which the particles were to be counted was chosen to be as shown in Fig. 9:2 and held constant throughout all $\bar{N}_c$ counting processes.

When the cine films were projected onto the counting screen the scale relationship was held at 3.5 times the true size. The exact outline of the dead fluid region was superimposed upon the screen image of the wake to make the marking of the particles within the boundaries more convenient.

The marking and subsequent counts were made at intervals of five cine film frames, which corresponds to approximately 0.1 sec separation between the counts. With a cycle of $\tau = 1.47$ sec this rate of counting yielded 15 sets of data for each vortex shedding cycle. This rate proved adequate to show the desired details of the particle accumulation. These data were plotted in the form shown in Fig. 5:10 to show the relationship between the elapsed time and the particle accumulation in the dead fluid region.

The data provided in Fig. 5:10 are those which were required in the last section of Chapter 3 to confirm the solution of Eq. 3.15 and thus establish the correct value of:

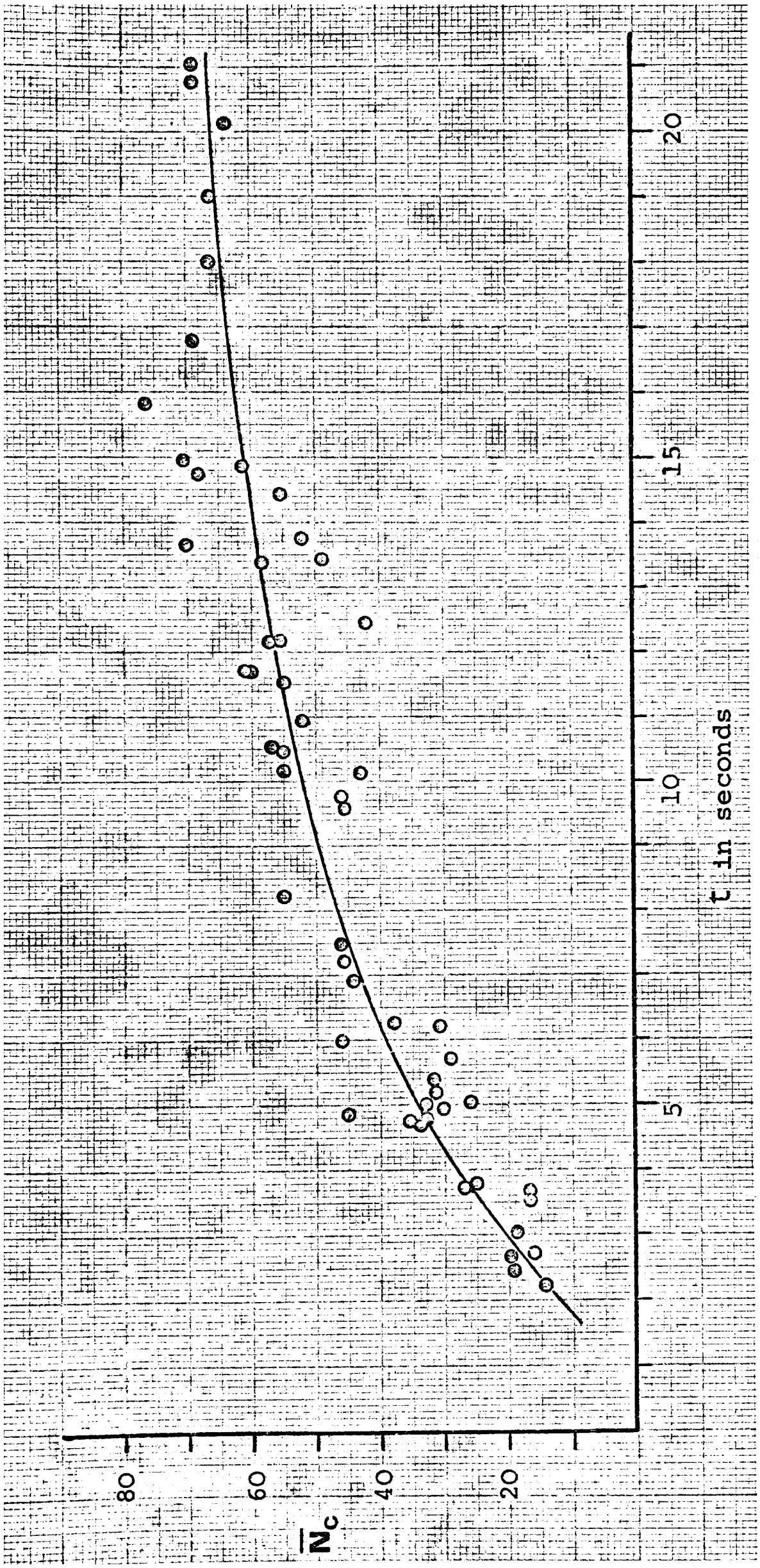


Fig. 5:10 Particle Counts $\bar{N}_c$ as a Function of Elapsed Ejection Time.

$$\alpha = \frac{N_c}{N_o}$$

By superimposing the mean value curve of the data given in Fig. 5:10 upon the solution set of Eq. 3.15 for α, it is shown in Fig. 5:11 that the correct value of α lies between

$$0.036 < \alpha < 0.043 \qquad 5.7$$

Recalling that the exact mode in which circulation bearing fluid is propelled into the quiescent dead fluid region is not known, there is good agreement between the experimental results and those deduced by solving Eq. 3.15.

This is particularly so, if cognition is taken of the fact that the theoretical development implies that the input of circulation represented by the particles starts immediately at the beginning of the cycle and remains constant throughout the cycle.

It was shown (page 103) in the general investigation of the wake that this is not quite so. There is a small but discernible interval between the time at which the shear layer begins to roll up into a vortex and the time at which fluid from this shear layer penetrates into the dead fluid region carrying that proportion of the circulation which ultimately will be cancelled there. It is also implied in the theoretical arguments that the particle distribution is instantaneously uniform throughout the dead fluid region. The first of these demands is of course not met and the second only after a cycle or two after the particle ejection process is initiated. Although the injection of fluid into the dead fluid region and the subsequent distribution occur very rapidly they do take a finite amount of time. The theoretical predictions for the initial one or two cycles do therefore not quite depict the truth, and under these circumstances the agreement between the

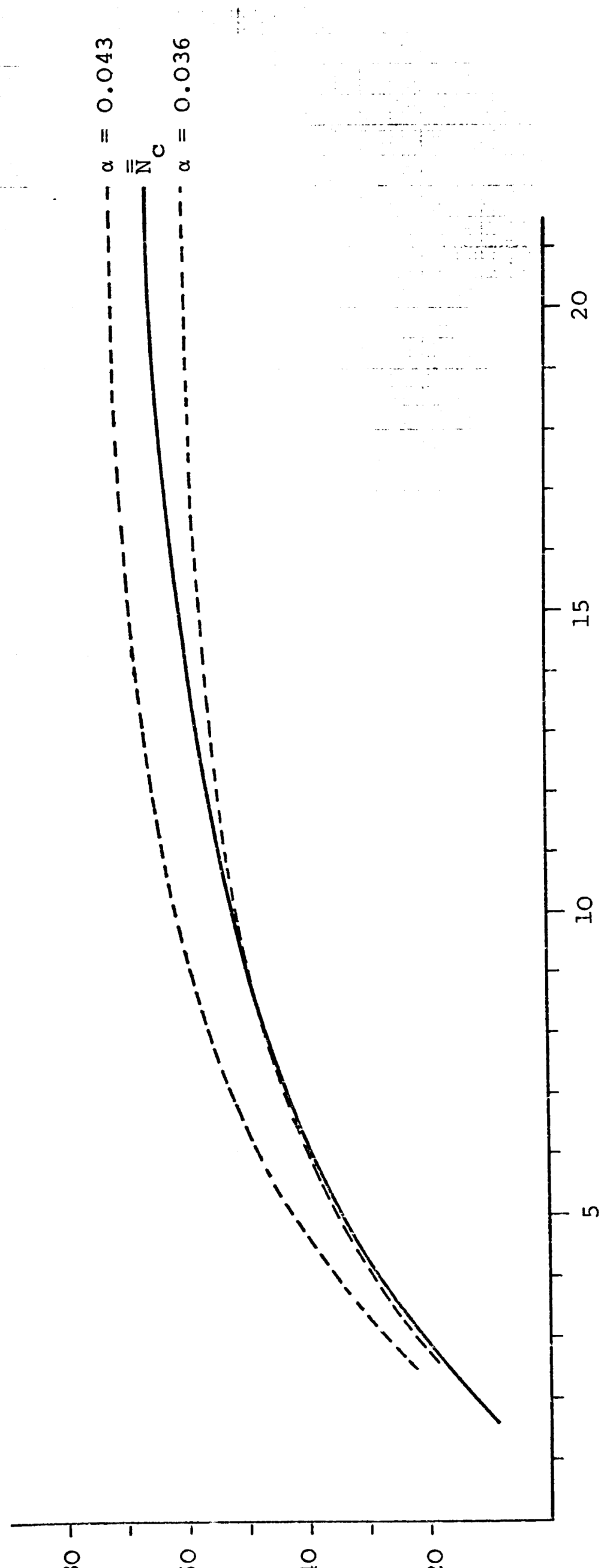


Fig. 5:11 The Mean Value Curve of the Experimental Counts $\bar{\bar{N}}_c$ (Fig. 5:10) Superimposed Upon the Solution of Eq. 3.15.

theoretical and the experimental results for α is good.

This value for α can now be compared with the value for Γ_c/Γ_o which was determined by the solution of Eq. 3.12 performed in the first section of this chapter. This solution gave a value of

$$\frac{\Gamma_c}{\Gamma_o} = 0.04 \qquad 5.6$$

We have just shown that

$$\frac{N_c}{N_o} \cong 0.04 \qquad 5.7$$

These two results were determined completely independently and the significance of these data can be understood by recalling from Eq. 3.8 and Eq. 3.10 that

$$\frac{N_c}{N_o} = \frac{\Gamma_c}{\Gamma_o}.$$

There is thus a very good agreement between the quantitative results obtained by the two different methods. It may therefore be stated that the proportion of circulation, which is carried into the dead fluid region once during each cycle as Γ_c, amounts to 4% of the total shed circulation Γ_o.

If furthermore the established values for Γ and Γ_o are used to estimate the distribution of circulation downstream of the dead fluid region the following result is had:

From

$$\Gamma_o - \Gamma - \Gamma_c - 2\Gamma_{ab} = o \qquad 3.4$$

and by substitution of the derived values of Γ and Γ_c

$$2\Gamma_{ab} = 1 - 0.66 - 0.04 \cong 0.3$$

$$\Gamma_{ab} \cong 0.15 \qquad 5.8$$

Thus the proposition of circulation transported across the wake as Γ_{ab} amounts to 15% of the total available circulation

Γ_o. Of course, a further loss is also caused by the arrival in the sheet of an equal amount $-\Gamma_{ab}$, but of opposite rotation as indicated by the sign.

With these results at hand, the thesis problem has been solved, because it was intended to provide a quantitative estimate of the distribution of circulation in the periodic wake according to the model suggested by Gerrard.

The soundness of his model is verified not only in quantitative terms by the solutions presented above; but also by the visual evidence showing that the circulation did only move to and become distributed in the three major regions proposed in the model.

CHAPTER VI

SUMMARY AND CONCLUSIONS

The Experimental Results

The results of this study indicate that the explanation of the mechanism responsible for the vorticity distribution and loss in the formation region, is substantially correct in the form given by Gerrard in 1966.

The clarity, with which the paths of the fluid are shown to carry the particles and thus the elements of circulation into the three major regions of the wake, serves well to reinforce the Gerrard concept in general.

In his model it is suggested that the fluid which carries circulation across the wake does travel along two paths - one which leads into the nascent vortex on the opposite side and one leading to the shear layer just ahead of the vortex. This small point could not be substantiated by either observation or measurement with the methods employed here.

Not only has it been shown that the ciculation was transported only in the three major regions in the formation region, respectively denoted by the nascent vortices in the two rows and the dead fluid region, but it was also possible to formulate the analytical expressions from which the quantitative data were computed, virtually without modification of the basic concepts.

Computation of the quantities revealed that only 66% of the circulation shed at either point of separation during each cycle survived the passage through the formation region to form the characteristic vortices in the periodic wake. If we consider one side of the wake only, the total loss during the cycle was shown to be composed of three losses which occur sequentially during the vortex formation process by quantities of circulation becoming annihilated in each of the three major

wake regions mentioned above. The loss in the dead fluid region was determined to be 4% of the total loss, while 15% is lost by transfer to and subsequent annihilation in the opposite shear layer. A further reduction is caused by the arrival one half cycle later of an equal quantity of circulation having opposite rotation and thus by annihilation causing also a 15% loss in the circulation available for subsequent vortex formation.

At this point it should be noted, that these exact values of the quantities of distributed circulation do of course only hold for this particular experimental situation; although the author sees no reason why they should not be near to those which would be attained in similar systems, because there is reasonable agreement as to the approximate value of the overall loss.

In this application the total loss is 34% which by comparison with the values given by other investigators (50% by Fage and Johansen 1927; 50% by Roshko 1955; 40% by Wood 1967 and 33% by Eskinazi 1967) is close to the recent and somewhat lower than the earlier given data.

This reduction in the loss is attributed to the very low level of ambient turbulence which was maintained in all experimental work. Because it was shown how devastating the effects of high levels of ambient turbulence could be upon orderly wake formation, very great care was taken to eliminate all possible sources.

The effects of ambient turbulence manifested themselves in particular by causing non-systematic variations in the length of the formation region and in general by the overall untidy appearance of the wake; whereas in absence of turbulence the wake formation was clear, repeatable and orderly in all aspects.

As well as it could be ascertained, the wavelength of the wake system remained the same irrespective of the level of induced, ambient turbulence.

The method of tracing the elements of circulation by following the motion of small particles is new and untried. It was however treated exhaustively, until it was shown that without fail the particles remained with the elements of circulation wherever they moved in the wake. In this context it was also shown that the particles were not expelled by the presence of circulation in the fluid also harbouring the particles.

A laser doppler velocity sensor was employed at one stage of the work. By virtue of its capability to measure velocities independently of the presence of particles, it was used to measure flow velocities in regions where particles were temporarily or permanently absent.

On Future Work

The results of this investigation warrants some suggestions concerning the direction of future work, both with respect to further research on the periodic wake and continuation of the development of the experimental technique employed during the course of this investigation.

The experimental technique could immediately benefit from a better knowledge of the exact particle size and the application of an illumination system which allows use being made of the very favourable forward light scattering properties of the particles.

The cumbersome and time devouring data retrieval could be accelerated by recording the wake movement not on cine film, but on video tape which could be processed directly by projecting

it onto the screen of a flying spot scanner and letting this device establish the particle counts.

Furthermore certain aspects of the flow visualization technique could be combined with the capabilities of the optical velocity sensor technique to explore flow regimes which do not tolerate the presence of sensors and probes.

A natural step would be to apply these particle counting methods and the doppler technique to the periodic flow created by a cylinder. Certain problems would arise with respect to particle ejection since the separation points wander during the shedding cycle,but they are not insurmountable. It would be of the utmost interest to compare the data for a model with fixed separation points with data from a cylinder of corresponding dimensions.

PART II

PROPERTIES OF THE PARTICLES USED IN THE FLOW VISUALIZATION PROGRAM

PART II

CHAPTER VII

THE STATIC PROPERTIES OF THE PARTICLES

In Part I, Chapter 4 (page 36) volume measurements were used to determine the number of particles present at any time in the ejaculate head tank. No explanation was given at that stage of the method by which these numbers were calculated as this would have interfered with the continuity of the argument. The necessary discussion and analysis of these matters is therefore presented below as a separate chapter.

By virtue of their very small size (D < 0.5 mm), the total number of particles per unit bulk volume will vary considerably with even small changes in size.

It was therefore necessary to obtain detailed information about the mean particle size, the size distribution in arbitrary volumes and the accumulation behaviour of the particles when they were collected in bulk for volumetric measurements.

Determination of the Particle Size

The determination of and control over the particle size was established by sieving a 5-6 litre sample of particles in a mechanical shaker between mesh screens until approximately 500 cm^3 remained in the sieve between the 360μ and 190μ screens.

This 500 cm^3 sample was further separated into its size components by repeating a simple sedimentation process until a sample was had in which the size range remained within

$$D = 365\mu \pm 8\mu.$$

This procedure yielded 300 cm^3 which proved adequate for all the experimental work.

Numerical Count of Particles in Unit Bulk Volumes

It was intended to establish the particle ejection rate and the subsequent consumption from measurements of volumes of particles accumulated in bulk in measuring vessels. Therefore it was necessary to determine the numerical particle

density per unit volume.

Due to their spherical shape and the nature of their deposition in the measuring vessel, the accuracy with respect to the total number of particles per volume depends on the detailed knowledge of the stacking mode which the particles assume in the bulk columns.

When a large number of equally sized particles accumulate in layers by deposition in a sedimentary process, they assume some characteristic system or mode of stacking. If undisturbed during the deposition process, they may form a rather loose and disordered structure, whereas with assistance such as vibration it is feasible to cause the particles to arrange themselves into a repeatable, ordered lattice system, which closely approaches the maximum theoretical packing density.

Variations in lattice structures formed by assembled mono-sized spheres was studied by Graton and Fraser (1935). They employed a term denoted by "the co-ordination number" C_o, which they defined to be the number of particles that are in contact with one selected particle in a lattice system.

Two characteristic lattice structures will be discussed in detail here: one is the cubic lattice, the nature of which is easily understood; but seldom found in its perfect state; the other is the rhombohedral lattice which is the optimum mode, allowing the maximum number of spheres to be contained within unit bulk volume.

The appearance of these lattices is shown in Fig. 7:1:

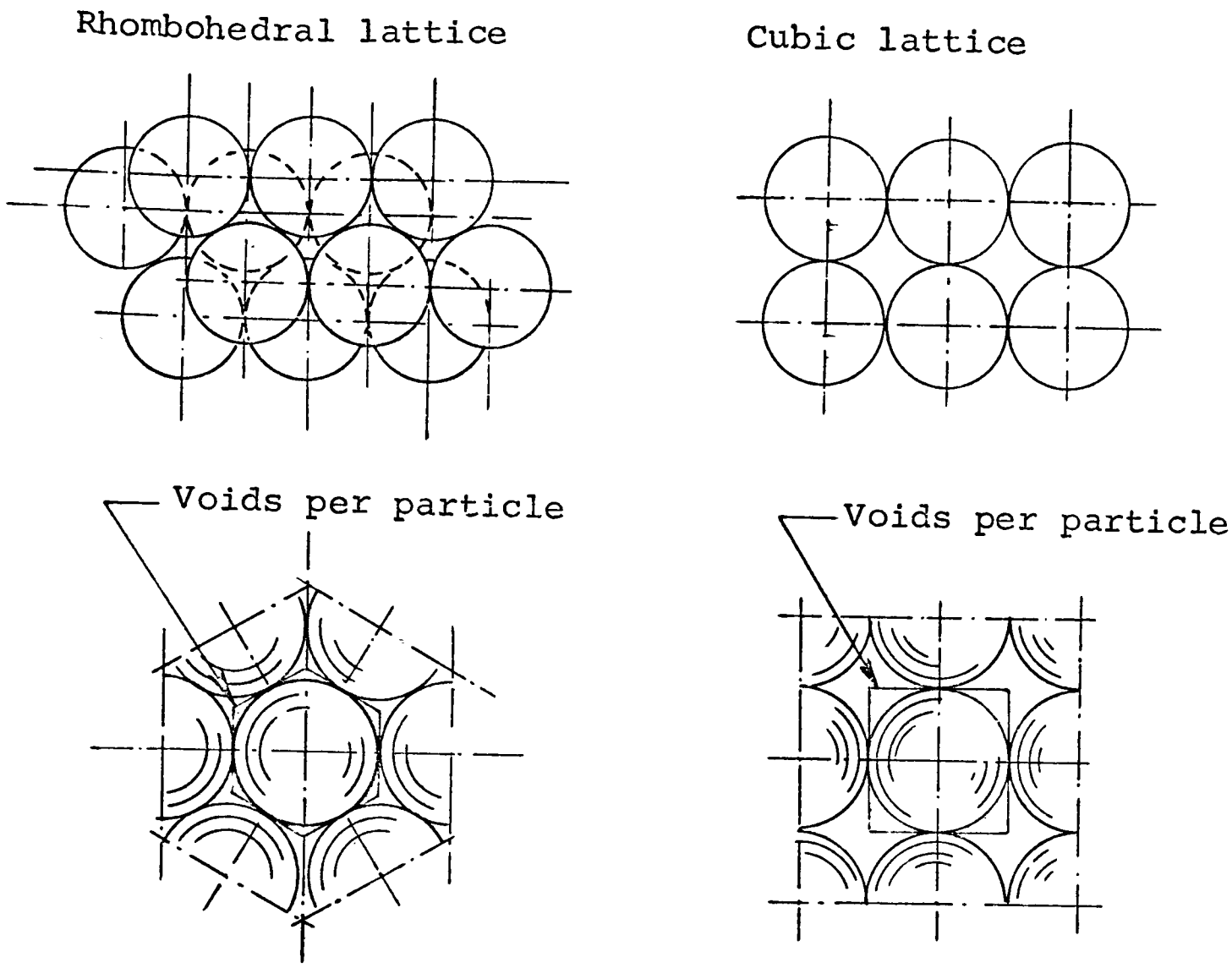


Fig. 7:1 The Characteristic Stacking Geometry of the Cubic and Rhombohedral Lattices

The co-ordination number C_o is equal to 6 for the cubic lattice and equal to 12 for the rhombohedral lattice.

It is also evident that each independent stacking mode is associated with only one characteristic geometry of the voids between the assembled spheres. Therefore it becomes convenient to differentiate between the virtual volume occupied by the solid particles and the exterior volume controlled by the configuration of the stacking lattice assumed by the particles. The efficiency of any stacking mode can be expressed by use of the non-dimensional void coefficient defined by:

$$\beta = 1 - \frac{V_{particle}}{V_{lattice}} \qquad 7.1$$

This parameter and the co-ordination number C_o are sufficient and necessary to describe any stacking lattice of

mono-sized spheres, and to determine the number of particles contained in bulk volumes displaying specific lattice structures.

In the case of the cubic lattice the significant volume which is shown in Fig. 7:2 is a prism whose dimensions are

$$D_x = D_y = D_z$$

and its significant volume is therefore

$$D_x \times D_y \times D_2 = D^3$$

hence

$$\beta_{C_o=6} = 1 - \frac{Vpart}{Vsignificant\ volume}$$

$$\beta_{C_o=6} = 1 - \frac{4/3\ \pi(D/2)^2}{D^3} = 0.476$$

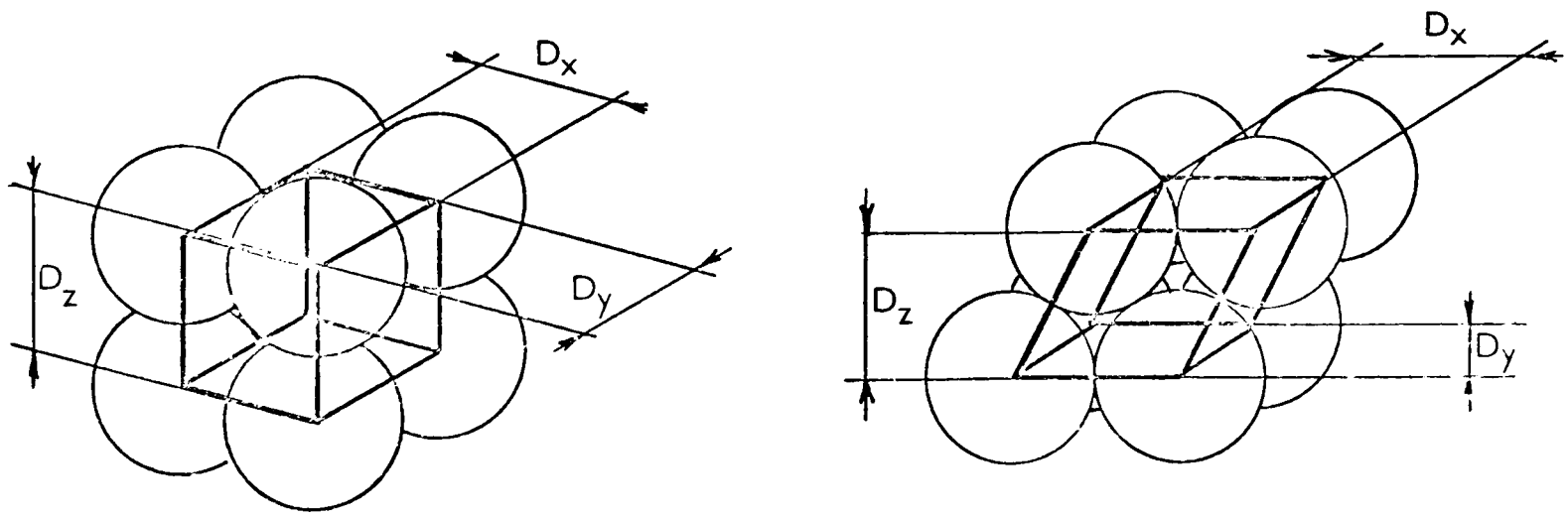


Fig. 7:2 The Significant Volumes of Cubic and Rhombohedral Stacking Lattices

In the case of the rhombohedral lattice the voids have been considerably reduced by rotating the significant directions in the lattice and changing the shape of the significant volume from a cube to a parallel sided prism as

shown in Fig. 7:2.

The volume of this prism is therefore

$$D_{x_2} \times D_{y_2} \times D_{z_2} = V_2$$

$$D_{x_2} = D_{x_1}$$

$$D_{y_2} = D_{y_1} \times \frac{3}{2} \sqrt{1/3}$$

$$D_{z_2} = D_z \times \sqrt{2/3}$$

Then $$V_2 = D_{x_1} \times D_{y_1} \times D_{z_1} \times \sqrt{1/3} \times \sqrt{2/3} \times 3/2 = D^3 \times 0.707$$

therefore, from Eq. 7.1

$$\beta_{C_o=12} = 1 - \frac{\text{Vparticles}}{V_2} = 0.26.$$

This represents the ideal stacking mode for mono-sized spheres - but it is unattainable unless each particle is placed individually in the system. When the particles are accumulated by normal sedimentation, the ideal stacking mode is never achieved. Furthermore, it is possible to obtain variations in β for the same co-ordination number C_o. For example if an event known as twinning occurs in the lattice, a decrease can be obtained for β from .476 to .396, while the sphere still is contacted only by six other spheres, thus not violating the definition of the co-ordination number C_o.

This anomaly was investigated by Bernal and Mason (1960) and Wadsworth (1961). They determined the probability distribution for haphazardly deposited mono-sized spheres which is shown in Fig. 7:3.

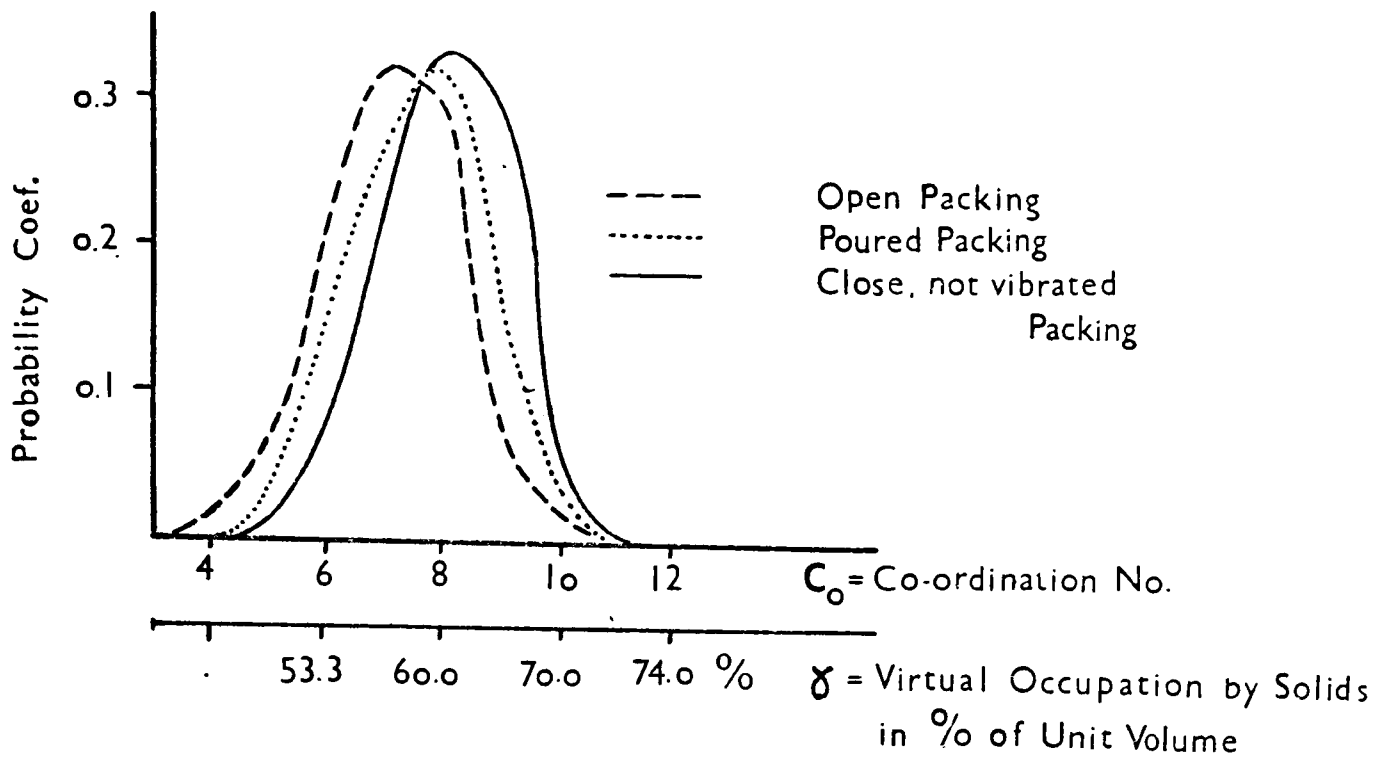


Fig. 7:3 Probability Distribution for the Co-ordination Number which is obtainable with a given Stacking Mode

This indicates the magnitude of C_o and the occupation coefficient which may be expected under the stated conditions for packing of mono-sized spheres. These data were however collected while using dry particles, while in this experimental application the column formed by the particles in the measuring vessel is saturated with water when being vibrated before measurements. The water acts as a lubricant between the particles and aids the growth of a systematically packed particle system.

Furthermore if the deposition of the particles is initiated on a horizontal plane there is a predominant trend towards the generation of a rhombohedral lattice structure. Although an equal amount of right and wrong cavities are exposed after the first layer of the bed has been deposited in a rhombohedral pattern, Graton and Fraser (1935) showed that the chance of spheres arriving and occupying the correct cavity was better than half, thus improving the probability of a higher co-ordination number being prevalent throughout the bed.

Such a bed cannot be expected to possess a large scale recognizable lattice pattern; but Levene and Chernik (1969) showed that if the macrostructure of such a bed is examined, the position of spheres in the vicinity of any single sphere indicate that ordered clusters prevail and can be repeatably observed throughout the bed structure.

It is assumed by the author that these favourable trends can be maintained in the experimental procedures, and furthermore that they will be augmented by mechanical vibration to aid the compaction. The effects of vibration are discussed by Gray (1959) who states that violent mechanical agitation, which temporarily can lift many of the spheres by a considerable fraction of their radius, will reduce the voids substantially in haphazardly packed regions. This improvement in packing which is contributed by mechanical assistance can amount by itself to a decrease in β up to 3% for materials having a coefficient of restitution similar to that of polystyrene.

Finally, it was shown by Westman and Hugill (1930), Scott (1960) and MacRae and Gray (1961) that, when mono- and near mono-sized spheres are haphazardly packed under non-varying conditions, the value for the void coefficient β is reliably repeatable to within 0.1%.

By summation of this evidence, we find that:

a: The probability of a high co-ordinate number is good even for non-systematic packing procedures (see Fig. 7:3).

b: The co-ordination number concept holds for mono-sized particle stacking systems.

c: Lubrication improves the stacking of particles.

d: There is a prevalent trend towards formation of rhombohedral clusters.

e: Although the macrostructure may be unordered, the particles tend to stack in ordered clusters.

f: Considerable improvement arises from vibration of the particle column during settling.

g: The value for β is repeatable within 0.01%.

Furthermore, it was also ascertained that polystyrene particles of the type used throughout this investigation accumulate in close, ordered systems, which exhibit a definite rhombohedral lattice structure as shown in Fig. 7:4.

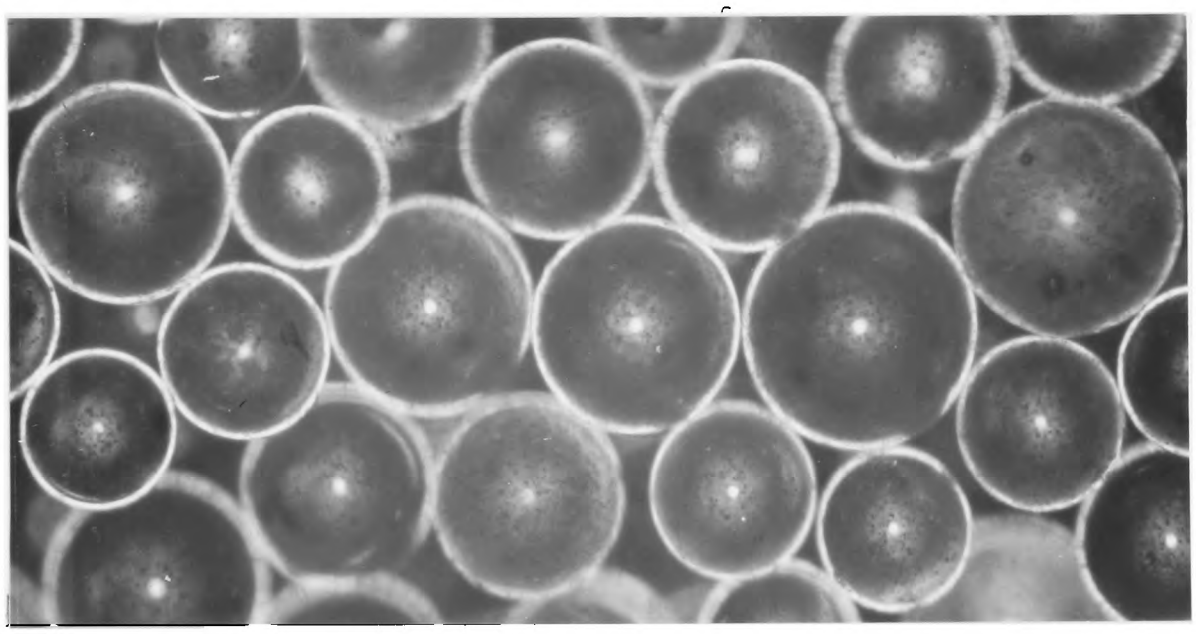


Fig. 7:4 The Experimentally Obtained Stacking Mode of Polystyrene Particles in a Lubricated, Vibrated Bed.

Most of the favourable trends listed in the summation of evidence were verified by the qualitative demonstration (in Fig. 7:4) of the existence of close, ordered stacking in the polystyrene particle bed. The number of particles, which are present in such a compacted bed measured by its bulk dimensions, can therefore be determined after having considered the reduction of the voids caused by the vibration and as well as the remaining trends in (a-g).

Referring to Fig. 7:3 the data given there for close, but not vibrated packing, which resemble the present experimental

application the closest, indicate an optimum value for C_o of 8 with a corresponding β of about 40%. In the present case it is considered that some improvement in β could be obtained by including an improvement of 2.5% to be contributed by the vibration technique alone, and a further 2.5% improvement from the combined effects of the remaining favourable trends a-g, and thus achieving a total reduction of 5% in the magnitude of β.

The final value of the void coefficient is therefore expected to be: β = 35%, so that the total volume occupied by particles and voids is equal to $^1/0.65$ = 1.571 times the actual volume of solid particle matter.

The validity of this approach is corroborated well, by comparison with the data presented in Fig. 7:5 which were obtained by actual counting of large spheres in systematic assemblies and relating their volume to that occupied by the bulk volume of the bed.

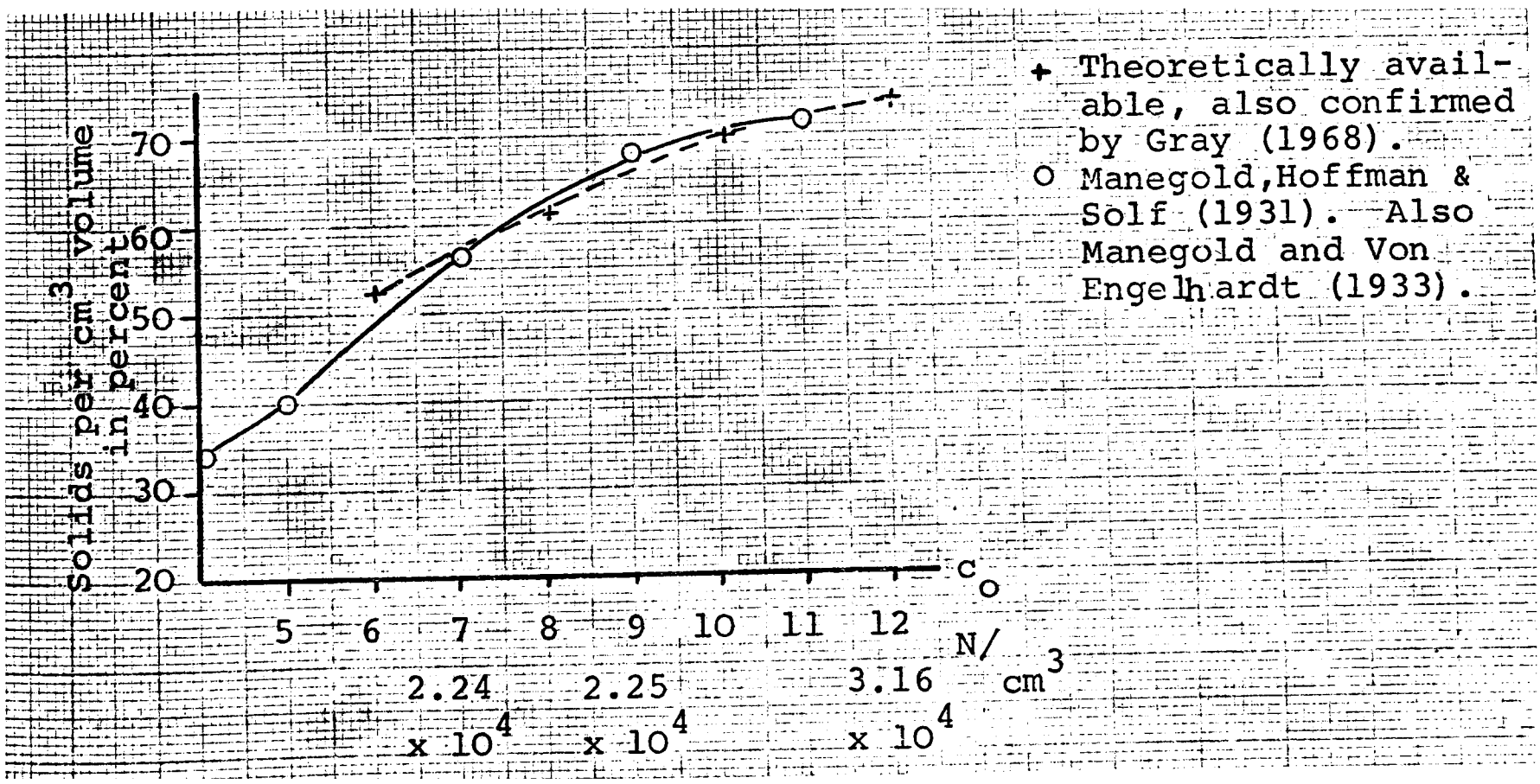


Fig. 7:5 Occupancy by Solid Matter in Percent of Unit Volume as a Function of C_o, for Mono-Sized Spheres in Systematic Assemblies

For the present particle diameter

$$D = 0.365 \text{ mm} \pm 0.008 \text{ mm}$$

and for

$$1 - \beta = 0.65$$

the total volume occupied by N particles will be in cm^3

$$\frac{4}{3}\pi(0.0365)^3 \times {}^{N}/_{0.65}$$

i.e. the number of particles per cm^3 bulk volume is

$${}^{N}/_{cm^3} = \underline{2.55 \times 10^4 \text{ particles}/cm^3}.$$

Due to the circumstances in the experimental work where considerable amounts of water was used to clean and flush the ejection mechanism for particles, and the very slight difference in specific gravity between the particles and water, it was not convenient to measure the particle numbers by weight. Therefore as mentioned earlier all determination of large numbers of particles was done by bulk volume measurements.

The Measurement of Bulk Volumes

The solution of particles and water, in which the number of particles were to be determined, was placed in a calibrated graduated cylinder and the height of the column formed by the stacked particles was measured within 0.01 mm by a depth micrometer using the ground top of the cylinder as a datum face.

In order that the maximum packing efficiency could be attained, the column was vibrated vigorously prior to each measurement until no further settlement could be detected with the micrometer within the limit of resolution: 0.01 mm.

Effects on the Solution Viscosity due to the Presence of Solid Particles

Although the ejaculate is a very weak solution of particles

and water, one further point of interest is the effect on fluid properties due to the pressure of the particles in the fluid. Solids suspended in a fluid cannot partake in any smooth deformation process which the fluid may undergo. This discontinuity in the deformation process manifests itself as an apparent increase in viscosity, as the presence of the solids makes itself known as an increased resistance to shear. This phenomenon was investigated by Einstein (1906) who developed the expression:

$$\nu_{F+P} = \nu_o(1 + \lambda C) \qquad 7.2$$

in which

ν_{F+P}: is the viscosity of the suspension

ν_o: is the viscosity of the clear fluid

λ: is a constant equal to 2.5 for rigid spherical inertialess solid particles

C: is the volume concentration of the solids.

This relationship was used to test the effect of the suspension ratios employed in the experimental work and found to be of no consequence.

CHAPTER VIII

THE PARTICLE RESPONSES TO UNSTEADY AND SHEARING FLOWS

SECTION I

Particle Response in Unsteady Flow

During the investigation of particle packing and determination of numbers of particles contained in bulk volumes, it was established that the particles in use were 0.365 mm ± 0.008 in diameter. It is also known that their specific gravity was 1.05.

It is also necessary to verify that particles of this type are capable of following the motion of water not only in irrotational steady motion, but also under accelerated flow conditions and particularly when strong shear gradients are present.

Consequently it was necessary to examine the particle motion in some detail to deduce the extent to which the particle tracks remain a true indicator of the velocities in accelerated flows.

Particle Response to Accelerations in the Flow Field

If a velocity fluctuation occurs such that the velocity difference $U_F - U_P = \Delta U$ between the particle and the fluid surrounding it, approaches but does not exceed that velocity for which the Reynolds number of the particle exceeds unity, then Stokes law can be applied.

If

$$\frac{\Delta U \times D_p}{\nu} = Re_p \leq 1$$

then for the present particle diameter

$$U_F - U_P \leq 0.35 \text{ cm/sec.}$$

The time response of the particles to velocity changes such that $U_F - U_P \leq 0.35$ cm sec^{-1} can now be deduced from a force balance using Stokes law

$$\sum M \frac{dU_P}{dt} = (6\pi r.\mu(U_F - U_P)) \qquad 8.1$$

where

$\sum M$: is the effective mass which includes both the mass of the particle and the virtual mass of the surrounding fluid.

The accepted value of the virtual mass associated with the motion of a sphere in a three-dimensional unbounded fluid is one half of the fluid mass displaced by the sphere.

Hence

$$\sum M = (\frac{4}{3}\pi r^3 \rho_P + \frac{2}{3}\pi r^3 \rho_F) \qquad 8.2$$

Combining Eq. 8.1 and Eq. 8.2 yields:

$$\frac{dU_P}{dt} = \frac{6\pi.r.\mu(U_F - U_P)}{(\frac{4}{3}\pi r^3 \rho_P + \frac{2}{3}\pi r^3 \rho_F)} \qquad 8.3$$

for convenience

$$= \Phi(U_F - U_P).$$

Solving the expression for the time dependant particle velocity U_P and noting the boundary conditions yields

$$U_P = U_F(1 - e^{-\Phi t}) \quad \text{for } U_P = 0 \text{ at } t = 0 \qquad 8.4$$

The constant Φ is given by

$$\Phi = \frac{6\pi r\mu}{(\frac{4}{3}r^3\pi\rho_P + \frac{2}{3}r^3\pi\rho_F)} = \underline{4.22 \times 10^2 \text{ sec}^{-1}}$$

Substitution of this value of Φ into Eq. 8.4 and subsequent examination for the smallest time interval of interest which as explained (page 37) in the discussion of the illumination system was 0.01 sec, revealed that:

$$\text{at } t = 0.01 \text{ sec} \quad \frac{U_P}{U_F} = 0.985$$

so that any velocity discrepancy reduces to 1.5% of its initial

value within the smallest time interval used in the investigation. An even more favourable situation exists of course when the cine film technique is applied, as the smallest time interval of interest in this case is 0.02 sec.

It is therefore safe to assume that errors from particle response lag due to velocity changes are too small to effect the experimental results when:

$$\Delta U < 0.35 \text{ cm sec}^{-1}, \quad \text{i.e. } Re < 1.$$

This conclusion is supported by Allen (1968), who states that under these conditions, which are met in sedimentation and elutriation processes, the assumption that the terminal particle velocity is reached instantaneously, introduces only a negligible error.

When the velocity difference and hence the Reynolds number exceed the stated limits such that

$$U > 0.35 \text{ cm sec}^{-1} \quad \text{and} \quad Re_p > 1$$

Stokes law is in theory no longer applicable, since it predicts too low a value for the drag coefficient of the sphere. However this observation is in itself sufficient to indicate that the particle response improves at supercritical Reynolds numbers, so that their response time will be yet shorter.

This general conclusion is supported by Clamen and Gauvin (1969). In an investigation of the effects of turbulence on drag coefficients of spheres in flows which were supercritical with respect to the particle Reynolds numbers, they found that small particles of low density invariably tended to assume a fluctuating motion of their own particularly at high turbulent intensities. This indicates that as the difference in density between particles and the carrier fluid becomes smaller, drag phenomena tend to control the motion of the particle.

Attention is also called to the fact that the preceding inquiry has dealt with single particles only; but that the principles and conclusions are assumed to apply to collections of particles also.

In this context it should be noted that Happel and Brennan (1965) in an inquiry on mono-sized particle assemblies established that: if two identical particles separated only by a few diameters move along the same path through a fluid, the combined flow field around the particles is affected in such a way that the sum of the resulting viscous force is greater than the sum of those which acts on a single particle.

In the intended application this can only be beneficial as the groups of suspended particles would remain with the fluid elements even more diligently than individual particles.

The conclusions will therefore be that the flow photographs may be used to obtain information about velocity and velocity changes from the particle tracks, since the particles remain with the fluid elements and are not affected by velocity fluctuations.

SECTION II

Particle Response when Immersed in a Shearing Flow

In the preceding section it was shown that the particle motion does represent the flow field motion in unsteady flow. But, as the particles are initially injected into the shear layer, it is also necessary to inquire into the particle behaviour, when they are immersed in a shearing flow field.

Effects of Circulation upon the Particle Behaviour

In two-dimensional flow a body develops lift if it possesses a circulation Γ and has some velocity ΔU relative to the surrounding fluid. The lift force is given by

$$\hat{L} = \rho(\hat{\Gamma} \times \Delta\hat{U}).$$

This effect could cause the flow visualization particle to migrate sideways out of the shear layer.

Jeffreys (1929) showed that this effect could take place when the circulation resulted from the presence of a shearing flow field. He presented an analytical solution to the problem of an infinite cylinder resting on a surface when subjected to a two-dimensional flow perpendicular to the cylinder axis and parallel to the surface. From the present point of view, the important conclusions of Jeffreys' work was that once it had been lifted from the surface, the cylinder accelerated horizontally until it reached the stream velocity and therefore $\Delta U = 0$. In this condition the lift vanished and the cylinder sank back to the surface. There is a clear indication in this result, that provided the particles move at the same streamwise velocity as the local fluid, they will not migrate sideways, but follow the fluid streamlines.

An inquiry of this point in the present application is complicated by the fact that the flow is not two-, but three-

dimensional around the individual particles, which limits the applicability of Jeffreys' conclusions concerning migration in two-dimensional flow.

Further doubt arose from the fact that an experimental investigation by Segre and Silberberg (1962) had indicated, that particles migrate in laminar tube flow. They demonstrated how particles immersed in a Hagen-Poiseville flow migrated into an annular configuration within the confined flow and congregated in an equilibrium position approximately 0.6 of the radius away from the centre of the tube.

This migration occurred in a highly laminar flow as the Reynolds number range remained between $3 < R_e$ No. < 520 during their experimental work.

They do not however state the length of tube required for the annular configuration to become established, but only that their observation station was located 110 tube diameters from the entry. The migration rate could have been very slow indeed. Also their particles were rather large with diameters up to 30% of the tube radius.

Their findings may therefore not be important in the present application, where we are concerned with the possibility of lateral migration in at most 2 cm of laminar shear layer of particles which are small in comparison with the shear layer thickness. Furthermore, although the shear layer in the present experiment was observed to be almost entirely laminar, evidence of transition was observed occasionally at a distance of 1.5-2.0 cm from the separation point. This is significant because Segre and Silberberg found that migration effects vanish completely as transition is approached.

The evidence just presented must however be regarded

as purely qualitative, because it is not known how the velocity gradients in the abovementioned experiments compare with those occurring in the wake shear layers.

If however it can be shown that velocity gradients which are equal to or stronger than those encountered in the wake, are unable to induce migration; then it can be assumed that particles in a weaker shear are even less inclined to migrate and thus will remain faithfully with the elements of fluid in which they originally were entrained

Quantitative-Determination of Particle Response to a Shearing Flow

In order to verify the validity of this assumption it was necessary to perform controlled experiments in which shear layers were formed such that by comparison

$$\frac{\frac{\partial u}{\partial y}(\text{wake})}{\frac{\partial u}{\partial y}(\text{experiment})} \leq 1 \qquad 8.5$$

For this purpose a system was designed in which a steady shear flow was produced by passing water from a constant head tank through a 2.5 cm by 2.5 cm square perspex tube 125 cm long.

The mean flow rate was monitored by rotameters, while the velocity gradients in the shear flows were determined by flow visualization photography and verified by application of an optical doppler shift technique, which operated totally independant of the flow visualization technique, but measured velocities in exactly the same location.

The general arrangement of the experimental equipment is shown in Fig. 8:1.

Illumination for the flow photographs of the shear layers was provided by a flat ribbon of laser light, which for timing

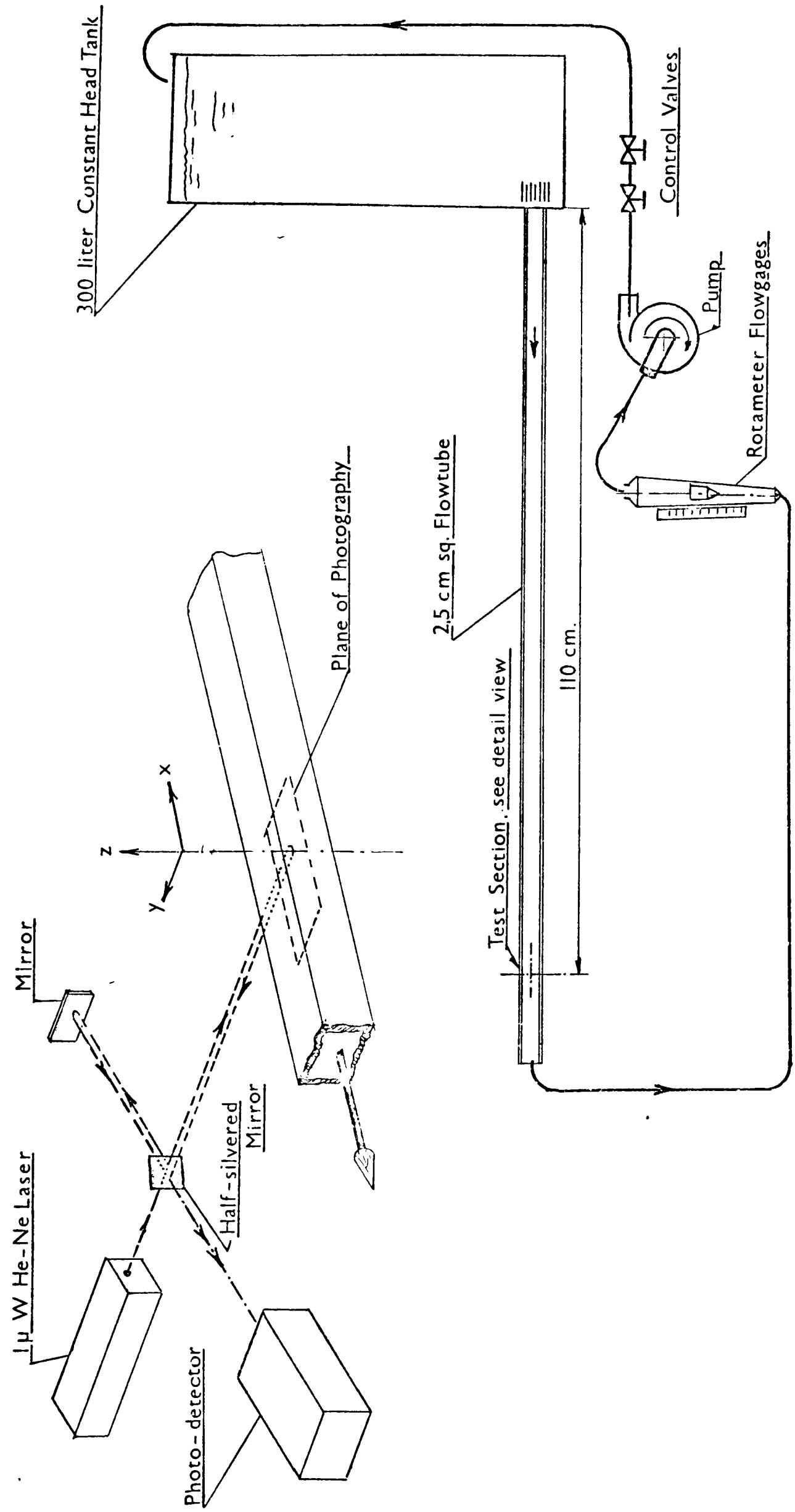


Fig. 8:1 The General Arrangement of the Equipment used in the Determination of the Particle Behaviour in Strong Velocity Gradients in the Shear Layers.

purposes was chopped into light pulses by passing the beam through a rotating, slotted disc. The timing accuracy was assured by driving the disc with a synchronous motor.

The chopping of the light converted the particle streaks into rows of dots on the flow photographs, so that particle velocities could be deduced by measuring the separation between the dots and correlating these measurements with the pulse rate of the light.

The particle measurements provided a complete picture of the velocities in the tube flow field from which the desired velocity gradients could be determined. But, as the particle streaks will also be used in the wake to determine the velocity gradients there, comparison between the two sets of flow field data is non-conclusive until it is established that the particle streaks represent the tube velocity at that point in the flow.

For this verification the optical doppler shift technique was employed because it measures exact velocities in the flow whether or not there are particles present in the location where measurements are being taken.

The velocity range to be surveyed is only that which causes laminar flow in the tube, as it was shown earlier that migration ceases completely at the onset of turbulence. If the transition is considered to occur at Re $\geq$ 2000 then

$$0 \leq U_{crit.} \leq 8 \text{ cm/sec}$$

Since water flow velocities have been measured as low as $U = 7 \times 10^{-3}$ cm/sec (Yeh, Y. and Cummins, H.Z., 1967), and as high as $U = 10^{2}$ cm/sec (Foreman, Jr., et al, 1966) by laser doppler shift sensors, they are fully capable of measuring the velocity span of interest in the present experiments.

When this technique was applied to the present system

it proved possible to measure velocities anywhere in the plane transverse to the fluid flow to within 0.025 cm of the walls of the perspex tube.

The measurements in the shear layer were taken simultaneously with the flow photographs, and upon subsequent comparison of the longitudinal velocities deduced by either method, no difference was found.

It is therefore concluded that velocities determined from the flow visualization photographs are true and do accurately represent the velocities in the shear layers.

The first part of the initial question concerning migration can now be answered. When flow photographs of the shear layer in the tube as shown in Fig. 8:2 were examined on the travelling microscope, no misalignment could be detected between the centrelines through the particle rows of dots and the centre axis of the tube within the limit of resolution which for this instrument is one minute of arc.

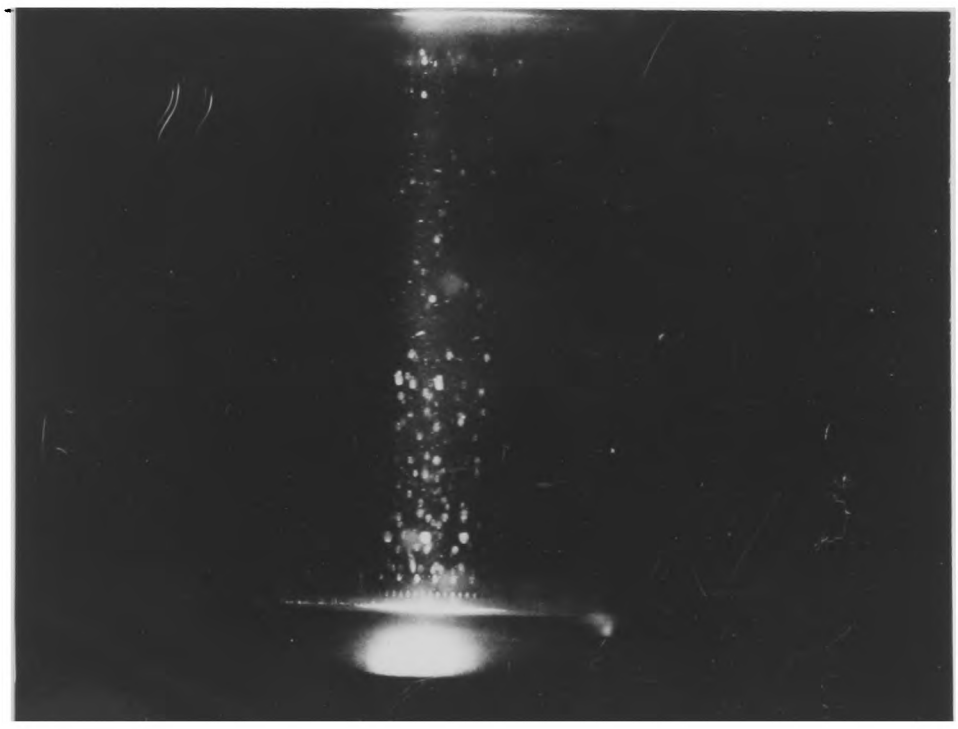


Fig. 8:2 Particle Paths in the Shear Layers

When furthermore the velocity gradients in the tube

shear layers were compared with velocity gradients deduced from measurements on wake photographs by substitution into Eq. 8.5, the result was that

$$\frac{\frac{\partial u}{\partial y}(\text{experiment})}{\frac{\partial u}{\partial y}(\text{wake})} \lesssim 2$$

Since the shear existing in the tube was shown not to cause migration, there is little chance that the weaker wake shear can expel the particles. It may therefore safely be concluded that the particles do remain in the fluid into which they originally were entrained also when these fluid elements are contained in a shear layer.

In summary it can be stated:

It was required (page 12) that the particles remain with the fluid and circulation elements in which they were entrained.

This demand has been satisfied since it was shown that the particles were not adversely affected by the velocity fluctuations, nor were they expelled from shearing flows; but remained with the fluid elements into which they were entrained.

Therefore, since the circulation remains with the fluid elements and the particles remain with the fluid elements, the particles must remain with the circulation.

PART III

CHAPTER IX

A GENERAL WAKE INQUIRY

Having established that the particles do remain with the elements of circulation and that by tracing the history of the particle motion knowledge can be obtained about the distribution of circulation, it is now possible to use these findings for a general examination of the wake produced by the bluff body shown in Fig. 4:2, Chapter 1, Part I, and outlined by particles ejected from the model.

A general investigation of the wake is desirable because in the course of presenting the main parts of the thesis, emphasis was concentrated upon those aspects which were directly relevant to the distribution problem. There are however many other points of great interest which were treated while work was proceeding on the main topic. These other subjects are therefore considered here.

The wake was produced in all experimental work by towing the model at one speed only, 9.30 cm/sec. This particular velocity yielded a model Reynolds number of

$$Re \simeq 1.5 \times 10^4$$

which should cause laminar boundary layers to prevail.

The particle ejection and wake formation sequences were cine and still filmed and timed for subsequent scanning and counting purposes.

SECTION I

Particle Motion History in the Wake

Visual examination was made of approximately 2000 vortex shedding cycles produced under identical circumstances. It was observed that those particles which originally were contained in the shear layer did without exception enter and entrain only in the three major regions of the wake, the dead fluid region and the vortex clouds in the two vortex rows.

In fact several attempts were made to direct the particles towards some other regions in the wake - but to no avail. If the particles were originally contained in the shear layer emanating from the separation point, they entrained in an orderly fashion into the regions of vortical activity.

It can therefore be concluded, that when the particles are injected into the circulation bearing shear layers, a large majority of the particles find their way into the semi-ordered vortex clouds and a small, but countable number enter the zone immediately behind the bluff base known as the dead fluid region. This general process of particle distribution is illustrated in Fig. 9:1a-k by a series of photographs of a typical vortex shedding cycle in the wake.

The first photograph in Fig. 9:1 depicts the approximate moment of the start of a cycle. It is at this point that the shear layer first exhibits a reversal in curvature, and it is therefore convenient to consider that at this moment a new cycle starts. It can be observed how the initially almost straight particle laden shear layer begins to roll up into a vortex cloud. When this cloud has reached a finite size, which varied very little from cycle to cycle, the feeding sheet is abruptly severed from the vortex (see g.) which begins to move downstream in the



Fig. a Frame: 110

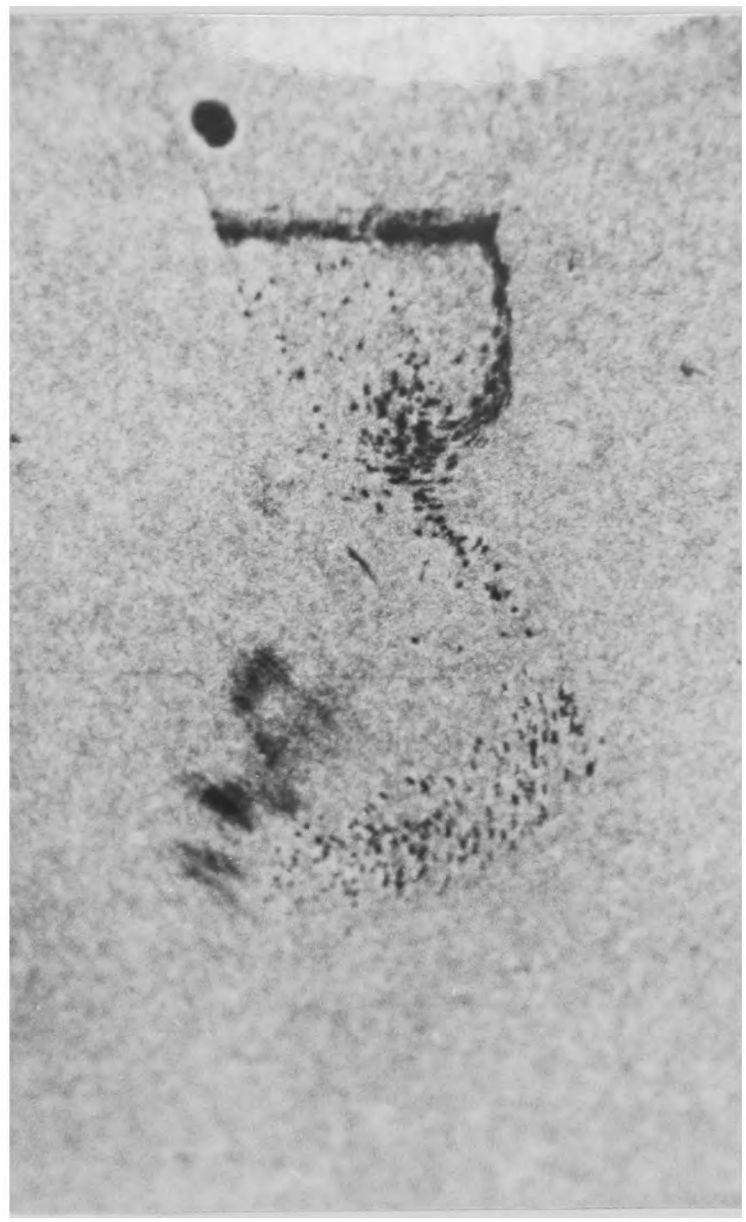


Fig. b Frame: 115



Fig. c Frame: 120



Fig. d Frame: 125

Fig. 9:1a-k A Complete Vortex Shedding Cycle shown at 0.04 sec per Frame Number



Fig. e Frame: 130



Fig. f Frame: 135



Fig. g Frame: 145

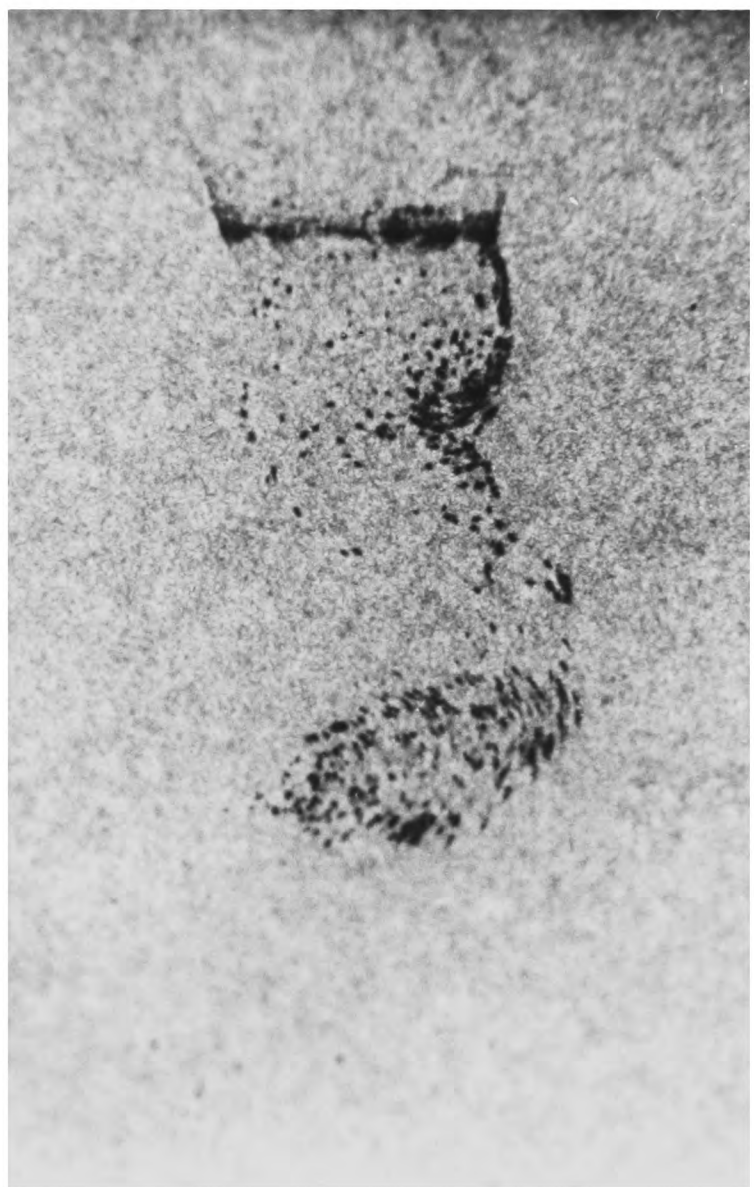


Fig. h Frame: 150

Fig. 9:1a-k

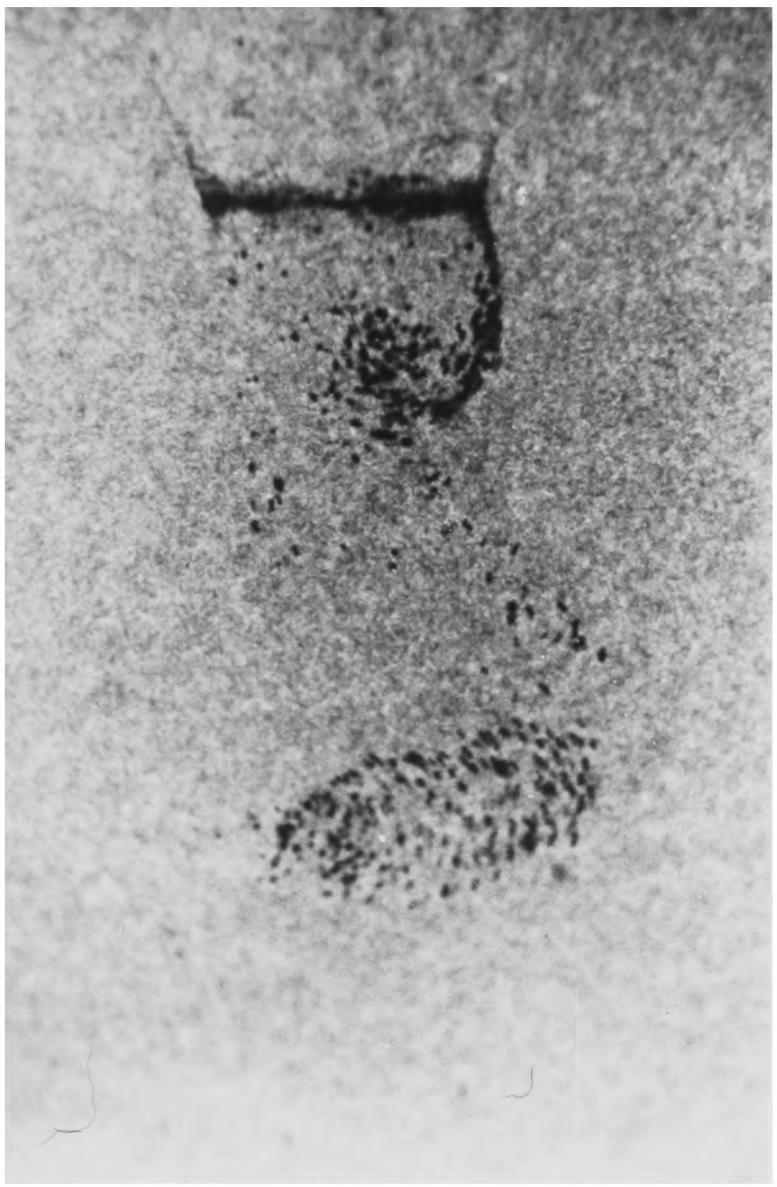


Fig. j Frame: 155



Fig. k Frame: 165

Fig. 9:1a-k

wake as a fully grown vortex cloud and the cycle repeats itself anew. The period of this separation was measured to be 1.47 sec/cycle.

Determination of the Downstream Counting Zone

Immediately after a vortex is separated from the feeding sheet it possesses its maximum strength. Therefore, the number of particles contained in the vortex cloud representing it must be determined shortly after the separation has taken place. However a compromise must be struck because in order to insure that all particles are counted, it is better to let the cloud diffuse slightly to eliminate image overlap. It was determined by visual inspection and repeated counting of control frames that constant, representative counts could be had if the counting zone was chosen to lie between 2h and 3h downstream of the base as shown in Fig. 9:2.

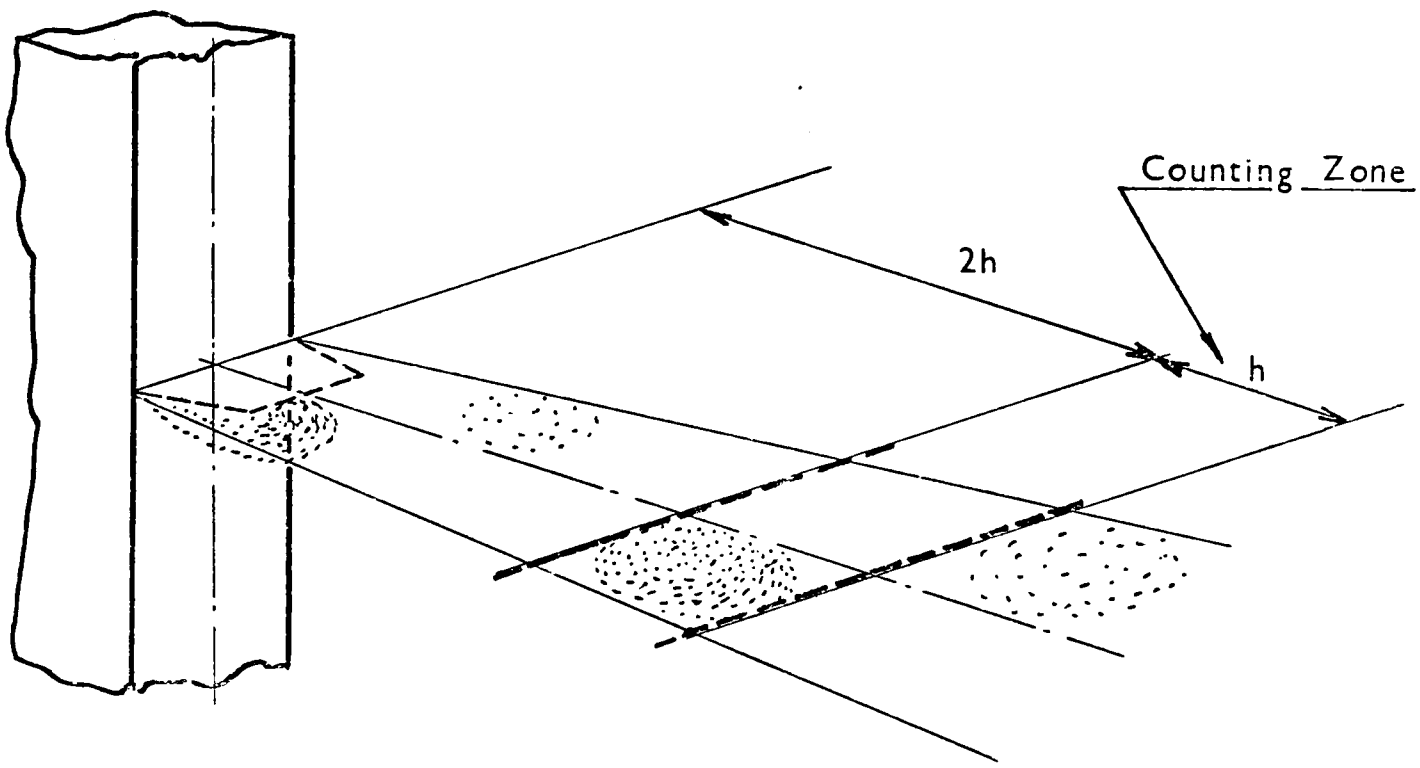


Fig. 9:2 The Dimensions and Boundaries of the Counting Zone

All counts of the number of particles in the fully formed vortices were taken within this region.

Since their downstream boundaries were without exception sharply defined (see k.), the arrival of the cloud could be determined with the accuracy inherent in the cine film framing rate. In fact the arrival of the downstream boundary of the vortex cloud at the imaginary 3h boundary could be timed even more exactly at 1.47 sec than the occurrence of the reversal of curvature in the shear layer. This provided a convenient confirmation of the period τ of the cycle measured earlier.

During the development of the circulation balance in Chapter 3, Part I (page 16), it was mentioned that no distinction could be made between the quantities of circulation denoted by Γ_a and Γ_b in the Gerrard hypothesis.

Considerable effort was made to attempt to distinguish between these quantities by using both dye and particle ejection technique, but with the present techniques to no avail.

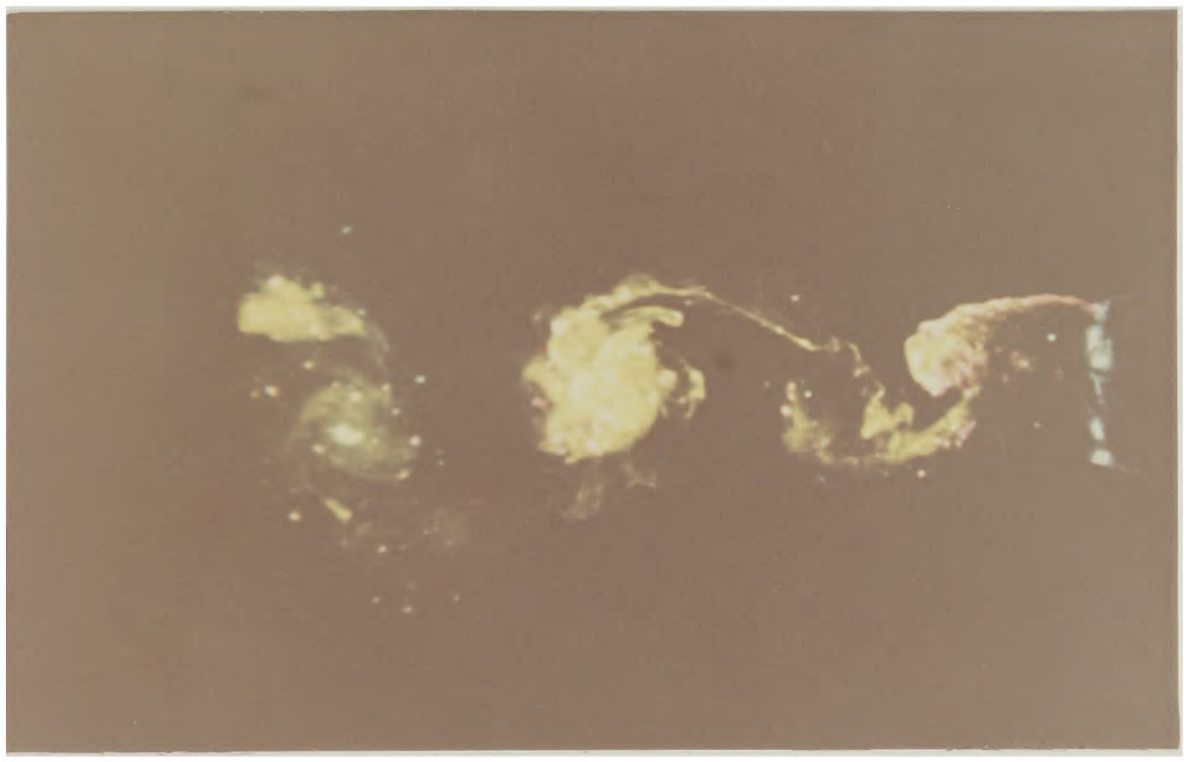


Fig. 9:3 Ejection of Dye into the Periodic Wake

Both techniques showed the general features of the wake in very good detail as shown earlier with particles and in Fig. 9:3 above with dye and gave qualitative information about the relative magnitude of the distributed quantities of circulation.

Nevertheless, it was impossible to separate the two quantities Γ_a and Γ_b and follow their individual history at any stage in the formation process, and they were therefore considered as a lumped quantity in the analysis.

Further qualitative information about the wake was obtained during the projection of the cine film records by tracking the history of arbitrarily chosen pairs of particles. These pairs were chosen while still located in the region where the roll-up occurs. Their motion was followed through approximately a full cycle by marking their positions every 0.04 sec. The paths of these particle pairs are shown in Fig. 9:4, in which the numbers refer to the consecutive frame numbers.

The position of each particle in the pair was marked by respectively a circle and a small bar on the counting screen as each new frame was projected. A pronounced rotation is indicated by the change in inclination of the lines connecting the pair in each new position. This tumbling occurs both in the formation region (frames 100-105, 100-110) and when the pairs are tracked in the downstream wake (as seen in frames 25-75) and may therefore be considered to constitute further visual evidence that the particles continue to represent the elements of fluid possessing the circulation also far downstream in the wake.

Particle Motion History in the Dead Fluid Region

It remains to examine both the wake flow into the dead fluid region as well as the region itself, because the number of particles which during each cycle were carried into this region was also to be determined. The examination was accomplished and the exact size of the region was determined from

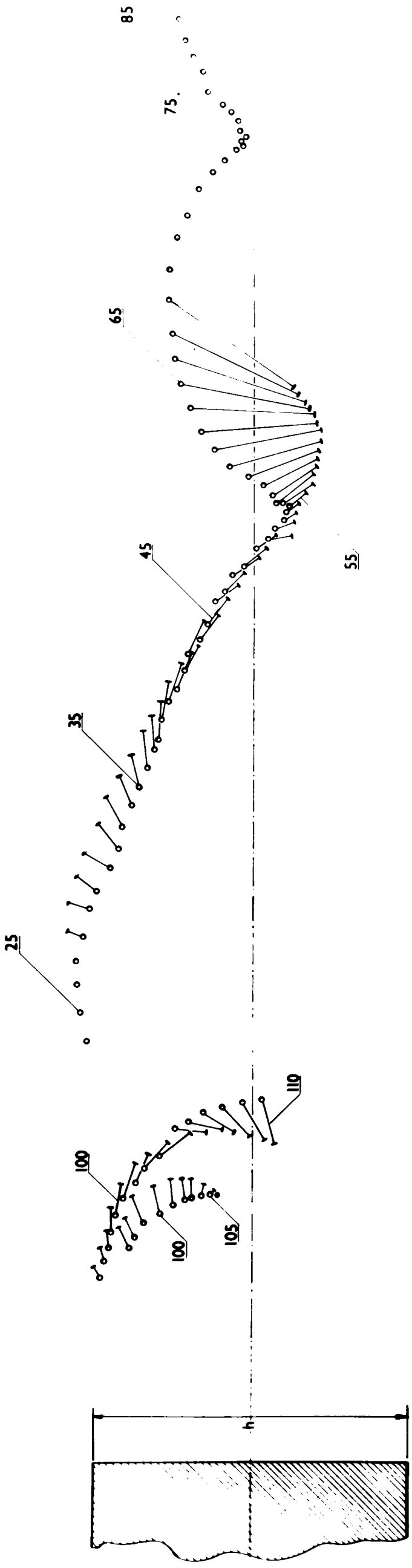


Fig. 9:4 The Translation and Rotation Exhibited by Pairs of Particles Visualized by Following and Marking their Position at 0.02 Sec Intervals for Approximately 1½ Cycle.

the cine film records of the processes whereby particles originating in the shear layer enter the dead fluid region.

At one point during the rolling-up process, while the diameter of the nascent vortex has been increasing steadily, suddenly particles are observed to enter the dead fluid region at rather high relative velocities. However, at the attainment of a certain diameter of the vortex, this particle flow is abruptly terminated and does not occur again until the next cycle is started. This injection process is outlined in Fig. 9:5a-h, in which the outline of the dead fluid region is superimposed upon the flow field.

Determination of the Boundaries of the Dead Fluid Region

The dimensions of this region were obtained by the following considerations.

The nascent vortex is observed to grow in diameter until its upstream boundary becomes tangent to an imaginary boundary 0.6h downstream of the model base, at which time the particle injection into the dead fluid region appears to start. Although the vortex continues to grow in size, its upstream boundary ceases to penetrate forward, but remains at the 0.6h position. Shortly thereafter the particle injection ceases, the vortex starts to move away and the flow reversal is seen to start anew.

The time at which these events occurred could be related to the time at which the flow reversal takes place to provide information about the injection mode within a single cycle as shown in Fig. 9:6.

It can be seen that the particle injection process never occupies more than about one third of the cycle and occurs late with respect to the start of the shear layer reversal.

The particles which were seen to cross the 0.6h boundary

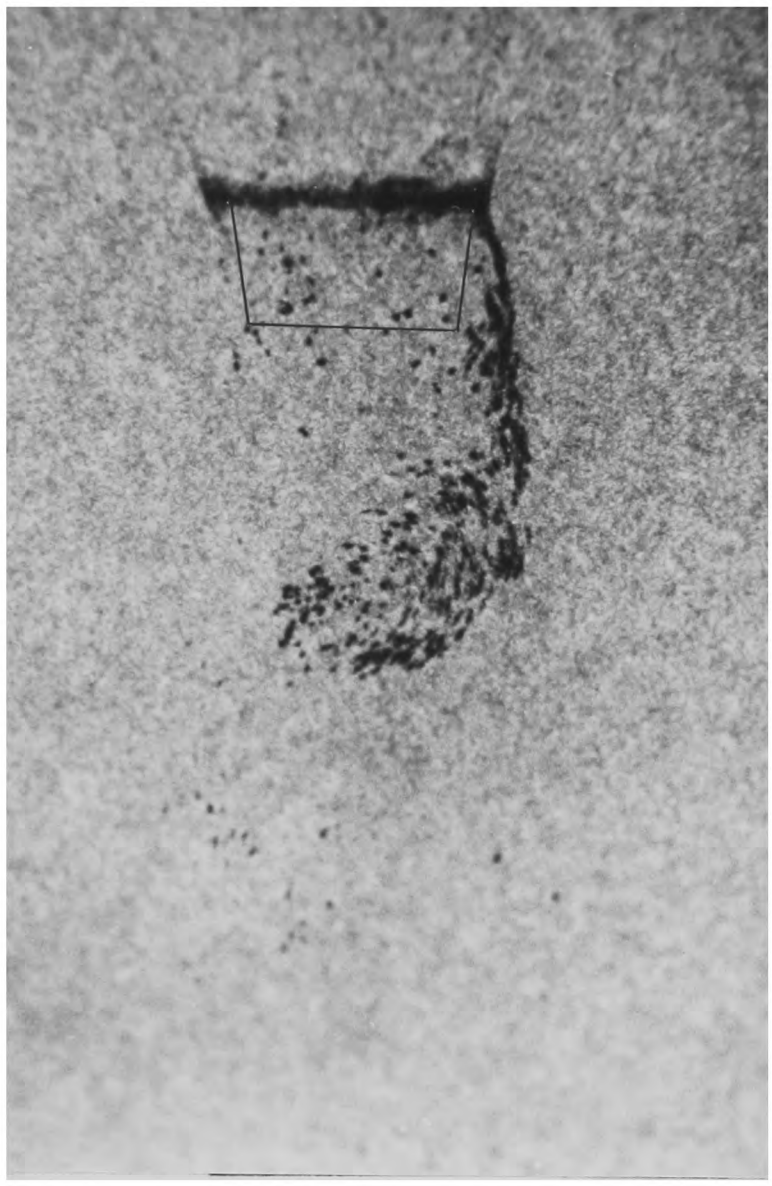


Fig. a Frame: 140

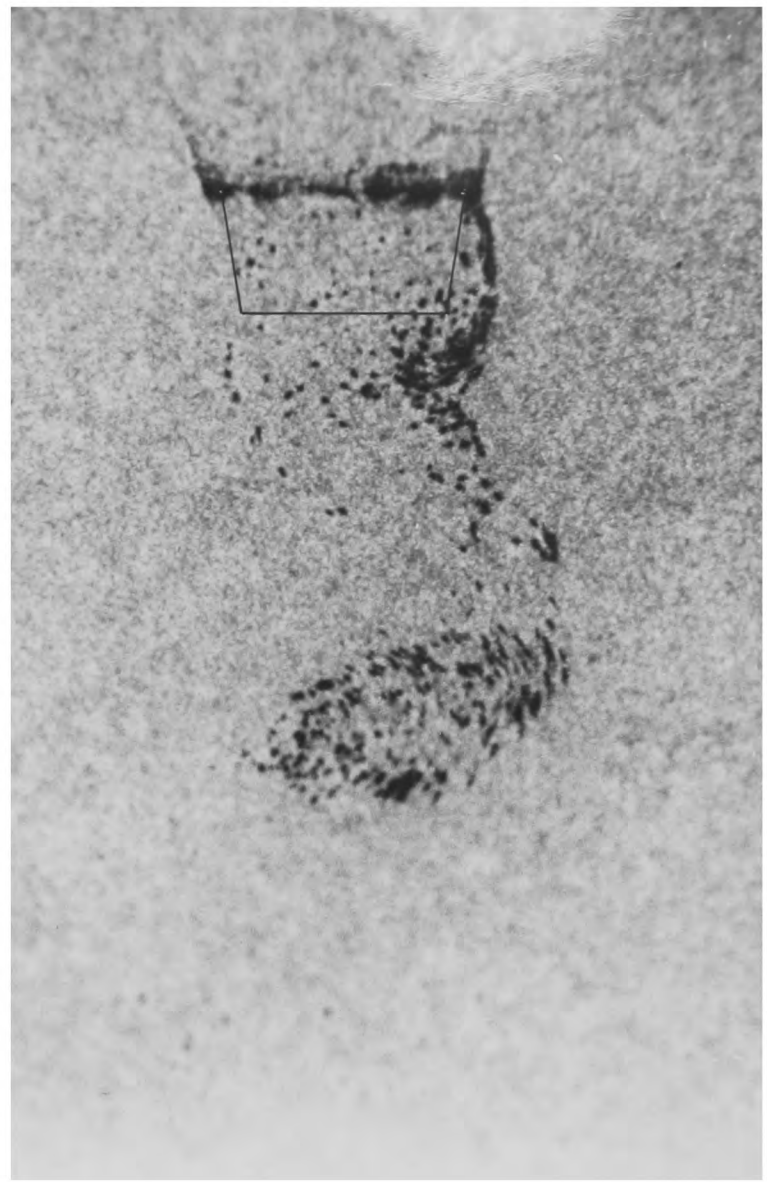


Fig. b Frame 150



Fig. c Frame: 160



Fig. d Frame: 165

Fig. 9:5a-h The Periodic Injection of Particles into the Dead Fluid Region shown at 0.04 sec per Frame Number



Fig. e Frame: 170

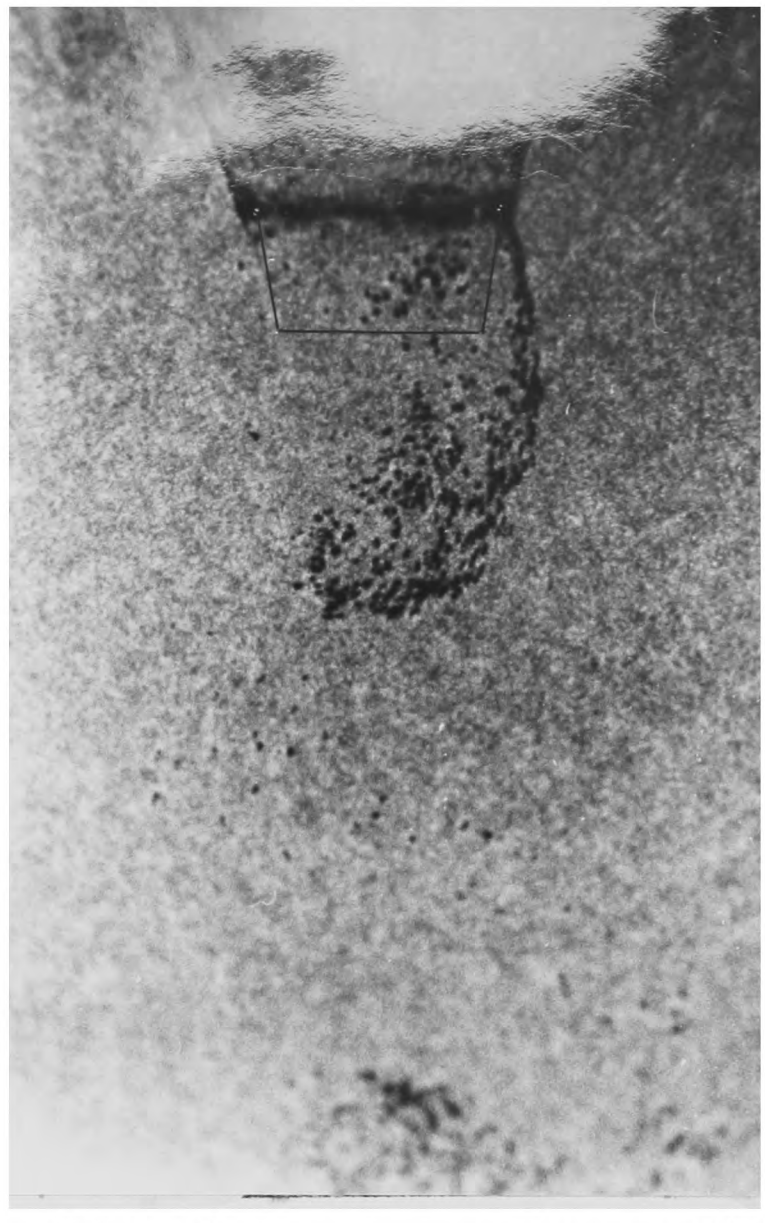


Fig. f Frame: 175



Fig. g Frame: 185

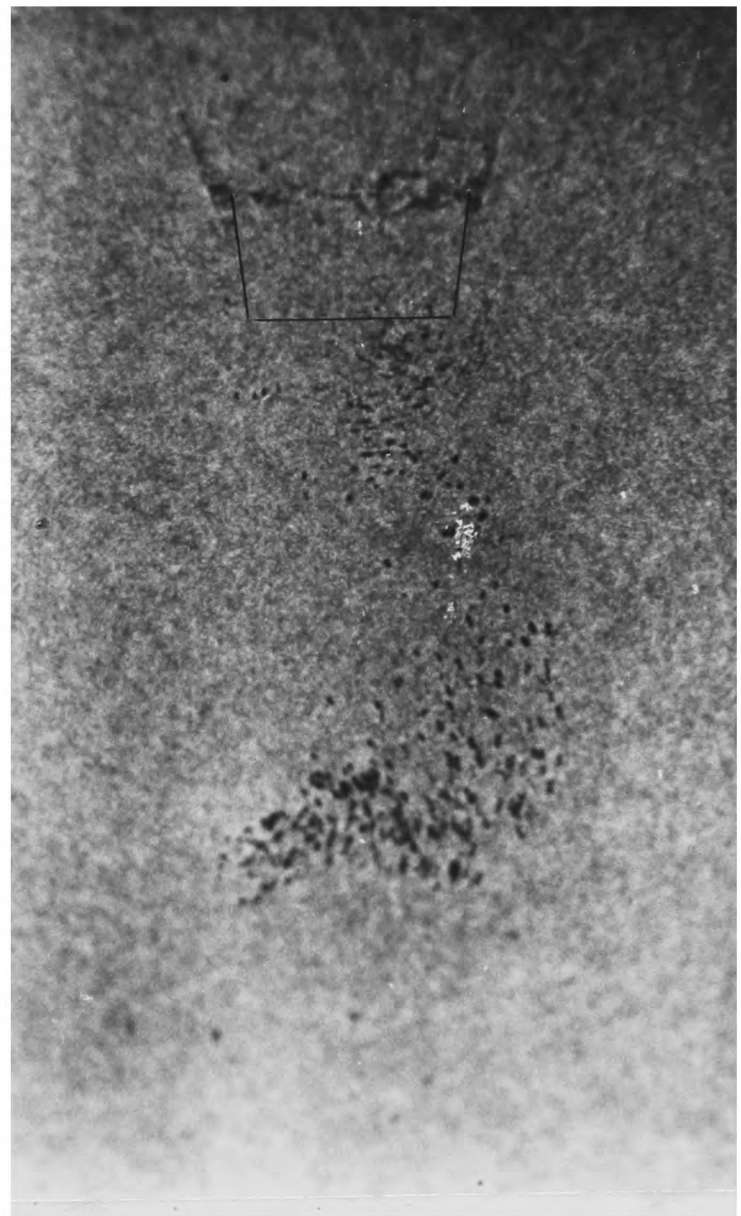


Fig. h Frame: 190

Fig. 9:5a-h

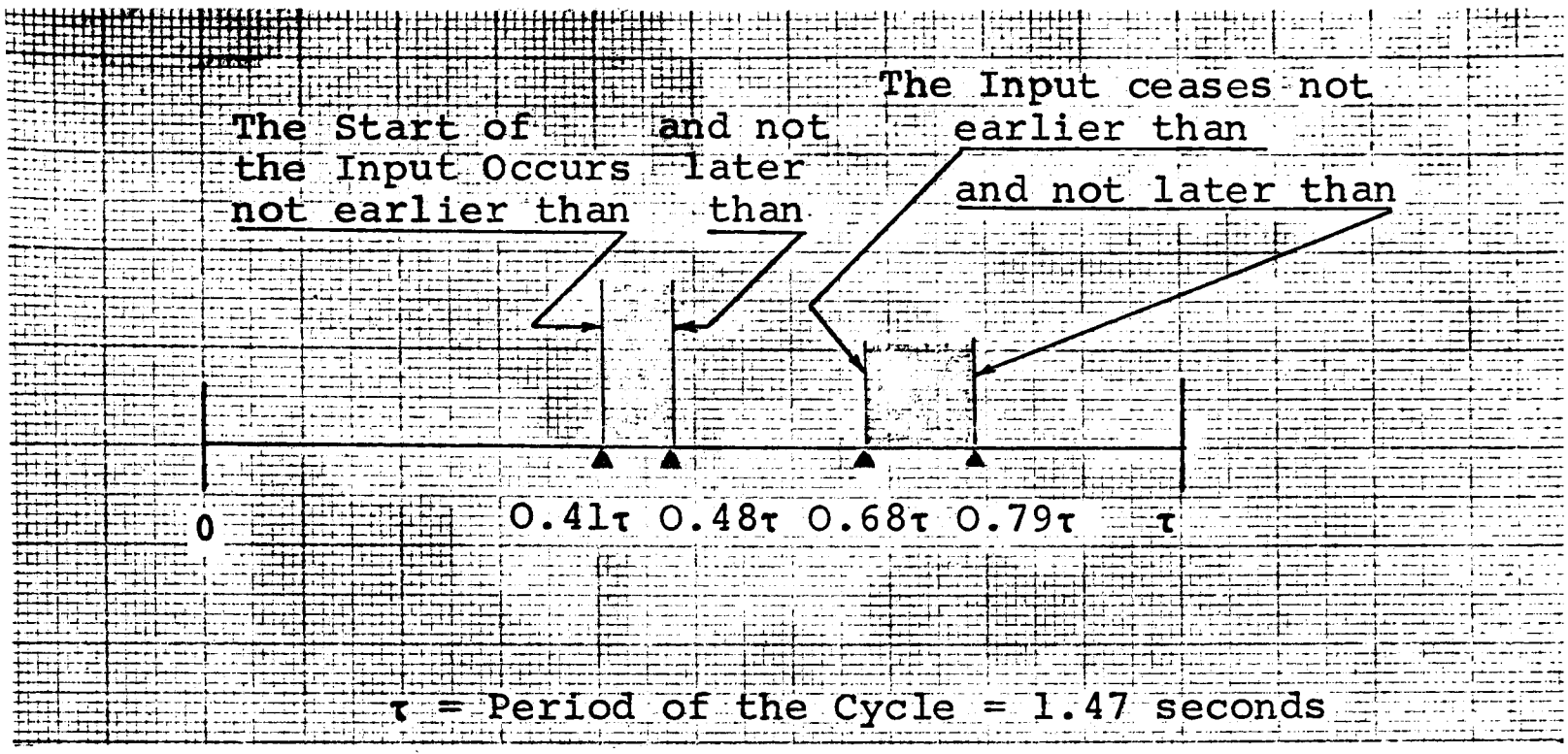


Fig. 9:6 The Timing of the Particle Entry into the Dead Fluid Region within the Cycle

at rather high velocities slowed down in a very short time. They then remained in sight for several cycles until eventually settling slowly out of sight without being swept out again to participate further in any wake activities.

Even when in close proximity with the inner boundary of the vortex sheet emanating from the separation point, the particles in the quiescent fluid of the dead fluid region were rarely if ever affected. Although visual evidence indicated that the shape of the region was a truncated wedge, experiments were made by counting particles within the rectangular slope bounded by the base width and the 0.6h. These counts varied too little from those taken in the conical area to be of any consequence. The length (0.6h) was shown to be the controlling dimension rather than the width.

Based on this evidence, the dead fluid region was determined to be of the configuration and have the dimensions shown in Fig. 9:7.

It was stated that once the particles were within the boundaries of the dead fluid region, they no longer participate

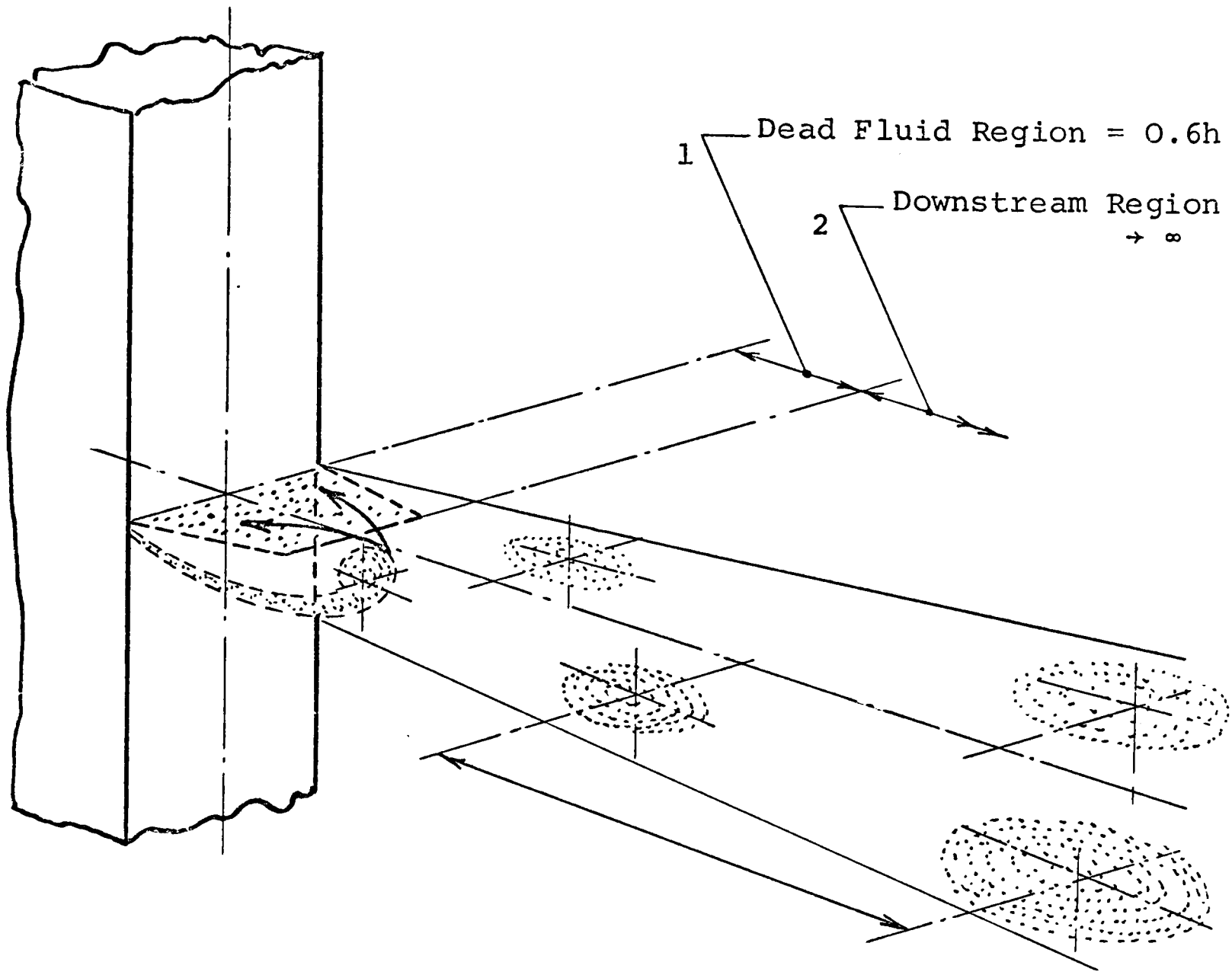


Fig. 9:7 The Boundaries and Dimensions of the Dead Fluid Region

in any wake activities, but only sink slowly away out of sight.

This is a very important point and therefore tests were made to ascertain whether this remained valid even under conditions of extreme turbulence. These tests were made both under normal experimental conditions, where the water in the tank had settled for several hours and when the turbulence level in the tank was so high that the wake appeared to be in a state of total disorder.

It was observed that even in the turbulent conditions, those particles which entered the dead fluid region behaved as explained earlier. Illustration of this point is provided in Fig. 9:8.

It can be seen that even at this disturbed state of the wake there is a clear separation between the dead fluid region



Fig. 9:8 Lateral View of the Particle Ejection and the Wake formed under Conditions of High Residual Turbulence

containing the particles and the particle free fluid downstream in the wake. This shows that the particles continue to sink vertically along the span and never leave the confinement of the imaginary boundaries of the dead fluid region, although of course they do sink out of the lit zone, when the wake is illuminated in the lateral plane.

Therefore the assumptionsstated earlier are valid and may be safely used in the analysis of the distribution of circulation by particle counts in the dead fluid region.

SECTION 2

Effects of Ambient Residual Turbulence

It was mentioned earlier that any residual turbulence in the towing tank was allowed to subside between each experimental run.

Although no systematic enquiry was made into the effects of waiting, it became evident very early in the work program that an extended settling period before each run provided much better definition of the vortices and particle clouds at the locations in the wake.

Qualitative observations were made of certain aspects of residual turbulence, which was produced by towing the model back and forth several times in the water tank. The presence of turbulence did not affect the particle ejection mechanism, but did at times have a visible effect upon the length of the formation region in the sense that its length was altered from that exhibited in a quiescent system.

This effect became more pronounced as the waiting time between the runs was decreased. The use of the indefinite term "altered" is intentional, since it was not possible to deduce how and what mechanism was responsible for the variations and disorder in the wake appearance. The effects of the turbulence were manifold. The vortices were strongly distorted, the length of the formation region varied up to 50 per cent from normal while untidiness and disorder prevailed in general throughout the wake.

One feature was however not affected. As well as it could be determined the frequency of the vortex formation in the wake was never altered. It appears that it would be necessary to change either the free stream velocity U_∞ or the base width

h of the model to change the wavelength of the wake system.

Some qualitative insight into the effects of the residual turbulence was obtained by photographing the particle ejection sequence from the side - not from above as previously. Three illustrations are provided in Fig. 9:9.

All parameters in the runs depicted here were the same with the exception of the settling time. In Fig. 9:9a the fluid was allowed to settle 6 hours, in Fig. 9:9b one hour and in Fig. 9:9c about 5 minutes which was the minimum time required to repeat an experiment.

An analogy can possibly be drawn here to the work performed by Schubauer and Schramstad (1947). On the basis of their work it is possible to surmise that if the intensity of the turbulence present in the tank is responsible for the variations in the length of the formation region, then there is a point at which it has decreased to a level, at which it is no longer capable of interfering with the formation region.

The length achieved by the formation region is then controlled by some internal mechanism or disturbance inherent in the wake, whereas above the critical level of turbulence intensity it is an external disturbance provided by the turbulence, which modifies the length of the formation region.



Fig. 9:9a Settling Time 6 hours

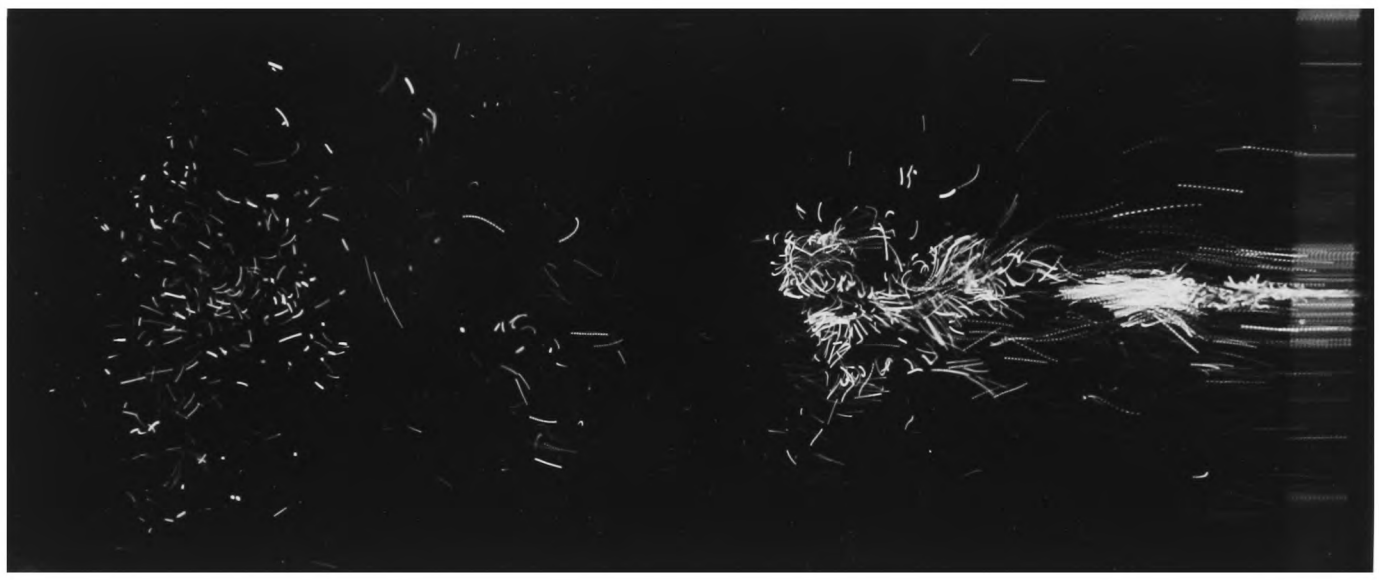


Fig. 9:9b Settling Time 1 hour

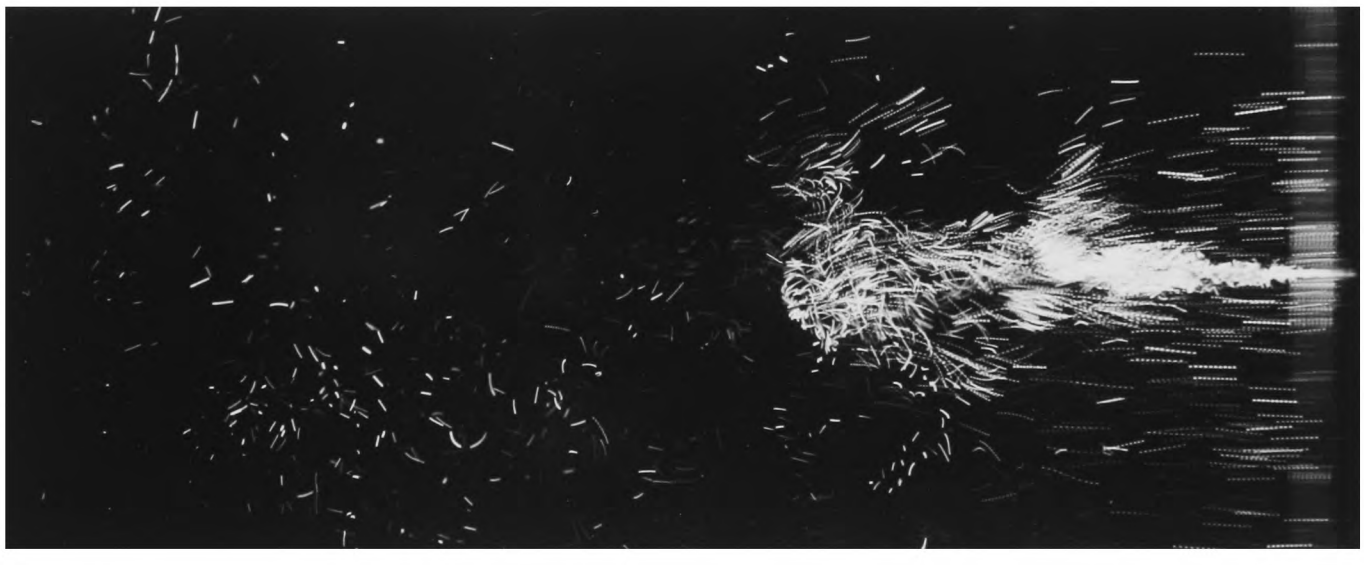


Fig. 9:9c Settling Time 5 min.

Fig. 9:9a-c Effects of Residual Turbulence upon Orderly Wake Formation

SECTION 3

Effects of Turbulence upon Residual Vortex Strength

It is evident that three dimensional effects become more pronounced as the interval between the runs were shortened. This may mean that even small levels of residual turbulence may have a profound effect upon the events occurring in the wake.

It is possibly a clue to the difference as regards residual vortex strength in the first fully formed vortices when the wakes are formed in different experimental facilities. Fage and Johansen (1927) established this residue in wind tunnels experiments to amount to about 50% of the total shed circulation, whereas careful measurements by Wood (1967) using flow visualization methods in towing tanks yielded a value closer to 60%. The author's value is about 65% for the wake formed in the very still conditions in the water towing tank.

Some attention was given to the search for spanwise occurrences of cells exhibiting turbulent characteristics at or before separation. The possibility of this phenomena occurring was not great but the Reynolds number range at which Humphreys (1960) discovered its presence is not too far above the range at which this work was conducted. It was however not possible to discover any trace of such behaviour in the flow photographs.

The conclusions from the results of the brief inquiry into the effects of residual turbulence resulted in the decision to allow 24 hours to pass between each and all experiments. It was found that under these circumstances the particle behaviour in the illuminated zone was controlled by two-dimensional effects as required by the initial premises and that any residual

turbulence had subsided to a level which could not be detected with the methods and apparatus used for the data analysis.

REFERENCES

Allen, T., 1968 — 'Particle Size Measurements', Powder Technology Series, Chapman & Hall Ltd., London 1968.

Batchelor, G.K.,1956 — A Proposal concerning Laminar Wakes behind Bluff Bodies at large Reynolds Numbers. J. Fluid. Mech., Vol. 1, Part 3, p.308, 1956.

Bernal, J.D. & Mason, J., 1960
Nature 188, p.910, 1960.

Clamen, A. and Gauvin, W.H., 1969
Effects of Turbulence on the Drag Coefficients of Spheres in a Super-critical Flow Regime. A.I.Ch. E. Journal, March 1969, p.187, 1969.

Clutter, D.W., Smith, A.M.O. and Brazier, J.G., 1959
Techniques of Flow Visualization using Water as a Working Medium. Douglas Aircraft Division, Report No. ES29075, April 1959.

Einstein, A., 1906 — Ann. Physik, Leipzig. Vol. 19, p.34, 1911.

Eskinazi, Salamon, 1967 — Vector Mechanics of Fluids and Magneto Fluids. Academic Press, New York, N.Y., 1967.

Fage, A. and Johansen, F.C., 1927
The Structure of Vortex Sheets. Aero. Res. Council, R. &. H. 1143, 1927.

Fage, A. and Townend, H.C.H., 1932
Proc. Roy. Soc. Ser. A, 135, p.656, 1932.

Foreman, J.W., George, E.W., Jetton, J.L., Lewis, R.D., Thornton, J.R. and Watson, H.J., 1966
Fluid Flow Measurements with a Layer Doppler Velocitmeter. IEEE Journal of Quantum Electronics, Vol. QE-2, No. 8, Aug. 1966, 1966.

Gerrard, J.H., 1966 — The Mechanics of the Formation Region of Vortices behind Bluff Bodies. J. Fluid Mechanics, Vol. 25, Part 2, p.401, 1966.

Goldstein, S., $(\frac{1938}{1965})$ — Modern Developments in Fluid Dynamics, 1938, Oxford.
New Edition 1965. Dover Publications Ltd. New York, N.Y. Chs. 13, 2 and 1.

Graton, L.C. and Fraser, H.J., 1935.
Journal of Geology 43, p.785, 1935.

Gray, W.A., 1959 — Ph. D. Thesis, Univ. of Leeds, 1959.

Gray, W.A., 1968 — The Packing of Solid Particles, Chapman & Hall, London, 1968.

Happel, J. and Brenner, H., 1965
Low Reynolds Number Hydrodynamics.
Prentice Hall, New York, N.Y., 1965.

Hooker, S.G., 1936 — The Spacing Ratio of a Vortex Street. Proc. Roy. Soc., Ser. A, Vol.154, p.170, 1936.

Humphreys, J.S., 1960 — 'On a Circular Cylinder in a Steady Wind at Transition Reynolds Numbers'. J. Fluid Mechanics, Vol. 9, pp.603, 1960.

Jeffreys, H., 1929 — On the Transport of Sediment by Streams. Proc. Camb. Phil. Soc., Vol. 25, p.272, 1929.

Kline, S.J., 1967 — Observed Structure Features in Turbulent and Transitional Boundary Layers. Symposium of Fluid Mechanics of Internal Flow, General Motors Press, Eisevier Press, Netherlands, 1967.

Kline, S.J., Reynolds, W.C., Schraub, F.A. and Runstadler, P.W., 1967 — The Structure of Turbulent Boundary Layers. Jour. Fluid Mechanics, Vol. 30, p.741, 1967.

Krzywoblocki, M.Z., 1953
Vortex Streets in Incompressible Media. Appl. Mech. Review, Vol. 6, No. 9, p.393, 1953.

Levine, M.M. and Chernik, J., 1965
Nature 208, p.69, 1969.

MacRae, J.C. and Gray, W.A., 1960
Brit. J. Applied Physics 12, p.164, 1960.

Manegold, E., Hoffman, R. and Solf, K., 1931
Koll. Z., 56, p.142, 1931.

Manegold, E. and Von Engelhardt, W., 1933
Koll. Z., 62, p.285, 1933.
63, p. 12 and p.149, 1933.

Marris, A.W., 1964 — A Review of Vortex Streets, Periodic Wakes and Induced Vibration Phenomena. Trans. of the ASME, J. Bas. Eng., June 1964, p.185, 1964.

Morkovin, M.V., 1964 — Flow around Circular Cylinder. ASME Symposium on Fully Separated Flow, Philadelphia, 1964.

Nash, J.F., 1962 — A Review of Research on Two-Dimensional Base Flow. Aer. Res. Council, R. & M. 3323, 1962.

Nash, J.F., 1967 — A Discussion of Two-Dimensional Turbulent Base Flows. Aer. Res. Council, R. & M. 3468, 1967.

Nielsen, K.W. and Berry, E., 1968
Development and Use of an Airborne Smoke Marker System for Atmospheric Research. D.R.I. Tech. Rept., Ser. P., P.S.P. Publication No. 3, Univ. of Nevada, Nevada, U.S.A.

Nielsen, K.W., 1969 Visualization of Separation in Base Flow. Interim Report to Ministry of Technology. Res. Agreement No. AT/2057/034, March 1969.

Prandtl, L. and Tietjens, O.G., 1934
Fundamentals of Hydro and Aero Mechanics. Dover, Inc., Engineering Societies Monographs, New York, N.Y.

Rosenhead, L., 1953 Vortex Systems in Wakes. Adv. in Appl. Mech., Vol. 3, p.185, 1953.

Roshko, A., 1954 On the Development of Turbulent Wakes from Vortex Sheets. NACA TN 1191, 1954

Roshko, A., 1955 'On the Wake and Drag off Bluff Bodies'. J. Aerospace Science, Vol. 22, No. 2, p.124, 1955.

Roshko, A., 1969 A Review of Concepts in Separated Flow. A Lecture presented at Canadian Congress of Applied Mechanics, Centennial Year, 1967. Université, Laval Québec.

Schaeffer, J.E. and Eskinazi, S., 1959
An Analysis of the Vortex Street generated in a Viscous Fluid. J. Fluid Mechanics, Vol. 6, Part 2, p.241, 1959.

Schmiescheck, U., 1936 Zeitschrift F. Tech. Physik, Vol. 17, p.98, 1936.

Schubauer, G.B. and Skramstad, H.K., 1947
NACA Wartime Rept. W8, April 1943. Or J. Aeronaut. Sciences, Vol. 14, p.69, 1947. Or NACA Tech. Rept. 909, 1948.

Scott, G.D., 1960 Nature, 188, p.908, 1960.

Segré, G. and Silberberg, A., 1962
Behaviour of Macroscopic Rigid Spheres in Poiseville Flow, Parts 1 & 2, J. Fluid Mechanics, 14, part I, p.115, 1962.

Wadsworth, J., 1961 Proceedings of International Developments in Heat Transfer Conference, Colorado, p.760, 1961.

Westman, A.E.R. and Hugill, H.R., 1930
J. American Ceramic Society 13, p.767, 1930.

Wille, R., 1960 — Karman Vortex Streets. Adv. in Appl. Mech., Vol. VI, p.273, 1960.

Wille, R., 1966 — Von Karman Vortex Streets. Progress in Aeronautical Sciences, Kucheman, D., Editor, Pergamon Press, Oxford.

Wood, C.J., 1964 — The Effect of Base Bleed on a Periodic Wake. J. Aeron. Soc., p.479, July 1964.

Wood, C.J., 1967 — Flow Visualization of an Incompressible Wake with Base Bleed. J. Fluid Mech. Vol. 29, part 2, p.259, 1967.

Wood, C.J., 1968 — A Travelling Microscope Unit with Semi-Automatic Digital Output. J. of Scient. Instr., Vol. 1, p.475. (J. of Physics E) 1968, Series 2.

Yeh, Y. and Cummins, H.Z., 1964 — Applied Physics Letters, Vol. 4, May 15, p.176, 1964.

Zdravkovich, M.M., 1969 — Smoke Observation of Vortex Street Formation. J. Fluid Mechanics, Vol. 37, part 3, p.491, 1969.